ERG

DRAFT

Technical Support Document

Optical Gas Imaging Protocol (40 CFR Part 60, Appendix K)

Prepared for:

Jason DeWees
U.S. Environmental Protection Agency
Office of Air Quality Planning Standards
Air Quality Assessment Division
Measurement Technology Group (E141-03)
Research Triangle Park, NC 27711

Prepared by:

Tracey L. Footer
Eastern Research Group, Inc.
601 Keystone Park Drive, Suite 700
Morrisville, NC 27560

Revision No. 5
August 11, 2015

DISCLAIMER

This document and related appendices are currently in draft format. Do not cite or quote. This document will continue to be developed based on the latest information. This draft report has been initially reviewed by the U.S. Environmental Protection Agency's (EPA's) Office of Air Quality Planning and Standards and has been approved in draft form.

Mention of or referral to commercial products or services and/or links to non-EPA websites does not imply official EPA endorsement of or responsibility for opinions, ideas, data, or products presented at those locations, or guarantee the validity of the information provided. Mention of commercial products/services and non-EPA websites is provided solely as a reference to information on topics related to environmental protection that may be useful to EPA staff and the public.

ABSTRACT

This technical support document (TSD) provides background, technical analyses, experimental results, and other supplemental information to support regulatory development of an optical gas imaging (OGI) protocol. OGI technology can be used to detect fugitive emissions of compounds such as methane and volatile organic compounds from industrial sources, including those within the refinery, oil and gas, and chemical sectors. The potential use of OGI technology has been presented in two *Federal Register* notices (77 FR 76248, June 18, 2012 and 79 FR 36880, June 30, 2014). A protocol for applying OGI technology will be codified at 40 CFR part 60, appendix K. This document presents a comprehensive regulatory history and results of a literature review on the technology development and observations of current application of OGI technology. The literature review identifies the technology, applications, and limitations of the current remote measurement and monitoring technologies. This TSD also contains the results from multiple efforts commissioned by the U.S. Environmental Protection Agency (EPA) for Eastern Research Group, Inc. (ERG) to perform laboratory studies, evaluate OGI technology, and research potential operations and procedures for detecting leaks using OGI technology. Laboratory studies include testing of the spectral limitations and gas sensitivity and determining the effect of various environmental factors on leak detection. Finally, the appendices of this document contain supplemental information to the laboratory studies.

TABLE OF CONTENTS

LIST OF TABLES

LIST OF FIGURES

LIST OF ACRONYMS

Å	Ångström (0.0001 μm)
AIMM	approved instrument monitoring method
API	American Petroleum Institute
AQCC	State of Colorado Air Quality Control Commission
AWMA	Air and Waste Management Association
AWP	Alternative Work Practice
BAGI	backscatter absorption gas imaging
CAA	Clean Air Act
CAAA	Clean Air Act Amendments of 1990
C-H	carbon-hydrogen
CLGS	custom controlled leak generation system
DI&M	directed inspection and maintenance
DIAL/LIDAR	differential absorption light detection and ranging systems
ELP	enhanced LDAR program
EPA	U.S. Environmental Protection Agency
ERG	Eastern Research Group, Inc.
ETV	Environmental Technology Verification program
FID	flame-ionization detector
FIP	federal implementation plan
FTIR	Fourier transform infrared spectroscopy
FOV	field-of-view
FPA	focal plan array
ft	feet
GF	GasFindIR
g/hr	grams per hour
GHG	greenhouse gas
GIT	Gas Imaging Technologies, LLC
GWP	global warming potential
HAP	hazardous air pollutant
HC	hydrocarbon
HgCdTe	mercury cadmium telluride
IMSS	image multi-spectral sensing
InSb	indium antimonide
IR	infrared
lbs	pounds
LDAR	leak detection and repair
LSI	Leak Surveys, Inc.
LSP	leak simulation platform
MDL	minimum detection limit
MDLR	minimum detected leak rate
mK	millikelvin
NECL	noise equivalent concentration length
NEIC	National Enforcement Investigations Center
NESHAP	national emission standards for hazardous air pollutants

NETD	noise equivalent temperature difference
NSPS	new source performance standards
OGI	optical gas imaging
OP-FTIR	open-path Fourier transform infrared spectroscopy
OP-TDL	open-path tunable diode laser
ORD	Office of Research and Development
ORS	optical remote sensing
PAT	Pacific Advanced Technology
PIA	pixel intensity analyzer
PID	photo-ionization detector
POL	point of limitation
PNNL	Pacific Northwest National Laboratory
ppm	parts per million
ppm•m	parts per million – meters
ppmv	parts per million by volume
RPM	radial plume mapping
RRF	relative response factor
SF_6	sulfur hexafluoride
SIP	state implementation plan
SOCMI	synthetic organic chemicals manufacturing industry
TSD	technical support document
UV-DOAS	ultraviolet differential optical absorption spectrometer
VOC	volatile organic compound
μm	micrometer

I. BACKGROUND

Fugitive emissions are a significant source of air emissions in the United States. The U.S. Environmental Protection Agency (EPA) defines fugitive emissions as emissions that could not reasonably pass through a stack, chimney, vent, or other functionally-equivalent opening. Examples of fugitive emissions include methane or volatile organic compounds (VOCs) from chemical plants or oil refineries, particulate emissions from handling solid raw materials in chemical or other manufacturing, or evaporative emissions of VOCs from wastewater treatment.

The magnitude of fugitive emissions can be significant for a source category. For example, at chemical processing plants, one study showed that about half of all hydrocarbon emissions typically stem from fugitive emissions from equipment.[35] An emissions inventory of four natural gas processing plants showed that more than 80% of methane emissions resulted from fugitive equipment leaks.[17] Emissions from the oil and gas industry, specifically from production, transmission, storage, and distribution, are currently among the largest anthropogenic sources of U.S. methane emissions.[129] In 2013, methane emissions from natural gas systems and petroleum systems[a] were 157.4 and 25.2 million metric tons of carbon dioxide equivalents, respectively, representing 69% of methane emissions from the energy sector. Fugitive methane emissions from compressors, including compressor seals, are the primary emission source from natural gas processing.[49] In emission projections to 2018, fugitive emissions continue to be the largest emission source category for the oil and gas sector.[49] For the purposes of this document, fugitive emissions are the unplanned losses of gaseous compounds from pipes, valves, flanges, and other types of industrial equipment.

A. Leak Detection and Repair

Leak detection and repair (LDAR) programs are standardized regulatory work practices that are designed to reduce fugitive emissions of air pollutants from industry by identifying leaking equipment for repair.[119] Regulatory LDAR programs first appeared in EPA regulations in 1983 and continue today. Regulatory LDAR programs typically involve several elements: an inventory of equipment that could be leaking; monitoring the equipment to determine if there is a leak (as defined by the applicable regulation) using sensory monitoring (i.e., audio, visual, olfactory) or EPA Method 21, and performing corrective action on equipment that is found to be leaking. EPA Method 21 (Determination of Volatile Organic Compound Leaks) is the most common method for identifying leaking equipment. Method 21 monitoring requires the use of a portable instrument to detect VOC leaks above a certain action level from equipment such as valves, flanges, pressure relief devices, pump seals, compressor seals, agitator seals, connectors, open-ended lines, sampling connections, and other common industrial connections at individual sources.

In 2008, the EPA introduced the Alternative Work Practice (AWP) as an option to replace standard work practices that use only Method 21 monitoring. The AWP allows LDAR programs the flexibility to implement OGI techniques for screening in lieu of Method 21. Instead of using a portable instrument to detect and measure the concentration of VOC leaks using a

---

[a] IPCC source category 1B2a (onshore and offshore crude oil production, transportation, and refining operations).

photoionization detector (PID) or flame ionization detector (FID), OGI technology utilizes an infrared (IR) camera to make equipment leaks visual by means of thermographic imaging.

Because OGI technology continues to evolve and improve, the EPA is conducting research into the current state of OGI technology to help standardize its use for regulatory purposes. The potential use of OGI technology has been presented in two *Federal Register* notices (National Uniform Emission Standards for Storage Vessel and Transfer Operations, Equipment Leaks, and Closed Vent Systems and Control Devices at 77 FR 76248, June 18, 2012; and Petroleum Refinery Sector Risk and Technology Review and New Source Performance Standards at 79 FR 36880, June 30, 2014). A protocol for applying OGI technology will be codified at 40 CFR part 60, appendix K.

B. Purpose and Scope of this Document

The purpose of this document is to provide technical background information on OGI. Information presented in this document will help the EPA in developing, evaluating, and promoting standardized prescriptive procedures for source characterization and compliance monitoring related to the use of OGI technology to detect fugitive gas emissions of VOCs, hazardous air pollutants (HAPs), and greenhouse gases (GHGs) (i.e., methane, sulfur hexafluoride) from industrial environments.

Since the formation of the EPA in 1970, the issue of management and mitigation of the fugitive emissions from industrial activities to ambient air has received a lot of attention because of fugitive emissions' direct effect on human health and the environment. This document reviews the evolution of federal regulations designed to control the amount of fugitive HAPs and VOCs released by leaking industrial equipment up to the current implementation of LDAR programs and the recent increase in use of OGI technology to assist these programs. The information presented in this document includes a review of publically available literature. This document focuses on the theory and performance of OGI technology application for LDAR programs and presents results from controlled laboratory studies aimed at characterizing the performance of OGI technology for leak detection.

Following are the main organizational compartments of this document:

- Section II – A summary of the regulatory history that covers regulatory and policy development up to today.

- Section III – A technical literature review that discusses commercially available OGI technologies and associated studies.

- Section IV – Research commissioned by the EPA for ERG to evaluate technology performance and methods related to the application of OGI for leak detection.

- Section V – Summary and observations.

- Section VI – Appendices and supporting documents.

II. POLICY AND REGULATIONS

A. History of LDAR Based on the 1990 CAA Amendments

Coincident with the formation of the EPA in 1970, Congress passed the Clean Air Act (CAA), which required the EPA to develop national ambient air quality standards (NAAQS) and establish measurement methods for criteria pollutants. Additionally, in response to the CAA's directive to establish federal standards of performance for new sources within categories of sources contributing significantly to air pollution, the EPA launched the new source performance standards (NSPS) program. The intention of the NSPS program is to control emissions from new, modified, or reconstructed stationary sources by setting standards that limit emissions through the use of the best system of emission reduction, which takes into account the cost of achieving such reductions. Existing sources were regulated through state implementation plans (SIPs) or the federal implementation plan (FIP).

Federal leak standards were first introduced when the NSPS for synthetic organic chemicals manufacturing industries (SOCMI) and petroleum refineries were promulgated in October 1983 and May 1984, respectively. These actions required monitoring of specific types of equipment in VOC or HAP service[b], depending on the regulation, using EPA Method 21 or other equivalent monitoring. The types of industrial equipment targeted in these actions included pumps, valves, compressors, pressure relief devices, sampling connection systems, open-ended lines, flanges, and other connector types.[118] Along with the first leak standards, Method 21 was first promulgated in 1983 at 40 CFR part 60, appendix A.

During the first two decades after being founded, the EPA began to investigate the level of hazard associated with individual HAPs that were listed in the CAA and developed a list of stationary sources that emitted these HAPs. The EPA developed national emission standards for hazardous air pollutants (NESHAP) to reduce, by the maximum degree, the emissions of HAPs from these source categories.

With the rise of new environmental issues getting public attention (e.g., inability to control HAP emissions from industrial sources, continued NAAQS non-attainment, increased emissions from automobiles, and acid rain), Congress passed the reauthorization of the CAA complete with over 600 additional pages of amendments, known as the Clean Air Act Amendments of 1990 (1990 CAAA).[103] Following passage of the 1990 CAAA, the EPA developed a new strategy for addressing HAP issues that involved shifting the focus from individual HAPs to source categories that may emit multiple pollutants.[102] This shift in regulatory approach resulted in the addition of source-specific NESHAPs based on Maximum Achievable Control Technology (MACT). MACT standards aim to reduce HAP emissions from stationary sources by requiring all sources to reduce their emissions to the levels of emissions achieved by the best performing sources in a source category. In 1990, with the introduction of the 1990 CAAA, Method 21 was revised to its current form.

---

[b] In VOC or HAP service means that the equipment is expected to come into contact with and/or contain a liquid or gas with VOC or HAP, generally above a specific level (e.g., greater than 10% by weight). The definition of in VOC or HAP service varies by regulation.

The control of fugitive emissions (and, therefore, LDAR programs) is mostly implemented through these two major regulatory programs today: the NSPS and NESHAP programs. Table 2-1 lists the major regulatory milestones that shaped current LDAR programs and requirements. Table 2-2 lists the federal regulations that require a formal LDAR program as of 2015.

Table 2-1. Timeline of Major Regulatory Milestones Leading to Current Status

Year	Common Name	Document
1955	Air Pollution Control Act	Public Law 84-159
1963	Clean Air Act (CAA)	Public Law 88-206
1967	Air Quality Act	Public Law 90-148
1970	National Environmental Policy Act (NEPA)	Public Law 91-190
1970	Clean Air Act of 1970 (1970 CAA)	Public Law 91-604
1983	NSPS LDAR and Method 21 Promulgation	48 FR 37598
1984	NESHAP (Part 61) LDAR Promulgation	49 FR 23513
1990	CAA amendments extend LDAR provisions to NESHAP MACT; (1990 Clean Air Act Amendments (CAAA))	55 FR 25602, Public Law 101-549
2000	Consolidated Federal Air Rule (CAR) for Equipment Leaks	65 FR 78268
2008	Alternative Work Practice (AWP) Promulgation	73 FR 78199 (40 CFR 60.18, 63.11, and 65.7)
2008	Greenhouse Gas Reporting Rule	74 FR 56260
2011	Proposed Uniform Standards for Equipment Leaks	77 FR 36248 (40 CFR 65)

Table 2-2. Federal Regulations Requiring LDAR Programs with Method 21 Leak Monitoring[22, 119]

40 CFR Part and Subpart		Regulation Title
Part 60		Standards for Performance of New Stationary Sources (NSPS)
Subpart	VV	Standards of Performance for Equipment Leaks of VOC in the Synthetic Organic Chemicals Manufacturing Industry for which Construction, Reconstruction, or Modification Commenced After January 5, 1981, and on or Before November 7, 2006
	VVa	Standards of Performance for Equipment Leaks of VOC in the Synthetic Organic Chemicals Manufacturing Industry for Which Construction, Reconstruction, or Modification Commenced After November 7, 2006
	XX	Standards of Performance for Bulk Gasoline Terminals
	DDD	Standards of Performance for Volatile Organic Compound (VOC) Emissions from the Polymer Manufacturing Industry
	GGG	Standards of Performance for Equipment Leaks of VOC in Petroleum Refineries for which Construction, Reconstruction, or Modification Commenced After January 4, 1983, and on or Before November 7, 2006
	GGGa	Standards of Performance for Equipment Leaks of VOC in Petroleum Refineries for Which Construction, Reconstruction, or Modification Commenced After November 7, 2006
	KKK	Standards of Performance for Equipment Leaks of VOC From Onshore Natural Gas Processing Plants for Which Construction, Reconstruction, or Modification Commenced After January 20, 1984, and on or Before August 23, 2011

Table 2-2. Federal Regulations Requiring LDAR Programs with Method 21 Leak Monitoring[22, 119]

40 CFR Part and Subpart		Regulation Title
	QQQ	Standards of Performance for VOC Emissions From Petroleum Refinery Wastewater Systems
Part 61		National Emissions Standards for Hazardous Air Pollutants (NESHAP)
Subpart	F	National Emission Standard for Vinyl Chloride
	J	National Emission Standard for Equipment Leaks (Fugitive Emission Sources) of Benzene
	L	National Emission Standard for Benzene Emissions from Coke By-Product Recovery Plants
	V	National Emission Standard for Equipment Leaks (Fugitive Emission Sources)
	BB	National Emission Standard for Benzene Emissions From Benzene Transfer Operations
	FF	National Emission Standard for Benzene Waste Operations
Part 63		NESHAP for Source Categories – Maximum Achievable Control Technology (MACT)
Subpart	H	National Emission Standards for Organic Hazardous Air Pollutants for Equipment Leaks
	I	National Emission Standards for Organic Hazardous Air Pollutants for Certain Processes Subject to the Negotiated Regulation for Equipment Leaks
	J	National Emission Standards for Organic Hazardous Air Pollutants for Polyvinyl Chloride and Copolymers Production
	R	National Emission Standards for Gasoline Distribution Facilities (Bulk Gasoline Terminals and Pipeline Breakout Stations)
	S	National Emission Standards for Hazardous Air Pollutants from the Pulp and Paper Industry
	U	National Emission Standards for Hazardous Air Pollutants Emissions: Group I Polymers and Resins
	W	National Emission Standards for Hazardous Air Pollutants for Epoxy Resins Production and Non-Nylon Polyamides Production
	Y	National Emission Standards for Marine Tank Vessel Loading Operations
	CC	National Emission Standards for Hazardous Air Pollutants from Petroleum Refineries
	DD	National Emission Standards for Hazardous Air Pollutants from Off-Site Waste and Recovery Operations
	GG	National Emission Standards for Aerospace Manufacturing and Rework Facilities
	HH	National Emission Standards for Hazardous Air Pollutants from Oil and Natural Gas Production Facilities
	OO	National Emission Standards for Tanks – Level 1
	PP	National Emission Standards for Containers
	QQ	National Emission Standards for Surface Impoundments
	SS	National Emission Standards for Closed Vent Systems, Control Devices, Recovery Devices, and Routing to a Fuel Gas System or a Process
	TT	National Emission Standards for Equipment Leaks – Control Level 1
	UU	National Emission Standards for Equipment Leaks – Control Level 2
	WW	National Emission Standards for Storage Vessels (Tanks) – Control Level 2
	XX	National Emission Standards for Ethylene Manufacturing Process Units: Heat Exchange Systems and Waste Operations
	YY	National Emission Standards for Hazardous Air Pollutants for Source Categories: Generic Maximum Achievable Control Technology Standards

Table 2-2. Federal Regulations Requiring LDAR Programs with Method 21 Leak Monitoring[22, 119]

40 CFR Part and Subpart		Regulation Title
	GGG	National Emission Standards for Pharmaceuticals Production
	HHH	National Emission Standards for Hazardous Air Pollutants from Natural Gas Transmission and Storage Facilities
	III	National Emission Standards for Hazardous Air Pollutants for Flexible Polyurethane Foam Production
	JJJ	National Emission Standards for Hazardous Air Pollutant Emissions: Group IV Polymers and Resins
	MMM	National Emission Standards for Hazardous Air Pollutants for Pesticide Active Ingredient Production
	OOO	National Emission Standards for Hazardous Air Pollutant Emissions: Manufacture of Amino/Phenolic Resins
	PPP	National Emission Standards for Hazardous Air Pollutant Emissions for Polyether Polyols Production
	VVV	National Emission Standards for Hazardous Air Pollutants: Publicly Owned Treatment Works
	EEEE	National Emission Standards for Hazardous Air Pollutants: Organic Liquids Distribution (Non-Gasoline)
	FFFF	National Emission Standards for Hazardous Air Pollutants: Miscellaneous Organic Chemical Manufacturing
	BBBBB	National Emission Standards for Hazardous Air Pollutants for Semiconductor Manufacturing
	GGGGG	National Emission Standards for Hazardous Air Pollutants: Site Remediation
	HHHHH	National Emission Standards for Hazardous Air Pollutants: Miscellaneous Coating Manufacturing
	BBBBBB	National Emission Standards for Hazardous Air Pollutants for Source Category: Gasoline Distribution Bulk Terminals, Bulk Plants, and Pipeline Facilities
	VVVVVV	Hazardous Air Pollutants for Chemical Manufacturing Area Sources
Part 65		Consolidated Federal Air Rule
Subpart	F	Equipment Leaks
Part 98		Mandatory Greenhouse Gas Reporting Program
Subpart	W	Petroleum and Natural Gas Systems
Part 264		Standards for Owners and Operators of Hazardous Waste Treatment, Storage, and Disposal Facilities
Subpart	BB	Air Emission Standards for Equipment Leaks
Part 265		Interim Status Standards for Owners and Operators of Hazardous Waste Treatment, Storage, and Disposal Facilities
	BB	Air Emission Standards for Equipment Leaks

B. Regulatory Status

Both the EPA and industry encountered unexpected challenges in implementing LDAR programs with Method 21 following initial establishment of the LDAR programs listed in

Table 2-2. EPA Method 21 involves positioning an instrument probe near the source of a potential equipment leak and measuring the VOC concentration as the probe is judiciously (and slowly) scanned around the potential leak source. A formal LDAR program requires that the facility maintain an inventory of all equipment at the facility subject to the regulation, complete with unique equipment IDs, leak definition, monitoring frequency information, and previous screening and repair results. If the survey result for an individual piece of equipment is above the regulatory leak definition, then the equipment is considered to be leaking and must be repaired and rescreened within a prescribed time frame. With individual facilities easily having thousands of pieces of equipment to monitor, this process immediately becomes a heavy resource burden to industries seeking compliance.

The following paragraphs present some of the challenges and findings of implementing LDAR programs using Method 21.

1993. Methane is a potent GHG that is estimated to have 28-36 times more global warming potential (GWP) than carbon dioxide on a 100-year time frame.[51] The overall threat of increasing GHG emissions to hasten global climate change compelled President Clinton to announce the Climate Change Action Plan of 1993. As a part of this plan, the EPA created the Natural Gas STAR program in 1993 to increase the awareness of methane emission sources and to serve as a platform for sharing emissions reduction innovations and best practices throughout the oil and natural gas industry.[25] The primary goal of the Gas STAR program is to offer a voluntary, flexible, and cost-effective partnership between the government and the oil and natural gas industry. By volunteering to become a partner of the program, companies exchange information with the EPA and, in turn, the EPA provides news, updates, and regular transfer of information meetings to assist their facilities with emissions reduction in all areas of operations, including those that were not regulated.

1995. Around this time, the term "Directed Inspection and Maintenance" (DI&M) started to appear in the literature relative to cost-effective strategies implemented by the facilities to proactively find and fix leaks. DI&M was one of the recommended practices introduced to industry in 1995 through the Gas STAR program. Industry began to realize that reducing fugitive emissions also meant reducing product loss and therefore could lead to improved economic performance. With a highly profitable product that was difficult to contain, the oil and natural gas industry was particularly interested in how to prevent methane product loss. However, not all companies willingly signed up for the Gas STAR program, and simply implementing the DI&M programs did not necessarily ensure that a facility using the practice was in compliance with all regulatory emissions control requirements. (DI&M does not satisfy the requirements for regulatory LDAR programs.)

1997. In 1997, the American Petroleum Institute (API) commissioned a study to investigate the possibility for conducting LDAR surveys in a more efficient manner.[1] This study collected data from seven Los Angeles, California refineries over 5.5 years for a total of 11.5 million refinery equipment measurements. Results showed that valve equipment in gas and light liquid service combined contributed an average of 68% of the total facility fugitive VOC emissions, while connectors in the same service contributed only 28% of the total facility fugitive VOC emissions, but were three times as abundant as valves by count of equipment monitored. A major discovery from this study was that *92% of the controllable*

fugitive emissions (non-zero screening values) were attributed to just 0.13% of the total equipment monitored (as represented by Figure 2-1), and the study concluded that the current leak detection practice spends about 98% of the LDAR program's effort monitoring non-leakers. The study went on to propose that a more cost effective method for LDAR program compliance should focus more on the high emission rate leakers and avoid performing EPA Method 21 monitoring on all equipment types during every survey.
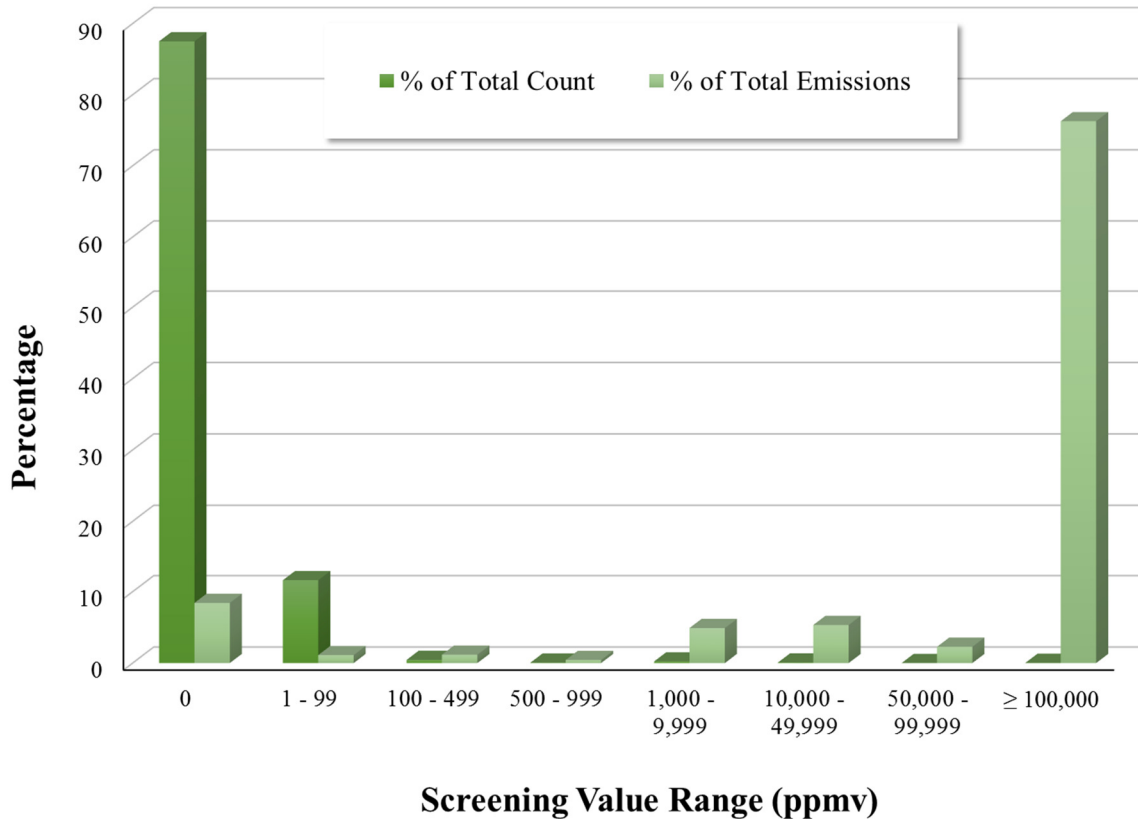
Figure 2-1. Distribution of the Total Equipment Counts and Estimated Emissions by Screening Range[1]

1997-1999. By 1999, it was obvious to the EPA that industry compliance reports were not matching up with results from comparison monitoring conducted by the EPA's National Enforcement Investigations Center (NEIC).[110] For example, 17 facilities were monitored during investigations by NEIC for several years, and while the average leak rate reported by facilities to the EPA was 1.3%, the NEIC found the average leak rate to be 5.0%. A potential explanation for this discrepancy appeared in a 1997 report by the Bay Area Air Quality Management District, whose findings showed that a one centimeter difference in analyzer position equated to a 57% chance of missing an actual leak.[110] This amount of sensitivity to operator error while performing Method 21, and the resulting under-reporting of potentially 80 million pounds of VOCs being emitted annually, fueled action by the EPA to find new ways to quickly and definitively identify significant leaks.

<u>1999</u>. Starting around 1999, to address poor performing LDAR programs, the Department of Justice teamed up with the EPA to issue civil penalties and consent decrees to industry LDAR programs that were found to be deficient. The consent decrees instructed the penalized facility to implement a stricter program of leak detection and repair monitoring called "Enhanced LDAR."[22,62] Enhanced LDAR programs (ELPs) go above and beyond regulatory LDAR requirements to systematically improve the performance of a facility's LDAR program. ELPs include tighter restrictions and/or more activity in subsections such as: documentation, monitoring frequency, LDAR action levels, repairs, delay of repairs, equipment upgrades, training, LDAR audits, recordkeeping, and reporting.[62] ELPs have resulted in considerable emissions reductions at individual facilities.[97]

<u>2002-2005</u>. Clearstone Engineering conducted two studies (in 2000[17] and 2004-2005[18]) that evaluated the potential for methane emissions reduction and cost-saving opportunities at gas processing facilities. In both studies, Clearstone found that fugitive equipment leaks contributed the majority of methane and non-methane hydrocarbon emissions and that, of the fugitive equipment leak emission categories, equipment that is associated with vibrational and heat-cycle services contributed a large majority of the total fugitive emissions. A significant result of the 2002 Clearstone report was that an estimated 94.9% of total natural gas losses would be cost-effective to reduce. However, similar to findings of the 1997 API study[1], both Clearstone studies found that only a small percentage (2.4% of all the equipment surveyed) under hydrocarbon service were determined to be leaking, in this case using a leak definition of 10,000 parts per million by volume (ppmv). The Clearstone studies also prompted the Gas Technology Institute (GTI, formerly known as the Gas Research Institute, GRI) to petition the EPA for acceptance of alternative work practices to Method 21 as early as 2000.[17]

The 2002 Clearstone study also indicated that using a HiFlow[TM] Sampler could provide more accurate estimates of actual leak rates versus Method 21. The HiFlow[TM] Sampler was developed by GTI as an economic means of estimating the emission rate from individual leaking equipment components with sufficient accuracy to allow an objective cost-benefit analysis of each repair opportunity. Leak source emission rate is the product of the measured pollutant concentration and the measured leak flow rate. Emission rates, as opposed to actual pollutant concentrations, provide an assessment of the severity of the leak in terms of air mass volume and time, which can in turn be used to determine long and short term exposure. In addition to tools such as the HiFlow[TM] Sampler, a more accurate way to determine the mass emission rate of fugitive gases from equipment leak sources is through "bagging[c]" or physical isolation techniques.[116] However, this technique is estimated to cost roughly $500 per equipment component; and with facilities having as many as a million components, this technique is impractical and prohibitively expensive.

---

[c]   Bagging is a method to measure the emission rate from an equipment component by isolating the component from ambient air to collect any leaking compound(s). A tent (i.e., bag) made of material impermeable to the compound(s) of interest is constructed around the leak interface of the piece of equipment. More information on bagging can be found in Section 4 of the EPA's Protocol for Equipment Leak Emission Estimates (http://www.epa.gov/ttn/chief/efdocs/equiplks.pdf).

EPA studies have correlated Method 21 concentration measurement values with a mass emissions rate from available bagging data as a way to estimate mass emissions rates for whole facilities.[116] However, because current OGI technology cannot reliably measure gas concentration values, a more resource intensive method such as EPA Method 21, bagging, or radial plume mapping with Fourier Transform Infrared Spectroscopy/Tunable Diode Laser/ Differential Optical Absorption Spectrometer (FTIR/TDL/DOAS) would still be required to estimate facility emission rates.[115]

Following the Clearstone report in 2002,[17] Natural Gas STAR began to publish "Lessons Learned" documents as technical references. Natural Gas STAR industry partners evaluated the effectiveness of DI&M programs to cut total facility emissions while also reducing facility costs. The projected cost curves from the Clearstone 2002 study indicated the likelihood that industry could make choices that would result in financial improvement with the added benefit of reducing fugitive emissions to the atmosphere, which appealed to state and federal regulators. Since 2002, the Natural Gas STAR program has published 19 Lessons Learned, covering sources such as compressors, dehydrators, and pneumatics and controls. The Lessons Learned serve as comprehensive guides for implementing methane emission reduction technologies and practices and summarize cost and benefit information.

2006-2007. Furry et al., 2006; Reese et al., 2007 and Trefiak, 2006 reported for industry on LDAR applications and technology challenges. These reports all agree that the implementation of Method 21 is timely and expensive, while advancing technologies offer promise to streamline and reduce the cost of routine monitoring.[35,80,98] A paper by Robinson et al. in 2007 found that using OGI technology to assist the periodic screening procedures increases the survey rate of equipment dramatically from about 60 pieces of equipment per hour with Method 21 to over 2,000 pieces of equipment per hour with OGI technology and that OGI technology-assisted surveys identified 97% of the total mass emissions detected from leaking sources with Method 21.[85] These studies provided evidence that using OGI technology to assist LDAR programs with their regular equipment surveys promises to be a quicker and more cost-effective method of identifying the largest sources of leaking emissions relative to Method 21 and will increase the amount of total facility fugitive emissions reduction because OGI technology can identify fugitive emissions from all equipment categories, regardless of whether that equipment is mandated for LDAR program compliance or not.

Grievances from industry, in addition to information on the difficulties of using Method 21, led to the proposal and ultimate promulgation of the AWP in 2008. The AWP, also commonly known as "Smart LDAR," gives LDAR programs the flexibility to implement OGI techniques for equipment screening in lieu of Method 21. Industry's initial response to the proposal of the AWP was favorable and even enthusiastic.[68,80,98] However, due to concerns raised during the proposal of the AWP about whether OGI technology could detect persistent low-leaking equipment, the EPA included an annual Method 21 survey requirement in the AWP, with a statement that this requirement would be revisited as people began to use the AWP and more information on OGI technology became available. This resulted in a lack of interest by industry to utilize the AWP in lieu of standard LDAR monitoring. Nonetheless, the promulgation of the AWP in 2008 was a catalyst for a flurry of studies and publications on its implementation.[10,11,68,78]

On March 26, 2012, the EPA proposed a set of emission standards for storage vessels and transfer operations, equipment leaks, and closed vent systems and control devices known as the "Uniform Standards" in an effort to ensure consistency and streamline recordkeeping and reporting requirements for facilities with sources subject to multiple regulations.[48,127] The requirements proposed in the Uniform Standards would be applicable only when referenced by a specific NESHAP or NSPS. As part of the Uniform Standards, the EPA proposed to allow the use of OGI technology in lieu of Method 21, as long as use of OGI technology followed the requirements of the protocol for use of OGI technology in 40 CFR 60, Appendix K, which has not yet been developed. The EPA recognized the potential in OGI technology for streamlining compliance activities related to emissions control, but because there is a well-documented need for OGI technology performance and operational studies,[94] the EPA still needed more data before concrete specifications could be outlined. The EPA received numerous comments on the proposal, but has not yet finalized the Uniform Standards.

States may opt to set emission standards that are more stringent than those required by the EPA. One such example is the enactment of Colorado's Air Quality Control Commission (AQCC) Regulation Number 7 in 2014, which covers the oil and natural gas sectors. This rule allows owners or operators to use one of the Approved Instrument Monitoring Method (AIMM), such as Method 21, OGI technology or any other Division approved instrument based monitoring device or method.[21] Some of the more progressive requirements included into Regulation 7 include:

- Provisions to reduce methane emissions from oil and gas development (first state in the nation to address methane);

- Increased control and inspection requirements for storage tanks (first standard in the U.S. to require tank emissions are captured and routed to control devices);

- Added requirement for well production facilities to connect their gas streams to a pipeline or control device from the first date of production;

- More stringent control requirements for glycol dehydrators;

- Extended the LDAR program requirements to include open-ended valves and lines; and

- Specifies the requirement of the use of best management practices (including increased use/allowance for OGI camera application and comprehensive recordkeeping and reporting) for well maintenance.

Colorado's Regulation 7 requirements prescribe LDAR program schedules according to threshold emission rates (in tons per year). This indicates that at least one LDAR screening survey is conducted via Method 21 or comparable quantification method. Thereafter, facilities are allowed to use AIMMs, such as OGI cameras, for LDAR surveys.

C. Costing Evaluations

[This section will discuss the results from studies performed on the financial burden and projected savings in relation to fugitive leak emissions reduction activities.]

III.   LITERATURE REVIEW

ERG searched the literature to identify the technology, applications, and limitations of the current remote measurement and monitoring technologies. This section presents the findings of the literature search.

A. Technology

1. History

Remote measurement and monitoring technologies have been available since the 1970s and extensive efforts have been made to make these technologies more widely acceptable to the monitoring community.[4,15,65,86,108,124] In late 2011, the EPA published the Optical Remote Sensing (ORS) for Measurement and Monitoring of Emissions Flux handbook,[71] which lists some of the more prominent technologies and applications, including:

- Ultraviolet Differential Optical Absorption Spectrometer (UV-DOAS)
- Open-Path Fourier Transform Infrared Spectroscopy (OP-FTIR)
- Raman spectroscopy
- Tunable Diode Laser (OP-TDL)
- Differential Absorption Light Detection and Ranging Systems (DIAL/LIDAR)
- OTM-10[d]/Radial Plume Mapping (RPM)
- Eddy Covariance Flux
- Optical Gas Imaging (OGI).

The application of some of these technologies has been difficult, especially with respect to LDAR programs. Roadblocks include: high cost, complex measurement theory, need for highly specialized operators, difficulty-of-use, identification of leak location, and inconsistent units of measure for data output to the end-user (e.g., parts per million – meters (ppm·m), path-averaged concentration).[124]

The scope of the literature search was broad initially, but ERG focused on leak detection technologies based on IR imaging (both active and passive) due to the potential for these technologies to reduce the time, labor, and cost of equipment monitoring for LDAR program compliance.[129] Of these technologies, the EPA selected only OGI cameras for implementation for the AWP. Other technologies were not selected because of the reasons above, in addition to technical limitations and interferences.[68] In-depth discussion on the different ORS technologies and their strengths, weaknesses, and applications can be found in the EPA ORS handbook[124]

---

[d] OTM-10 is "Other Test Method 10 – Optical Remote Sensing for Emission Characterization from Non-Point Sources" that contains various configurations of radial plume mapping or RPM. It is available from the EPA at http://www.epa.gov/ttn/emc/prelim.html.

2. Basis of OGI technology

OGI cameras produce images of gaseous emissions using one of two different IR sensing approaches: active or passive IR imaging. Active IR imaging provides the IR light source via controlled laser output to the environment that is then reflected off the background and attenuated or absorbed as it encounters gas species along the optical path. Passive IR imaging uses available IR radiation (anything with a temperature—above 0 K—produces IR radiation) to detect differences in the IR intensity between background IR and gas plume IR radiation. The type of gas species that will be imaged is a function of the spectral transmission window in the camera design. For example, many common OGI cameras for VOC detection have a bandpass filter that allows transmission of the 3.2 to 3.4 micrometer (μm) spectral region to the detector. This spectral region is characteristic of the stretching vibrational energy between a carbon-hydrogen (C-H) bond and is typically targeted when trying to detect or measure gases containing alkanes, alkenes, aromatics, and other hydrocarbons (such as methane, benzene, propane, butane and many others).[92] OGI cameras with bandpass filters that allow the transmission of different spectral windows can target different gas types; such as 4.52 – 4.67 μm for carbon monoxide, 10.3 – 10.7 μm for sulfur hexafluoride and anhydrous ammonia, and 8.0 – 8.6 μm for refrigerant gases.[34]

Active IR Imaging

Backscatter Absorption Gas Imaging (BAGI) cameras produce a live image by illuminating the viewing area with infrared laser light and detecting the amount of reflected (or backscattered) laser light returned to the instrument's detector. When the laser light of a specified wavelength is strongly absorbed by a gas, a shadowy cloud of that gas becomes visible as a darkened area in the live image.[84] This method of hydrocarbon gas leak detection works independently of ambient conditions but is limited by the laser wavelength output specified. Active IR imagers that use carbon dioxide lasers for their light source are unable to illuminate some target hydrocarbons such as methane. Sandia National Laboratories has developed two BAGI cameras to address the laser wavelength limitations: one for petroleum refineries, and one for the natural gas industry (to detect methane).

For the BAGI technology to image a leak there must be some sort of reflective surface close behind the leak.[84,85] A leak cannot be imaged against the sky or a distant background because the camera detector will not receive sufficient backscattered light intensity. As of 2007, BAGI cameras from Sandia National Laboratories and Laser Imaging Systems weighed between 20 and 30 pounds and could only run about 1 to 1.5 hours on battery power.[84,85] Quantification is not yet available with this technology and eye-safety for surrounding personnel is a concern due to laser output.

Passive IR Imaging

Due to the power demands and optical complexity of using controlled light sources with active IR imaging, manufacturers of OGI cameras will more commonly turn to passive IR imaging techniques to develop a more market viable system. Passive IR imaging cameras typically comprise an IR-transmissive lens, a staring focal plane array (FPA) detector, a cooling system,

and a processing system.[8,64] The selection of the FPA depends on the wavelength region of interest.

For detection of hydrocarbons, the region of interest is typically 3 – 5 µm, for which a detector made of indium antimonide (InSb) is the FPA of choice. However, in order to generate an image of sufficient contrast between gas plumes and the apparent background, passive IR imagers need stricter controls on the spectral bandwidth of the image and a reduction of signal noise. To address noise reduction in OGI detectors, a cooling module (like a Stirling engine) is incorporated into the camera design to cool the detector.

Recently there has been research and developments using microbolometer detectors which have resulted in products (such as Bertin Technologies' Second Sight[9]) now being commercially available. Microbolometer detectors do not need to be cryo-cooled; however, the physics behind the thermal conductivity response mechanism of microbolometer-based devices renders them slower and less sensitive than cooled photo-detection devices, like InSb FPAs. [50]

Two very different techniques have evolved to control the spectral bandwidth of passive IR imagers, band-pass filter and diffractive optics. Opgal and FLIR Systems, Inc. have each developed their own offering of an IR camera (the EyeCGas and GasFindIR 320 (GF320), respectively) based on OGI technology that restricts bandwidth to 3.2 – 3.4 µm. This bandwidth is spectrally harmonious with major absorption lines in the spectra of many target gases as mentioned above.[26] Because of the lack of complexity with this type of camera design, it is smaller, easier to use, and more robust.

Another way to control the spectral bandwidth is through methods called hyperspectral and multispectral imaging. Recent advances of this technology have increased the number of potential OGI instruments for leak detection applications since the start of this effort by the EPA to evaluate all commercially available OGI technology systems. Some of these upcoming instruments are not yet ready for commercial distribution and/or are so new that performance studies are either still underway or have yet to be planned. As this document is currently still in draft form, more analysis will be incorporated as newer OGI technology systems and relevant study data becomes available.

Gas Imaging Technologies, LLC (GIT) has developed the Sherlock® VOC OGI camera, which uses diffractive optics and multispectral image processing to image, speciate, and quantify fugitive gas emissions. The Sherlock® VOC camera operates based on the principles of image multi-spectral sensing (IMSS). IMSS is a form of diffractive optics whereby the incident light being received through the camera lens is both imaged and dispersed using a combination of a diffractive imaging spectrometer and an adaptive tunable filter.[40,42,43,44,45,46] Similar to a monochromator, where light is separated spectrally and the light that passes through the exit slit is scanned, with IMSS the light is spectrally dispersed using an optical lens that can be focused along the optical axis to produce images of narrow spectral bands that are measured sequentially in time on the FPA detector. See Figure 3-1 for an example of the basic concept of IMSS compared to a monochromator.
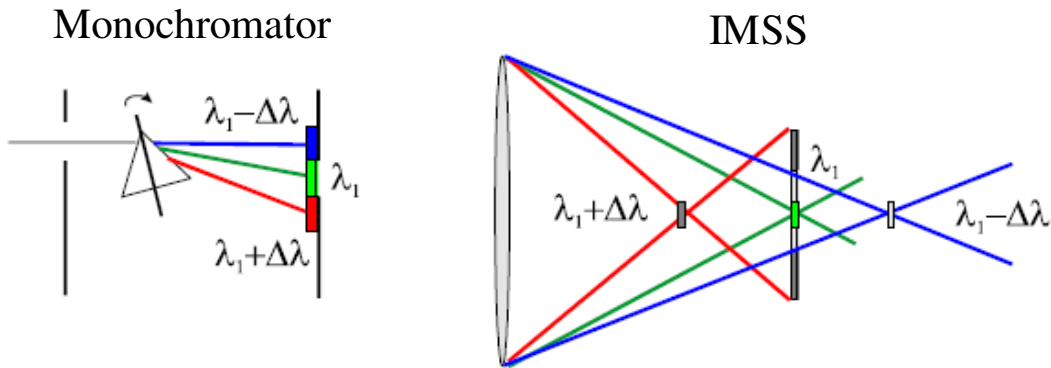
Figure 3-1. Basic Principle of IMSS Diffractive Optics[45]

The camera operator of a Sherlock® VOC has full control on the motion of the optical lens, allowing the operator to scan a series of wavelengths or dwell indefinitely on one wavelength.[46] The result is a frame-by-frame imaging of different spectral wavelengths that can be selected and combined with visual images to show gas leaks as false color. By selecting to visualize different wavelengths, it is possible to distinguish between gas species with the Sherlock® VOC; however, the exact identification and quantification of gas concentration procedures utilized by the associated software has not yet been evaluated in this document because it is proprietary. *Declaring that the Sherlock® VOC can quantify gas concentrations comes with a heavy caveat as verification studies by an external party has not yet been performed and QA evaluations on any measured gas concentrations produced by the Sherlock® VOC still need to be carefully studied.*

US Patent # 6680778[46] for the Sherlock® "Gas Leak Detector" states this technology determines concentrations of the target chemical by calculating the absorption (or emission) of the target chemical at its absorption (or emission) wavelength through the gas plume and comparing this value to absorption amounts at the same wavelength measured simultaneously from a background (out-of-plume) region. In a presentation at the 99th annual meeting of the Air and Waste Management Association (AWMA), Hinnrichs et al.[47] explained further that the log of the ratio of the signal intensity from the gas and the background is equal to the product of the absorption coefficient of the gas, the path length of the gas, and the concentration of the gas, as illustrated in the equation below. The plume depth (or path length) is determined by assuming the gas plume is symmetric and using the 2D pixel footprint of the image of the gas.[47]

$$-log\left(\frac{I_{gas}}{I_{background}}\right) = \alpha L c$$

The quantification of gas concentration by the Sherlock® VOC was compared with results from a FID at an oil and gas plant in Viggiano, Italy.[47] The study did not find many leaking equipment detected by EPA Method 21, and so the comparison was limited to six measurements. Of these six measurements, three had concentrations higher than the FID saturation level, and one was taken during rain, which interfered with the FID detection. The study claimed that the two remaining measurements agreed well, providing Figure 3-2 as evidence of good correlation. Where the FID measured 3,300 ppm, the Sherlock® VOC measured 4,530 ppm. And where the FID measured 9,155 ppm, the Sherlock® VOC measured 9,060 ppm. These measurements equate

to a relative percent difference of 31% and 1%, respectively. Added in the conclusions of this study is a statement regarding the need for more testing to better understand the accuracy of the Sherlock® VOC's gas concentration quantification performance.[47]
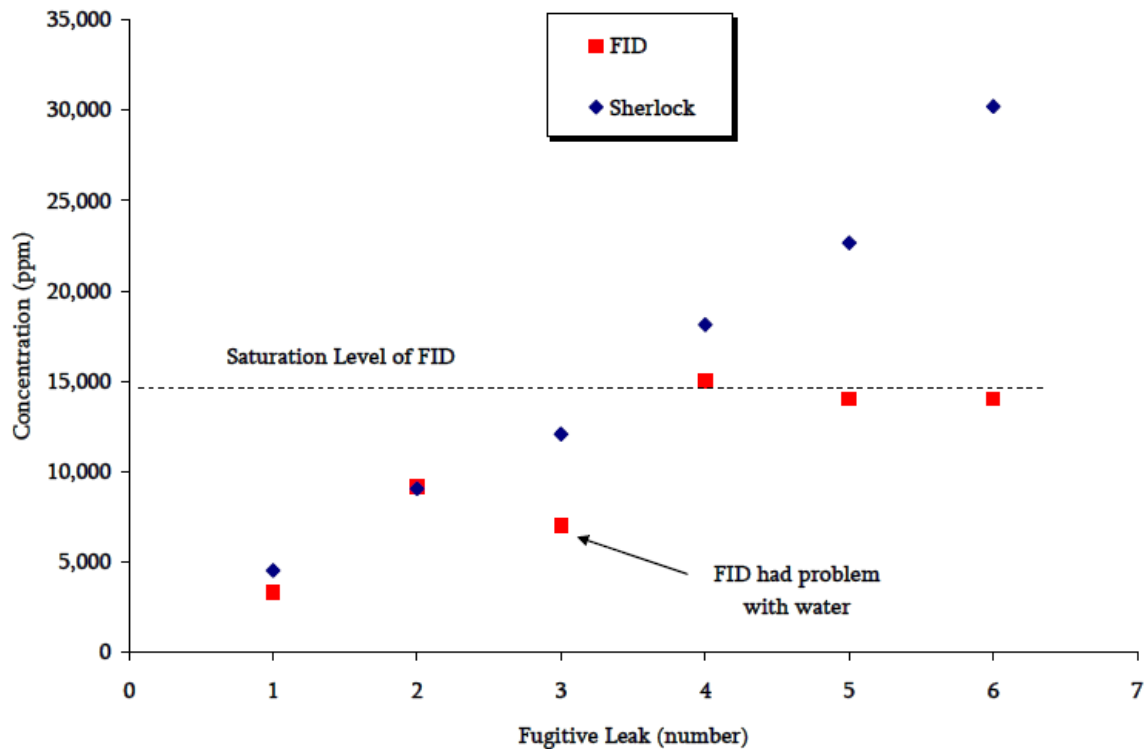
Figure 3-2. Correlation Between the Concentration Measurements Made by the FID Device as Compared to that Using the Sherlock® VOC[47]

Gas-imaging devices based on OGI technology operate by visually representing the temperature profile in a field of view where a gas cloud has a different thermal signature than its apparent background. The difference between the temperature of a targeted gas cloud and the temperature of the apparent background for that gas cloud is known as "delta-T" (ΔT). This is an important property to understand with respect to OGI technology because the greater the difference in temperature between the gas cloud and its apparent background (or the larger the absolute value of ΔT becomes), the higher the contrast between the two objects will appear in the OGI technology display and the more likely it will be for that leak to be detected by the OGI technology operator or automated display algorithm.

3. Available Technology

Both FLIR and GIT have long-wave IR options for imaging gases such as sulfur hexafluoride (SF_6) and ammonia (NH_3). As current LDAR activities focus principally on gases that absorb in the mid-wave IR ($3 - 5$ μm), so does this review. Commercially available OGI systems that operate in the mid-wave IR are displayed in Table 3-1 with estimated purchase costs, safety certifications, notes on the detector technology, and whether the manufacturer offers capability to quantify gas concentration (via software) or not.

Table 3-1. Currently Commercially Available Handheld OGI Camera Systems

Model	Make	Est. Cost	Intrinsically Safe?	Detector Technology	Quant?
GF320	FLIR	$85,000	No	InSb	No
EyeCGas	Opgal	$86,500	Yes	HgCdTe	No
Sherlock® VOC	Gas Imaging Technology	$100,000	No	Diffractive w/ InSb	Yes*

* The ability of the Sherlock® VOC to consistently provide a quantification value for gas concentration has not been sufficiently evaluated or verified.[41]

The allowance for the application of OGI cameras in regulatory LDAR programs through the AWP was partly to help alleviate the time, labor, and financial cost of compliance for industry and partly to help improve the rule effectiveness of LDAR programs. In order for the technology to meet these objectives, it must be able to consistently visualize target compound leaks at concentrations equal to the leak definition as specified by the applicable regulation. It also must be field portable so that an LDAR inspector can comfortably use the OGI technology for the duration of the LDAR survey without interruption for power (battery life), data (space), or physical demands (not too heavy or bulky). Ideally, the technology would be easy to deploy with minimal training and staffing requirements, have a reasonable cost for initial purchase and maintenance, and not endanger the OGI operators (be intrinsically safe in hazardous environments). The technology must be rugged enough for routine field use and provide a near real-time response with the capability of identifying the exact source of the leak.

Other potential units, such as Bertin Technologies' Second Sight TC and Telops Hyper-Cam have been excluded from this list due to the impractical weight and size of the units for LDAR application.[9,53,63] The Sherlock® VOC has also been determined impractical for LDAR applications by the EPA for similar reasons.[127] However, the Environmental Technology Verification (ETV) program did perform similar performance assessments on the FLIR GasFindIR™ MW (the predecessor to the FLIR GF320) and Sherlock® VOC cameras which demonstrated that the minimum detection limits (MDLs) for the Sherlock® VOC were generally higher and that the FLIR GasFindIR™ MW performed better overall. Results from these ETV assessments are provided in Table 3-2 and described in the next section.[10,11]

B. Observations and Improvements

Because of the importance proper leak identification and repair ultimately has on human health, safety, and the environment, many studies have been conducted to try and delineate the expected technology performance, limitations, and best practices associated with performing leak detection surveys using OGI cameras. This section presents summaries of key efforts at evaluating detection limit performance, operational conditions, and emission rate estimates.

1. Initial OGI Technology Performance Studies

After an intensive air quality study in Texas in 2000 revealed a discrepancy between aerial measurements of chemical species concentrations in the atmosphere over the Houston-Galveston area and what investigators expected the chemical species concentrations to be based on

available VOC emission inventory estimates, the Texas Commission on Environmental Quality (TCEQ) focused its efforts on better characterizing fugitive emissions through the development of additional leak detection and evaluation methods and using these new methods and conventional methods to update emissions factors and correlation equations.[24] The TCEQ funded studies to conduct evaluations of OGI technology to assist leak detection surveys at chemical and petroleum facilities. The ENVIRON International Corporation (Environ) was appointed by the Texas Council on Environmental Technology (TCET, which was later absorbed into TCEQ) in June 2003 to conduct the first of these studies.

TCEQ/Environ Study[24]

The main objectives for Environ in this study were to conduct a laboratory evaluation on OGI technology and to conduct a field evaluation on OGI technology for the development of a monitoring protocol using OGI technology for leak detection and updated emission factors and/or correlation equations.[24] Four OGI technology-based IR cameras were evaluated in the laboratory:

- Pacific Advanced Technology's (PAT) IMSS passive IR imaging camera (the predecessor to GIT's Sherlock® VOC)

- Laser Imaging Systems' Long-wave BAGI active IR imaging camera

- Sandia National Laboratory's Mid-wave BAGI active IR imaging camera

- Leak Survey, Inc.'s (LSI) Hawk passive IR imaging camera (the predecessor to FLIR's GasFindIR and GF320 cameras).

The tests were performed at the BP laboratory in Naperville, IL as detailed in the Environ report. The experimental set up that resulted from this effort was later used to conduct further OGI technology performance evaluations described later in this document. [5,10,11,74,75]

Delta-T (ΔT)

The TCEQ/Environ study employed a copper plate background painted flat black to assess the ability for PAT's IMSS and LSI's Hawk OGI cameras to detect gases as the ΔT approaches zero. Under controlled laboratory conditions, they found that both cameras were able to detect 60 grams per hour (g/hr) butane test gas with a ΔT as little as 0.5°C.[24] This result prompted the investigators to conclude that the ΔT parameter was not crucial in OGI technology leak detection as the OGI technology instruments were sensitive enough to be able to visualize gas leaks with very small ΔT values.

Laboratory Minimum Detection Limit Tests

The TCEQ/Environ study evaluated the minimum detectable mass emission rates of the four OGI cameras under controlled laboratory conditions for the following gas species of interest: ethylene, 1,3-butadiene, 1-butene, and propylene. Butane gas was also tested where time and resources allowed. All four OGI cameras were able to detect all test gases at mass emission rates less than 60 g/hr except the Mid-wave BAGI camera could not detect 1,3-butadiene and butane test gas was not evaluated for the Long-wave BAGI OGI camera. Table 3-2 summarizes the

results for each OGI camera under low wind conditions with a concrete background at a distance of 10 feet (ft) from the leak source.

Table 3-2. Average Minimum Detection Level Mass Emission Rates (g/hr), Number of Measurements in Parentheses[24]

OGI Camera	Ethylene	1,3-Butadiene	1-Butene	Propylene	Butane
PAT's IMSS	36 (3)	27 (3)	18 (3)	25 (4)	15 (3)*
Long-Wave BAGI	6 (5)	19 (3)	28 (3)	24 (3)	Not Tested
Mid-Wave BAGI	21 (3)	Not Detected Below 60 g/hr	8 (3)	17 (4)	1 (3)
LSI Hawk	14 (3)	18 (2)	5 (5)	7 (3)	5 (5)

* Results are uncertain and expected to be biased high due to a leak in the gas delivery system that was discovered after testing.

Other parameters expected to affect the leak detection capability of OGI cameras were tested during the TCEQ/Environ study. Two different backgrounds were employed to simulate various industrial conditions: concrete wall and metal gas cylinders (to represent metallic background equipment). Two different wind speeds were evaluated: low wind speeds (between 0 and 2 mph) and high wind speeds (between 3 and 5 mph). The leaking source was imaged at two distances (10 ft and 20 ft) to evaluate the impact distance from leak source had on leak detection capability.

To investigate the impact of a reflective background, the TCEQ/Environ study used metal cylinders as an experimental background. The results indicate that the "darker" areas of the metal cylinders prevented plume detection in those areas, but did not impact the overall minimum detection limits for any of the OGI cameras tested as the movement of the test gas plume was still visible in the "lighter" areas of the metal cylinder background. However, preliminary study data indicate that there is an impact on the minimum detection limit capabilities for each OGI camera by the other conditions tested (namely, higher wind speeds and farther distances from the leak source).

In February 2004, Environ carried out the field portion of a study on the performance of different OGI camera technologies.[24] This field study found that none of the four OGI camera technologies tested or Method 21, alone or in combination, detected all gas leaks. A total of 66 leaks were found at two study locations, representing normal industrial conditions for leaks of ethylene, propylene, butenes, 1,3-butadiene, and hexanes. The four OGI cameras found 31 of the 66 leaks (47%), and Method 21 found 49 of the 66 leaks (74%). Nonetheless, OGI camera surveys detected 533.9 g/hr of the overall 595.4 g/hr mass emissions found by Method 21 and measured by bagging, or about 90%, and indicate that the OGI cameras captured the majority of the larger leaks. Figure 3-3 is a graphical representation of the leaks seen or unseen by each OGI technology over the measured mass emission rate determined by bagging.[24]
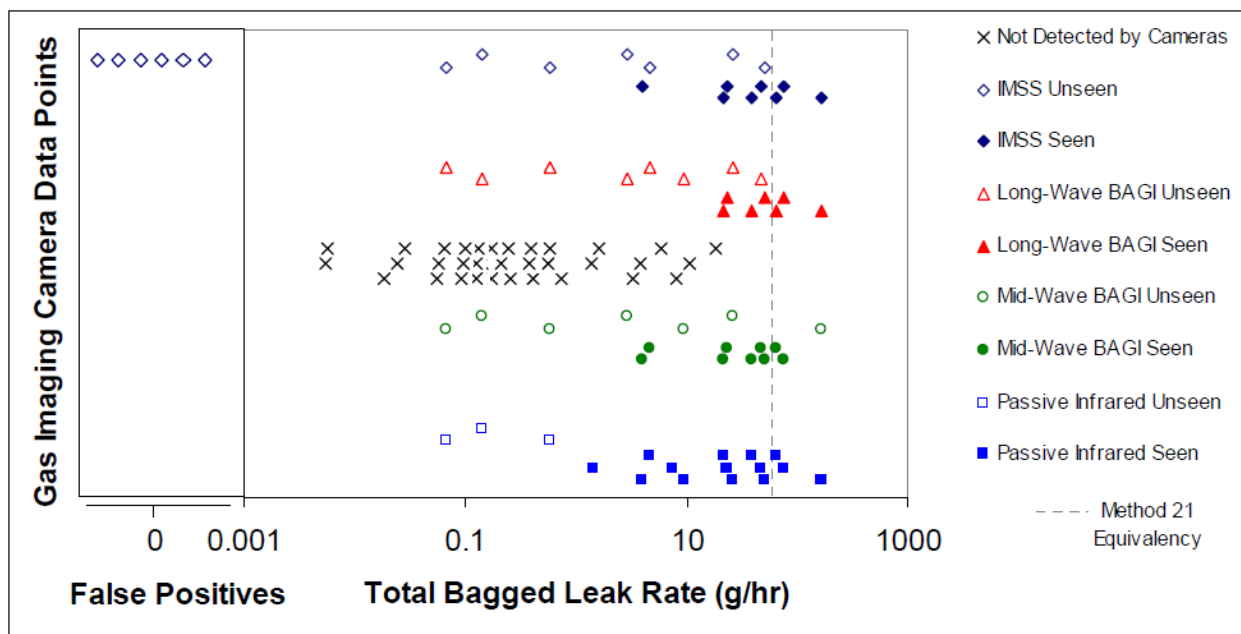
Figure 3-3. Field Survey Performance Summary of Infrared Cameras[24]

The y-axis in Figure 3-3 is unitless, the black X data points represent the leak rates of leaks discovered via Method 21 but not detected by the OGI cameras, and the hollow data points represent a bagged leak that was not detected by the camera. Of the OGI camera technologies tested, passive IR (the LSI Hawk, predecessor to the FLIR and Opgal OGI cameras) detected the lowest mass emission leak (1.4 g/hr), detected the most leaks, detected all leaks above the Method 21 equivalency leak rate[e] of 60 g/hr, and detected all leaks larger than 21 g/hr.[24] The other camera technologies tested missed leaks either near or above the Method 21 equivalency leak rate of 60 g/hr. The IMSS camera (i.e., Sherlock® VOC) detected leaks that could not be verified with Method 21, these were labeled as "False Positives" and are depicted on the left side of Figure 3-3 in the zero region.[24] According to this study—based on the OGI camera technologies available at the time of the study and the compounds detected—cameras designed with passive IR OGI technology are the most practicable and reliable for leak detection surveys.

Because LDAR applicable OGI cameras alone are not yet able to quantify the concentration or mass emission rates of fugitive gas emissions, and because there is still some concern remaining over OGI detection of very small leaks, other detection technologies may be useful when combined with AWP surveys. For example, a PID is a highly sensitive hand held device that can be extremely useful when coupled into an AWP program.[90] However, a PID will measure only gas concentrations and not direct mass emission rates, thereby, still requiring the application of correlation equations to calculate whole facility leak mass emission rates as with the current

---

e   Common Method 21 leak definitions of 500, 1,000, and 10,000 ppmv are employed by various LDAR program regulations to ensure a specific level of environmental protection from fugitive emissions. Monte Carlo analysis has been extensively studied as a way to determine the leak rate level that would result in an equivalent level of environmental protection when OGI technology is used in lieu of Method 21. For the purposes of AWP implementation, the EPA approved an equivalency leak rate of 60 g/hr when monitoring is performed on a bi-monthly frequency.[109]

work practice of Method 21. However, at the time of publication, the results of the TCEQ study gained OGI technology favorable attention from industry for its cost, size, weight, portability, performance, user-friendliness, and value as a potential tool to assist AWP leak detection surveys.[74]

2. API Follow-on Studies[5,74,75]

One year after the TCEQ/Environ study, the API sponsored continuation studies using the same laboratory facility in Naperville, IL to evaluate two newer OGI cameras: the FLIR GasFindIR, and the PAT Sherlock. Studies by Panek[74,75] and Benson[5] report on the results from these follow-on efforts.

Operational conditions such as lens focal length, gas temperature, background composition, steam presence, wind speed, and gas mixture versus pure compound were evaluated as possible convoluting factors when establishing new detection limits for FLIR GF-series OGI cameras.[5,74,75]

- The focal length of the lens did affect the detection capability of the camera. Using the same lens but increasing the distance to the target resulted in increased detection limits. Conversely, higher focal length lenses had better detection limits compared to shorter focal length lenses at the same distance.[5,75] Minimum detected leak rates (MDLRs) were plotted versus standoff distance in Figure 3-4 to illustrate this effect.

- Adding to the efforts of the earlier TCEQ study, Panek[75] found that an increase in the gas temperature increased the visible contrast of the gas plume against a uniform background (by increasing the temperature differential between the gas and the background) and lead to a reduction of detection limits.[75]

- The detection limits for imaging gas against a background of metal cylinders were higher than those with a uniform concrete background. It is assumed that this is because of a lack of thermal contrast between the gas and the cylinder background.[75]

- The Panek[75] study did not detect steam that was generated by a pump. However, when steam was produced using a hot vapor generator, the plume was easily visible.[75]

- MDLRs are presented for 20 compounds at three different wind speeds in Tables 3-3 through 3-5. These tables illustrate that higher wind speeds and measuring mixtures of the pollutants versus pure chemical both resulted in higher MDLRs.[5]
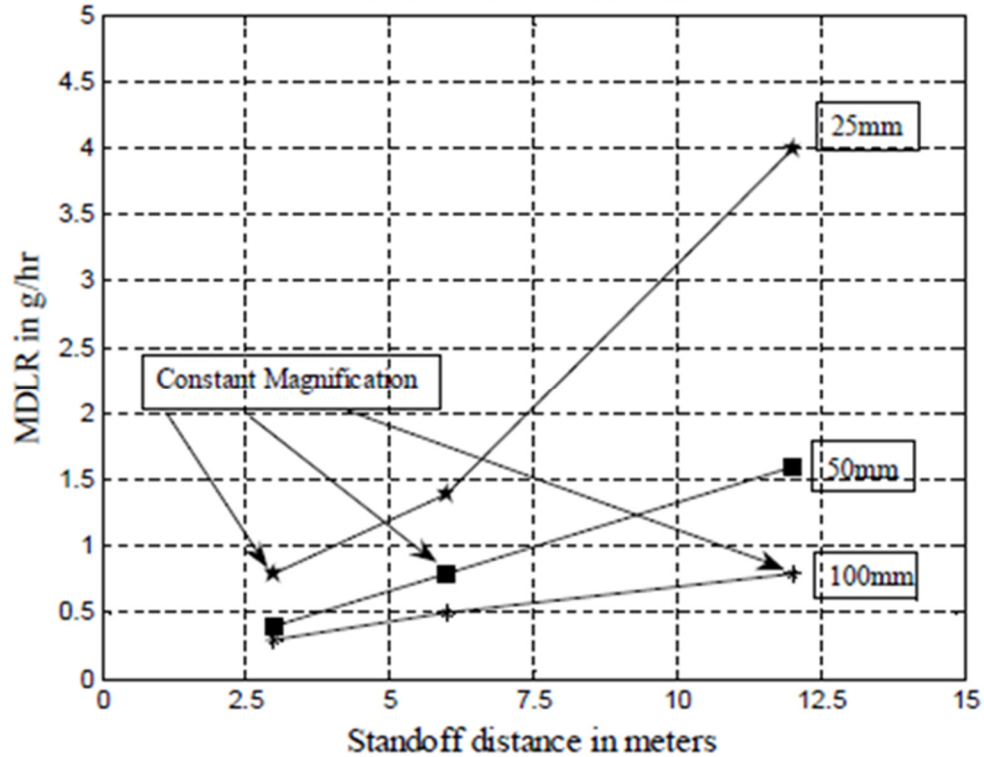
Figure 3-4. MDLRs Versus Standoff Distance for Three Lenses[5]

Table 3-3. Summary of Controlled Laboratory Testing Minimum Detection Limits (g/hr) at Various Wind Speeds[74]

OGI Camera	Sherlock			GasFindIR		
Compound	0 mph	2 mph	5 mph	0 mph	2 mph	5 mph
Benzene	34.72	>66*	ND	>70.1*	>70.1*	>70.1*
Ethylbenzene	20.6	48.9	ND	7.6	53.2	>75.9*
Heptane	13.55	28.8	>51.4*	3	21	48
Hexane	4.4	18.25	52.1	2.9	37.6	57.8
Isoprene	28.8	>51.4*	ND	32.8	59.6	>59.6*
Methanol	23.5	55.4	>153.9*	16.7	41.7	69.3
MEK	32.15	61.1	ND	5.3	60	>70.5*
MIBK	11.1	60.4	ND	7.01	24.6	70.1
Octane	11.1	31.7	ND	4.36	18.7	62.2
Pentane	Not tested	Not tested	Not tested	13.8	25.4	45.8
1-Pentene	9.85	>25.2*	ND	14	30.9	47.7
Toluene	34.3	>65.2*	ND	22.6	>75.3*	>75.3*
Xylene	30.75	64.9	ND	15.1	52.8	>75.3*

* The values in this table with a greater than sign indicate where the gas was imaged at a leak rate above that which the laboratory design was to quantify. This represents that the gas is able to be detected, but the MDLR could not be determined using the available equipment. ND = Not Detected.

Table 3-4. Summary of Controlled Laboratory Minimum Detection Limits (g/hr) for Pure Gases at Various Wind Speeds[74]

OGI Camera	Sherlock			GasFindIR		
Compound	0 mph	2 mph	5 mph	0 mph	2 mph	5 mph
Butane	Not tested	2.85	24.25	0.72	5.8	15.9
Ethane	Not tested	22.5	41.2	0.97	5.2	17.8
Methane	Not tested	32	80	3.96	20.8	49
Propane	Not tested	7.14	29.1	0.76	9.8	19.1
Ethylene	Not tested	Not tested	Not tested	13.9	53.7	104
Propylene	Not tested	Not tested	Not tested	4.37	15.6	59.8

Table 3-5. Summary of Controlled Laboratory Minimum Detection Limits (g/hr) for Gases Diluted with N_2 at Various Wind Speeds[74]

OGI Camera	Sherlock			GasFindIR		
Compound	0 mph	2 mph	5 mph	0 mph	2 mph	5 mph
Butane	Not tested	12.8	24.25	7.9	15.9	21.6
Ethane	Not tested	37.5	63.7	5.94	14.5	20.4
Methane	Not tested	68	159	19.8	45.6	65.4
Propane	Not tested	27.5	53.9	7.08	16.3	21.8
Ethylene	Not tested	Not tested	Not tested	90.1	>90.1*	>90.1*
Propylene	Not tested	Not tested	Not tested	24.7	47	62.4

* The values in this table with a greater than sign indicate where the gas was imaged at a leak rate above that which the laboratory design was to quantify. This represents that the gas is able to be detected, but the MDLR could not be determined using the available equipment.

FLIR developed a second generation GasFindIR and submitted this OGI technology update for testing later that same year on the same experimental apparatus at the Naperville, IL facility. The second generation FLIR GasFindIR camera achieved lower MDLRs for all gases tested and even challenged the lower release rate capabilities of the experimental apparatus. A summary of the MDLR values for the second generation FLIR GasFindIR is presented in Tables 3-6 and 3-7 for all gases and conditions tested. The values in Tables 3-6 and 3-7 for 0 mph wind speed conditions and pure gas are currently used by FLIR to describe the gas detection limits of their next generation GasFindIR OGI camera, the FLIR GF320.[33]

In a report prepared for FLIR on both GasFindIR studies, Panek[75] confirmed the conclusions resulting from the study conducted earlier that year, and reiterated that:

- The focal length of the lens did impact the detection capability of the camera;

- The temperature of the gas relative to that of the background (the ΔT) can potentially have large impacts on the MDLR for this OGI technology; and,

- The uniformity of the background does influence the MDLR for this OGI technology.

The report by Panek[75] reintroduced the importance of temperature differences and thermal tuning when operating OGI technology.[75]

Tables 3-6 and 3-7. MDLRs for Pure Compounds at Different Wind Speeds and Gas Mixtures at Different Wind Speeds[5,75]

MDLR's in Grams/Hr	Wind Speed in MPH		
Compound	0	2	5
Benzene	3.5	17.5	38.6
Ethanol	0.7	3.5	14
Ethylbenzene	1.5	7.6	17.5
Heptane	1.8	4.8	8.4
Hexane	1.7	3.5	8.7
Isoprene	8.1	14.3	38.8
Methanol	3.8	7.3	24.3
MEK	3.5	17.7	31.8
MIBK	2.1	4.9	13.3
Octane	1.2	3.4	8.7
Pentane	3.0	6.1	17.7
1-Pentene	5.6	19.7	43.8
Toluene	3.8	5.3	14.3
Xylene	1.9	9.1	18.9

MDLR's in Grams/HR	Wind Speed MPH					
Gases, Pure & †N$_2$ Mixture	0		2		5	
	P	N$_2$	P	N$_2$	P	N$_2$
Butane	0.4	6.5	1.5	7.3	4.2	13
Ethane	0.6	4.8	1.9	6.3	3.5	10
Methane	0.8	3.4	2.0	6.4	6.0	11
Propane	0.4	3.3	1.3	7.1	1.3	9.3
Ethylene	4.4	31	7.3	52	14	84
Propylene	2.9	14	8.9	30	16	35

†N$_2$ mixture flow rates were typically 3liters/minute.

* It is assumed that the cement board background was used (instead of the metal cylinder background) for this part of the study because the authors did not specify the exact background used.

* A hot nitrogen gas stream was flowed through a custom organic vapor generator system in order to generate the gases for the compounds listed in the table on the left, which are normally liquid at room temperature. To make direct comparisons between these MDLRs and those of the compounds from the table on the right (species that are gases at room temperature), the pure gases from the table on the right were diluted with nitrogen at a flow rate similar to that used for the vapor generator (about 3 L/min).

3. ETV Minimum Detection Limit Study

The EPA Environmental Technology Verification program conducted OGI technology verification studies on the second generation FLIR GasFindIR and the GIT (formerly PAT) Sherlock® VOC cameras in both laboratory (Naperville, IL facility) and field conditions in 2008. For the ETV MDL study, gaseous compounds were released from a 1 inch outlet valve under carefully controlled laboratory conditions for each of the compounds listed in Table 3-8 using the same Naperville, IL experimental apparatus discussed above. Three observers were used to confirm OGI camera detection. Starting at release rates in g/hr resulting from the Panek[74,75] and Benson[5] studies previously discussed as the limit of detection for each compound, the mass rate

was incrementally decreased if all three observers identified the leak. Once a leak rate that was not identifiable by all three observers was reached, the release rate was then increased until all three observers could again identify the leak with the OGI camera. This procedure was repeated under different test conditions, such as: stand-off distance, wind speed, and background material as performed initially during the TCEQ study. The minimum and maximum MDLs presented in Table 3-8 represent the range of MDLs measured over all test conditions.[10,11]

The ETV study also compared relative OGI camera agreement with an approved Method 21 monitoring device during laboratory testing. Once a detection level using the OGI camera was found for each test condition, gas concentrations were measured according to Method 21 using a PID and a leak definition concentration of 500 ppmv. For situations where the OGI camera MDL was above the highest reliable flow rate of the chemical delivery system, the OGI camera was noted as not being able to detect the compound under the specific test conditions. Similarly, if the Method 21 monitoring device produced a response equal to zero, then the monitoring device was considered unable to detect the chemical gas leak under the specific test conditions.[10,11]

If both the OGI camera and the Method 21 monitoring device proved capable of detecting the gas leak, then both units were considered to have agreed under the specific test conditions. Likewise, if either unit proved incapable of detecting the gas leak under the specified test conditions, then the units were considered to have disagreed. The relative agreement between OGI camera leak detection and a Method 21 acceptable monitoring device is listed by camera for each chemical compound tested in Table 3-8. Percent agreement was calculated where A was the number of tests that both units agree and T was the total number of tests in:

$$Percent\ Agreement = \left(\frac{A}{T}\right) \times 100$$

Table 3-8. Summary of MDLs and % Agreement with a M21 Monitoring Device during Lab Testing[10,11]

FLIR GasFindIR™ MW Camera				
Compound	**Method Detection Limit (g/hr)**		**Agreement with Method 21 Device**	
	Minimum	**Maximum**	**Total No. of Tests Performed**	**Percent Agreement**
1,3-butadiene	1.3	2.7	4	100%
Acetic acid	≤ 0.02	≤ 4.6 (b), (c)	11	100%
Acrylic acid	0.92	1.2	4	100%
Benzene	0.35	35 (c)	12	100%
Methylene chloride	4.9	> 70 (c)	No data (d)	
Ethylene	0.35	278 (c)	8	100%
Methanol	0.28	22 (c)	No data (d)	
Pentane	≤ 0.28	28 (c)	16	100%
Propane	≤ 0.44	13 (c)	No data (d)	
Styrene	0.35	0.70	3	100%
Sherlock® VOC				
Compound	**Method Detection Limit (g/hr)**		**Agreement with Method 21 Device**	
	Minimum	**Maximum**	**Total No. of Tests Performed**	**Percent Agreement**
1,3-butadiene	8.0	27	4	100%
Acetic acid	1.7	81	11	100%
Acrylic acid	0.92	7.4	4	100%
Benzene	3.2	≥ 70 (b), (c)	10	40%
Methylene chloride	≥ 70 (b)	≥ 70 (b)	No data (d)	
Ethylene	3.3	≥ 278 (b)	6	33%
Methanol	2.1	≥ 69 (c)	No data (d)	
Pentane	0.83	≥ 55 (b), (c)	12	75%
Propane	0.88	235 (b)	No data (d)	
Styrene	15	25	4	100%

(a) Minimum and maximum method detection limits were measured at a 0-mph wind speed unless otherwise noted.
(b) Measured at a 2.5-mph wind speed.
(c) Measured at a 5-mph wind speed.
(d) Percent agreement was not evaluated for methylene chloride, methanol, and propane because these compounds have an ionization potential greater than the energy that could be supplied by the Industrial Scientific IBRID MX6 with PID sensor.

The ETV assessment tests did find these same operational results for both cameras:

- Increased stand-off distance led to increased MDLs
- Increased wind speed led to increased MDLs
- The units were both easy to set up and ready to deploy in 10 minutes.

However, the GasFindIR™ MW was significantly lighter in weight (4.6 pounds (lbs)) versus the Sherlock® VOC (19 lbs), and optional lenses that are interchangeable with the GasFindIR™ MW offset the increase in MDL with distance from target. The Sherlock® VOC does not have this capability.

4. Attempts at Calibration and Performance Verification

Challenges to acceptance of OGI technology as a standalone technique for LDAR surveys include a lack of detailed information on standardized procedures to be followed, requirements for formal training of OGI technology operators, and conditions under which LDAR surveys with OGI technology should be performed.[68] Calibration verification is a quality assurance procedure typically implemented through prescriptive methods and/or standard operating procedures that objectively measures the performance of OGI technology prior to field deployment to ensure data of known quality. Calibration equipment and techniques are currently being discussed and refined, but in general include: the detection of a reference cell as compared to a cell filled with gas (see Figures 3-5 and 3-6) or an added calibration component to be attached to the OGI camera.

In the first calibration option, shown in Figure 3-5, a chambered vessel is filled with different gases of known concentrations and mounted onto the lens of the OGI camera. A video overlay allows the user to adjust camera settings to align the gain and level amounts to match with the desired gas at the desired concentration allowing the camera to be calibrated.[6]
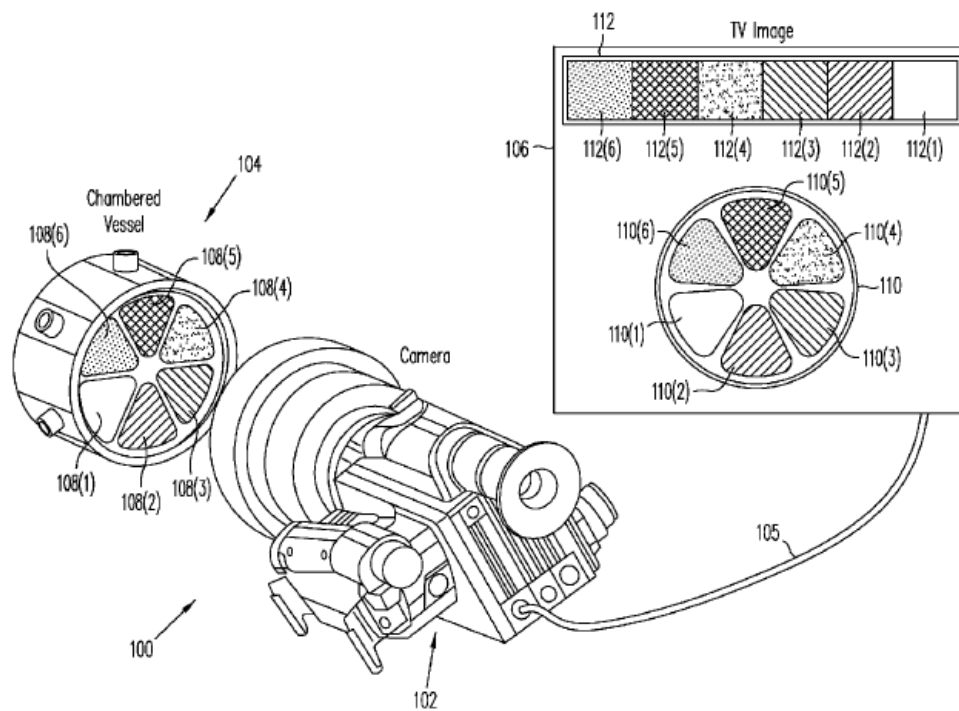
Figure 3-5. Calibration Chambered Vessel[6]

Alternatively, the raw pixel intensity from the OGI camera's detector can be used in a laboratory set up (shown in Figure 3-6) developed with a gas cell and a reference cell against a temperature controlled background. In this pixel intensity approach, the OGI camera images are processed with a pixel intensity analyzer (PIA)—or software algorithm that gathers and evaluates the raw pixel data from the detector—and are used to construct a quality control chart that defines the quality control criteria.[131] The following paragraphs discuss this calibration verification concept further; the use of a PIA to develop a quantitative OGI method will be discussed later in this document.

Using the set up illustrated in Figure 3-6, researchers[131] were able to develop theoretical relationships between the difference in pixel intensity measurements between the gas cell and the reference cell (ΔI) and the difference between the gas cell temperature and the background board temperature. Using a gas cell filled with a known gas at a known concentration and varying the temperature of the background board, a calibration verification quality control chart, such as the one calculated in Figure 3-7, can be developed as part of a daily OGI calibration check routine, complete with bound compliance criteria windows.[131]
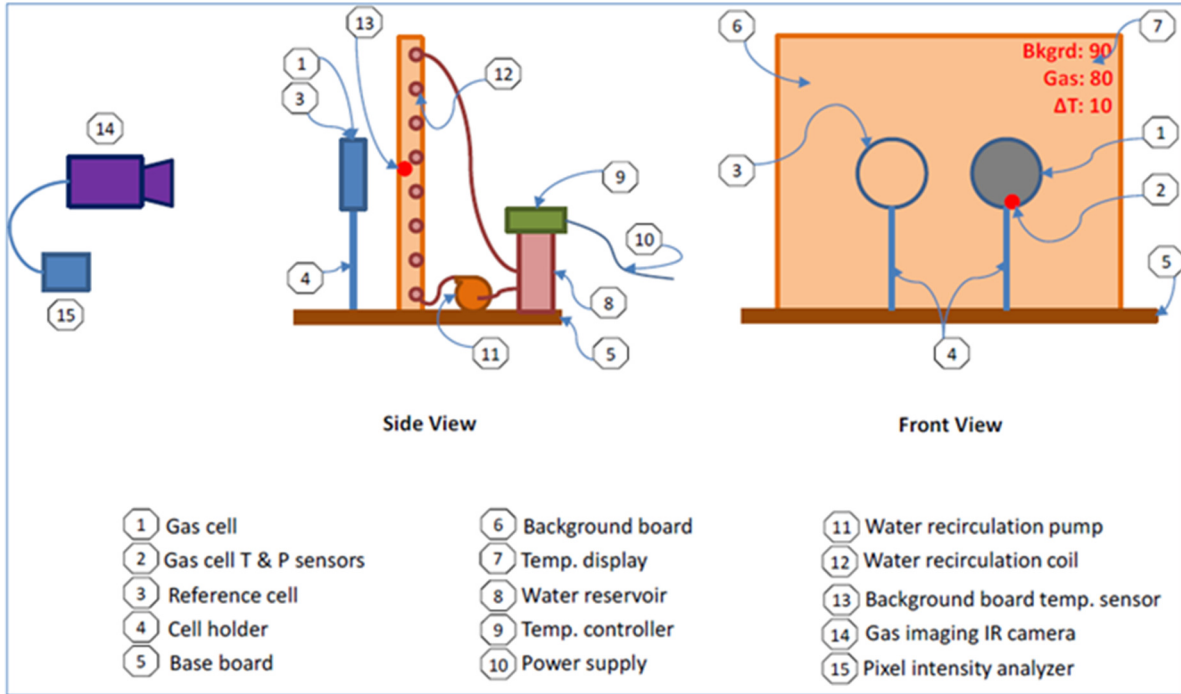
Figure 3-6. Gas Imaging IR Camera Verification and Calibration System[131]
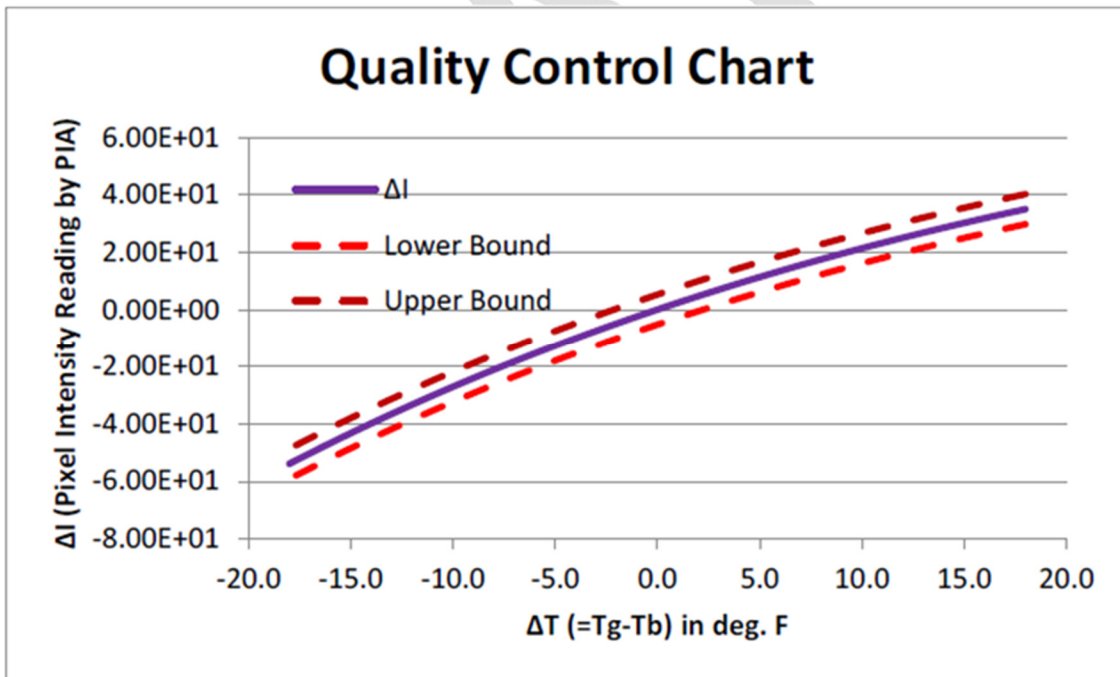
Figure 3-7. Quality Control Chart for IR Camera Daily Check[131]

Repeating this experiment with many different gases at many different concentrations yields a library of response clusters, such as the one in Figure 3-8. Therefore, being able to know the temperature difference (ΔT) between the target gas and the background—and if imaging a pure component or a specific mixture of components for which a cluster has been developed—allows the operator to determine the concentration-path length. For example, if the ΔT was 9°C (as

shown in Figure 3-8 with a dotted blue vertical line), then the camera operator should be able to determine the concentration-path length using a plot of the ΔI of the target plume and the background as demonstrated in Figure 3-9.[131]
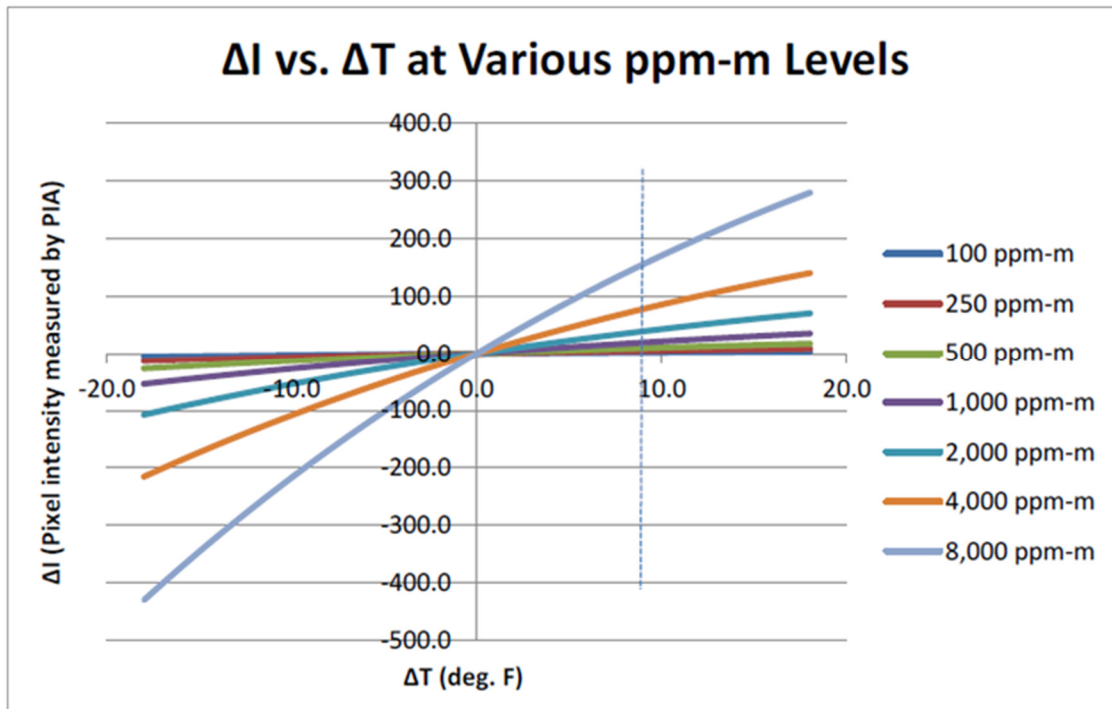
Figure 3-8. Example of a Cluster of ΔI vs. ΔT Curves for Different PPM-M Levels of Benzene[131]
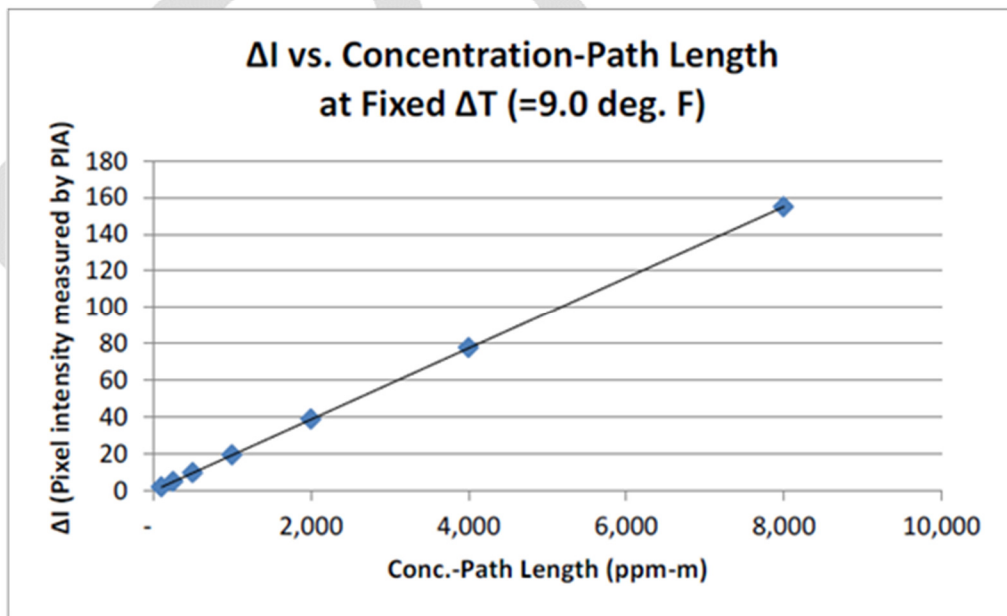
Figure 3-9. Example of a ΔI vs. Concentration-Path Length Curve[131]

A Benson et al. study[7] from 2008, which looked for camera signal intensity with gas reference cells (set up is shown in Figure 3-10), used the change in signal intensity (Figure 3-11) to develop OGI camera sensitivity functions. Plotting the amount of signal attenuation versus concentration in Figure 3-12 showed a way to predict OGI camera minimum detectable leak rates, and also illustrated the effect of maximum optical attenuation, the phenomenon by which an increase in gas concentration will no longer result in a larger signal because the optical signal has reached maximum attenuation. This is illustrated in Figure 3-12 as the point where the signal-to-noise ratio (S/N Ratio) begins to level off.
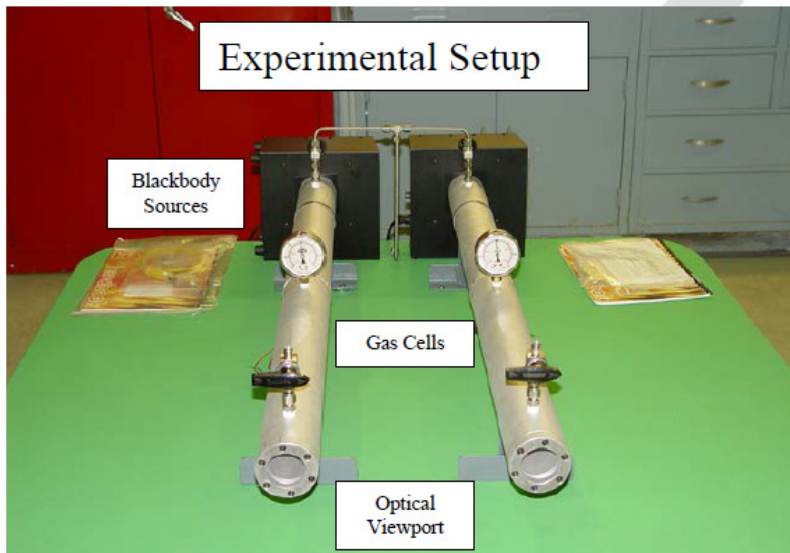
Figure 3-10. Experimental Set Up of Gas Cells with Controlled Blackbody Sources[7]
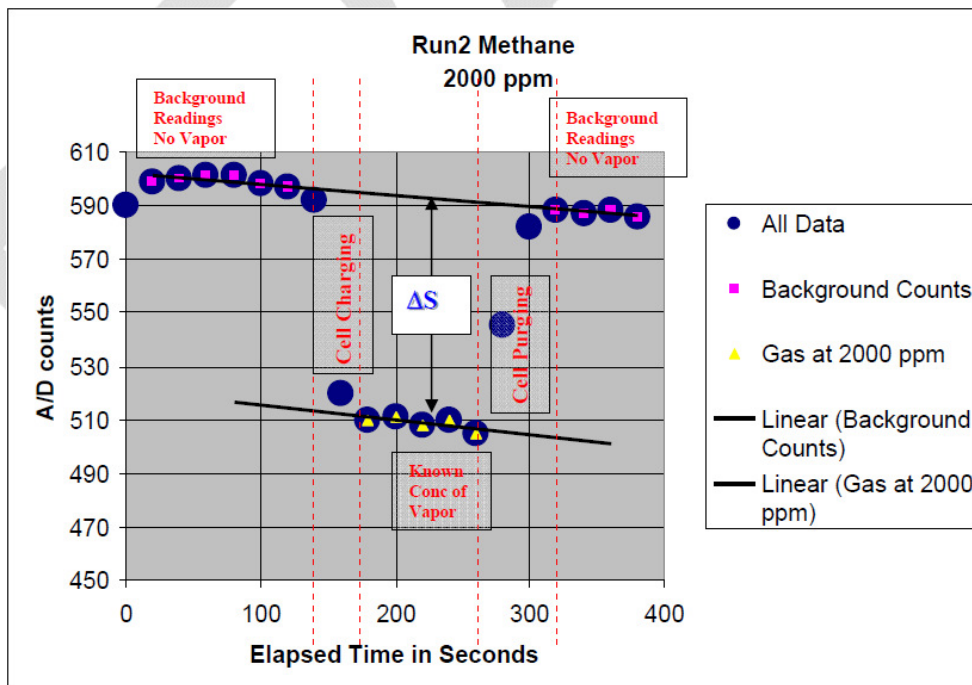
Figure 3-11. Measurement of the Signal Attenuation from 2,000 ppm of Methane[7]
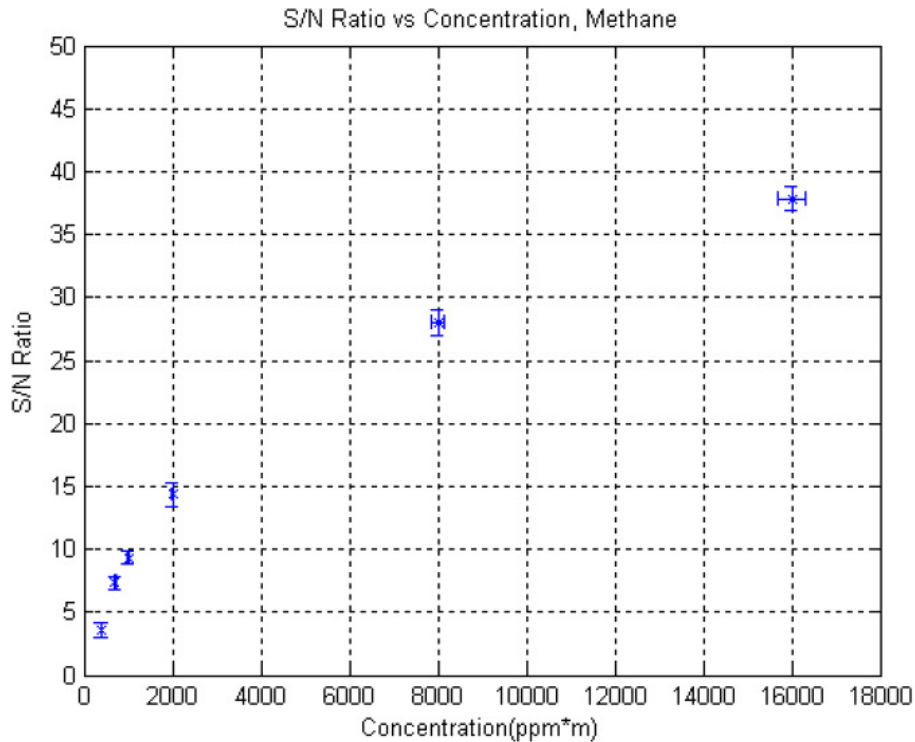
Figure 3-12. Signal Attenuation vs. Gas Concentration[7]

Recently, Sandsten et al. took this concept a step further and defined the noise equivalent concentration length (NECL) derived from OGI camera gas absorption curves as a promising metric for establishing OGI camera performance.[88] Similar to the way in which the noise equivalent temperature difference (NETD) is used to characterize the performance of thermometric instruments by defining the smallest amount of temperature difference that can be definitively measured above noise levels (like the limit of detection in analytical chemistry), the NECL describes the performance limitations for OGI cameras in terms of the lowest ppm•m that can be detected above the baseline noise. As a measure of the sensitivity of an OGI camera to a specific gas, the NECL value depends on ΔT, the concentration of the target gas, and the depth of the gas plume along the optical axis of the OGI camera. Their studies, presented in 2015, used a similar design to those mentioned above where a test cell of specified gas concentration (at ambient temperature) is placed between the OGI camera and a blackbody background able to maintain a stable temperature at 30°C (about 10°C above ambient), as illustrated in Figure 3-13. The gas concentration is varied by pre-filling gas cuvettes with different gas concentrations and placing them inside the holder (small white box in Figure 3-13) located 1.0 m away from the lens of the OGI camera.
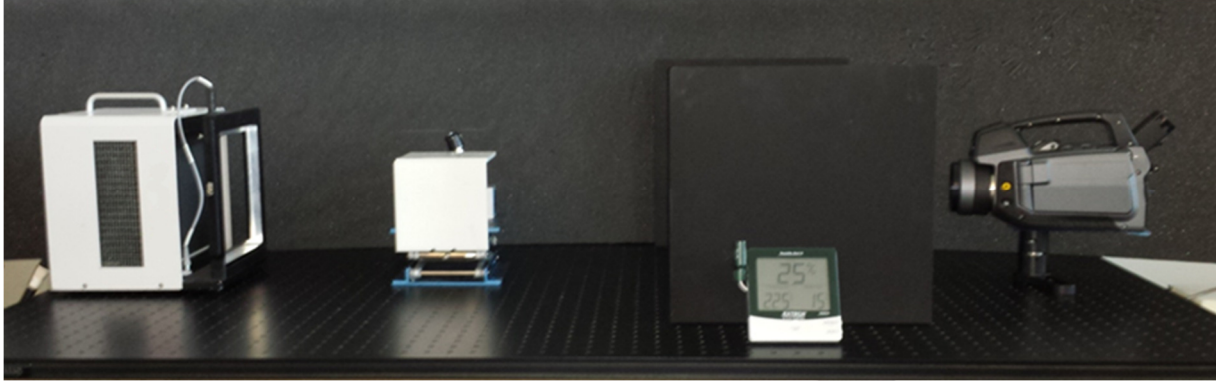
Figure 3-13. NECL Measurement Set Up[88]

A proxy measurement of the signal intensity is recorded from the set up in Figure 3-13 as apparent temperature of the black body background through the test gas and plotted over the path-integrated concentration length (CL, in ppm•m) in Figure 3-14. During these measurements, the ΔT was recorded by monitoring the temperature difference between the black body radiator and the test gas.
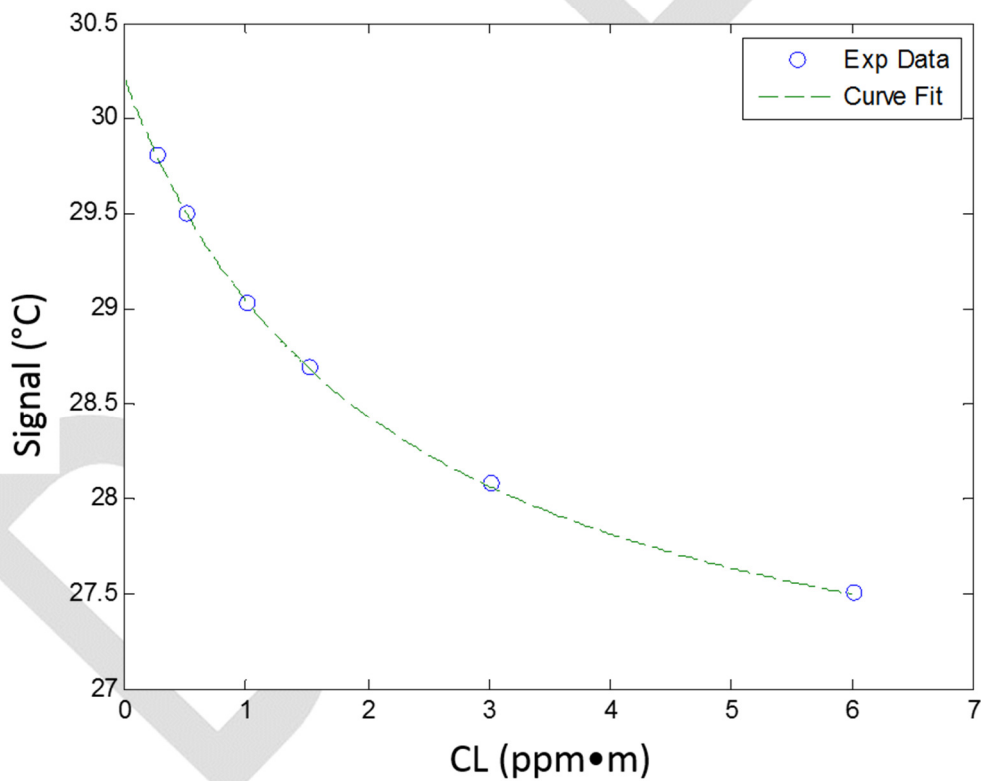
Figure 3-14. Signal Intensity as a Function of CL[88]

By developing a derivation of the Beer-Lambert law to integrate the signal over the OGI cameras spectral range of operation, Sandsten et al. calculated a line of best fit (green dashed line in Figure 3-14) through the experimental data obtained during their study (blue circles in Figure 3-

14) and extrapolated the line function to CL = 0 to find the NECL. The fit-function of the line in Figure 3-14 can be described by the following relationship:

$$S(CL, T) \propto \frac{A}{B + CL}$$

Where the radiative signal (*S*) for a given ΔT (*T*) and *CL* received by the OGI camera through a plume of pollutant are proportional to line fit factors *A* and *B* and the *CL*. In this way, Sandsten et al. determined the NECL of methane for the FLIR GF320 to be 13 ppm•m. Sandsten et al. verified this NECL result by simulating a theoretical value through calculations with spectral compound data from the HiTran database. These calculations are displayed in Table 3-9 where the empirical results are shown for different ΔT amounts with a measure of the instrumental error and the simulated results for comparison in parentheses.[88]

Table 3-9. Empirical Methane NECL Values for a FLIR GF320 OGI Camera[88]

CL (ppm•m)	ΔT = 2 °C	ΔT = 5 °C	ΔT = 10 °C
0	75 ± 4 (76)	28 ± 1 (28)	13 ± 1 (13)
10	76 ± 4 (77)	29 ± 1 (29)	13 ± 1 (13)
100	87 ± 4 (90)	33 ± 1 (34)	15 ± 1 (15)
1000	235 ± 3 (239)	88 ± 1 (90)	40 ± 1 (40)

In order to develop a standardized metric that objectively describes the performance of an OGI camera, Sandsten et al. proposed measurement conditions (highlighted in green in Table 3-9) that should remain constant so that the NECL results for multiple cameras of different types can be compared. These conditions are:

- ΔT = 10°C

- The OGI camera to be tested is set up 1.0 m from the gas cell

- After the line of best fit is optimized (through the A and B factors), the NECL is evaluated at a CL = 0 ppm•m.

Also, this metric can be applied to describing potential field performance. For example, a NECL of 13 ppm•m for methane with a gas plume that is 10 cm in optical depth translates to the OGI camera being technically capable of detecting the plume if it has a concentration greater than 130 ppm (13 ppm•m / 0.1 m). This limit of detection will increase, however, in a manner commiserate with field conditions at the time of detection (e.g., wind speed, leak exit velocity, background temperature and uniformity, distance from targeted equipment).

5. Studies to Compare OGI Technology to Method 21

Many studies have been conducted to evaluate the ability of OGI technology to perform comprehensive LDAR leak surveys and compare the results between OGI technology monitoring and Method 21 monitoring.

Robinson and Luke-Boone[84,85] performed a study that tested the capabilities of the active IR imaging BAGI camera at ethylene chemical plants and refineries. It was shown that the OGI camera was able to consistently detect unsaturated (gas feedstock has a higher percentage of olefinic—or unsaturated—chemical compounds) gas plant leaks at 20 g/hr or above as determined by bagging; however, a modified background (something to reflect the IR output, such as brightly reflecting Styrofoam) was needed to consistently image leaks at lower rates. The BAGI camera only missed 3 out of a total 27 leaks detected where all 3 of the missed leaks were measured to have a mass emission rate of 5 g/hr or less. However, it was observed during the surveys that multiple LDAR leak identification tags resulting from Method 21 surveys were actually misidentifications due to the lack of visual confirmation. Additionally, operators conducting LDAR surveys using Method 21 only were able to screen between 500 and 700 equipment components per day, whereas the OGI technology-assisted surveys increased that rate to 2,100 equipment components per hour. The study showed that the potential cost savings was outstanding based on the rate at which LDAR operators could perform the survey.[84]

The same screening rate inequality was found in a different study by Picard et al.[78] at a gas fractionation plant, where the implementation of OGI technology increased the screening speed nearly 10-fold.[78] For a two person team using Method 21, a rate of 240 components per hour was a reasonable pace. A two person team using OGI increases that rate to 2,300 components per hour.[81] Of the top 10 biggest leakers found during this study, operators only found 5 while using Method 21, but found 8 while using OGI technology (the other 2 leaks having sufficient mass emission rates to be detected by the camera, but were missed by the operator[f]). While the study emphasized the detection performance for the top 10 leaks, there was no comparison of performance over the entire size range of leaks. Additionally, this study found that as compared to Method 21, OGI technology had the following advantages and disadvantages.[78]

Advantages	**Disadvantages**
	Is not recommended for use during rain, fog, or in extreme cold. Also may not be as effective during overcast conditions.
Able to visualize difficult and hard-to-reach leak locations.	
Can clearly "see" the source of the leak.	Needs a knowledgeable operator.
Reduces equipment operator exposure to vapors.	Unable to quantify emissions.

---

f Operator sensitivity to contrast differences varies widely from person to person and depends on multiple factors such as pupil dilation. For more on the capabilities of the human eye, see Optical Modulation Transfer Functions of the Human Eye.[55]

During a study by Reese et al., 2006, it was determined that only two people were required for 2 days to do an OGI technology-assisted facility survey versus four people for 4 days using Method 21.[80] In this study, the authors allowed some leaks that were less than the regulation definition of 10,000 ppm to go unrepaired to evaluate the concern over the potential for leaks at lower mass emission rates to become bigger over time. These equipment leaks were re-surveyed three months after the initial Method 21 survey. Although some leak rates increased over that time, an equivalent amount of leaks decreased, resulting in no net change over time and resulting in the authors unable to find any correlation between leak rate and length of time.

Reese et al. reported that, during the last comparison survey conducted for this study, only one leak was detected with OGI technology and nine leaks were detected with Method 21 independently. In this example, although the Method 21 survey found more leaks, the maximum leak concentration detected by Method 21 was 5,817 ppm. In comparison, the one leak found by OGI technology measured 210,000 ppm; this was the largest leak of the study, and it was not detected via Method 21. Therefore, lower whole-facility emissions can result from the implementation of OGI technology-assisted leak surveys due to the greater probability of a large leak being detected with OGI versus Method 21 only. Reese et al.[80] reached this conclusion after observing that OGI consistently found the larger leaks, although some leaks were missed starting around 6,000 ppm (according to EPA Method 21 measurements) and less.[80] In the study, the authors applied the EPA correlation curves[106] to Method 21 screening values and the API leak/no-leak emission factors[2,3,59,60] to come up with whole facility emission rates of 9,099 pounds per year (lbs/yr) for Method 21 and 7,774 lbs/yr for OGI. This was a difference of about 15%, which was acceptable to the authors.[80] The study authors concluded that the use of OGI technology to assist LDAR surveys results in lower whole-facility emissions versus Method 21 alone and that the amount of emissions released by smaller leaks possibly missed by OGI technology-assisted surveys are offset by the faster identification (and repair) of larger leaks when surveys are conducted on a more frequent basis.

6. Studies Comparing OGI Technology to "Bagging" Techniques

While the fugitive emissions from individual equipment may be small, the large number of leaking equipment that can be found in typical refinery or petrochemical processing plants results in the total amount of emissions from this source category being about 50% of the total facility hydrocarbon emissions.[35] Developed in response to the 1997 API study,[1] which showed that a very small fraction of equipment leaks contribute a large majority of the controllable fugitive emissions, Smart LDAR programs target these larger leakers. OGI technology has the potential to assist LDAR programs by increasing the efficiency and cost effectiveness of leak detection surveys, but data on the applicability of OGI technology still needs to be collected in order to confirm the leak detection capabilities of this developing technology. The studies conducted by Furry et al., 2006[35] and Thoma, 2009[122] compared results between OGI technology and bagging techniques to add to the body of knowledge on OGI technology leak detection capabilities.

Furry et al., 2006 tried to validate the laboratory controlled minimum detection leak rates (MDLRs) for OGI technology previously developed by Panek et al.[74] and Benson et al.[5] by comparing these earlier published values with field data collected using Method 21 and bagging techniques from targeted chemical plant process unit areas.[35] The study team quantitatively

validated the OGI technology leak detections made in the field with a FLIR GasFindIR by obtaining a screening value for the leaks using a Method 21-approved PID/FID analyzer and "bagging" some of the leak emissions for laboratory gas concentration analysis and emission rate measurements. The results of this effort are illustrated in Table 3-10 where the MDLRs at various wind speeds determined from the Panek and Benson studies are compared to the results from the field study conducted for this effort.[35] The Panek and Benson results are discussed in detail in Section III.B.2 of this document, and it is worth noting that the range of MDLR values presented by Furry et al. in Table 3-10 for the Panek et al. study is for the first generation FLIR GasFindIR OGI camera. Therefore, evaluating Table 3-10 with respect to the range of MDLR values from the Benson et al. study, which were conducted on the second generation FLIR GasFindIR OGI camera, may be more useful, although it is unknown which generation FLIR GasFindIR OGI camera was used for conducting the field tests.

Table 3-10. Comparison of Field-Derived Values to Published Laboratory Detection Limits (g/hr)[35]

Chemical	Field Test	Panek et al., 2006[74]	Benson et al., 2006[5]
Methane	3.7	3.96 – 49	0.8 – 11
Propane	4.7	0.76 – 19.1	0.4 – 9.3
Butane	10.6	0.72 – 15.9	0.4 – 13
Propylene	23.8	4.37 – 59.8	2.9 – 35
Toluene	50.2	22.6 – 75.3	3.8 – 14.3
Xylene	17.8	15.1 – 75.3	1.9 – 18.9

In Furry's study, the monitoring team was able to screen at a rate of 3,600 components per hour and were able to confirm the applicability of lab-derived detection limits as predictive values for field operation. This study also showed that leaks were successfully detected against many different backgrounds representing various reflectivities, as long as there was a sufficient ΔT. It is worthwhile to note that wind speed, optical resolution, plume motion, and viewing angle are all parameters that will influence detection sensitivity, and so the comparison between the field-derived detection limits and the MDLRs determined under ideal laboratory conditions are expected to be different.[35] However, evaluating the field-derived MDLRs with respect to both published MDLR ranges in Table 3-10 shows that the laboratory results are able to provide predictive performance ranges for field applications of OGI technology.

In 2008, multiple interested parties collaborated on a study investigating fugitive emissions from petrochemical barges using OTM-10, OGI technology, and "bagging" techniques.[122] The activities included using the LSI Hawk (FLIR GasFindIR) to image barges from a helicopter, from the ground standing on the edge of the lock as vessels passed through channel locks, and from the ground on the barges themselves. The "bagging" technique was used to quantify emission rates visualized from the aerial survey, and OTM-10 with OP-FTIR was used to quantify emission rates from barge vessels as they moved through the channel locks. The following general conclusions were made from this study:[122]

- Aerial IR images from OGI technology identified barges, and even barge equipment, with big leaks, whereas ground-based and onboard IR images from OGI technology detected leaks at lower emission rates in addition to the larger leaks.

- OGI IR equipment was found to be robust, easy-to-use, and possessing sufficient detection sensitivity for all applications in this study.

- OGI technology detection was easier to perform during mid-day to late afternoon time periods because of more favorable background conditions during those hours. The higher sun position during those hours heated the background scenery (the barges) to effectively raise the ΔT while also reducing the interference caused by shadows.

- Onboard OGI technology detection was less sensitive to ambient conditions as compared to aerial observations.

- OGI technology measurements were able to detect leaks from barges in the lock that ranged from 169 to 12,204 g/hr alkane mixture as measured by OTM-10.

- Aerial images were identifying leaks that were quantified by bagging as being in the range of 252 to 20,772 g/hr for individual components, relating to total barge leak rates of 4,068 to 22,464 g/hr.

- In all, there were seven instances where leaks were detected from passing barges in the lock by OGI technology, but the plumes never crossed the optical path of the OTM-10, thereby missing the leak quantification via OTM-10.

C. Conclusion

Two commercially-viable cameras are on the market today and available for leak detection work: the FLIR GF320 and the Opgal EyeCGas provided by Guardian Compliance. These two units are extremely similar and operate based on the same passive IR OGI technology imaging principles. There are several key differences in the design and functionality of the camera systems (as shown in Table 3-11), including the type of FPA detector used and the ability to measure temperature as well as image the gas. In addition to the differences noted below, the EyeCGas is intrinsically safe whereas the GF320 is not.

Table 3-11. Comparison Between FLIR GF320 and Opgal EyeCGas Specifications[33,73]

Specification	FLIR GF320	Opgal EyeCGas
Field-of-View/minimum focus distance	24° x 18° / 0.3 m (1.0 ft)	18.2° x 13.6° / 0.5 m (1.6 ft)
Lens F-number	1.5	1.1
Thermal Sensitivity/NETD	<15 millikelvin @ 30°C	<12 millikelvin @ 25°C

Table 3-11. Comparison Between FLIR GF320 and Opgal EyeCGas Specifications[33,73]

Specification	FLIR GF320	Opgal EyeCGas
Focus Modes	Auto or manual	Manual
Zoom	1-8x continuous, digital	2x, 4x, digital
Focal Plane Array	InSb (3.2 – 3.4 µm)	HgCdTe (3 – 4 µm)
Spectral Filter	3.2 – 3.4 µm cold bandpass	3.2 – 3.4 µm hot bandpass
IR Resolution	320 x 240 pixels	320 x 240 pixels
Sensor Cooling Stirling Microcooler	FLIR MC-3	Ricor K563
Full Frame Rate	60 Hz	30 Hz
Display	Built-in, 4.3" LCD, 800 x 480 pixels	Built-in, 3.5" LCD, 640 x 480 pixels
Viewfinder	Built-in, 800 x 480 pixels	None
Automatic image adjustment	Continuous/manual; linear or histogram based	Automatic. Manual for Enhanced Mode adjustment
Manual image adjustment	Level/span	Enhanced Mode (depth/background)
Image modes	IR-image, visual image, High Sensitivity Mode (HSM)	IR-image, visual image, Enhanced Mode (Enh)
Temperature measurement range	-40 to +350°C	None (does not perform temperature measurements)
Temperature measurement accuracy	± 1°C for temp range 0 to 100°C, or ±2% of reading for temp range >+100°C	None (does not perform temperature measurements)
Meta data recording	GPS	Audio via Head Set
Video output	Removable SD (plus other connections) Visual image can be associated with video recording	SD not removable (USB connection) Visual image can be recorded in the same footage with the IR video image
Battery operating time	> 3 hrs @ 25 °C, typical use	> 4 hrs @ 25°C, typical use
Start-up time	< 5 min @ 25°C	< 8 min @ 25°C
Operating temperature range	-20 to +50°C	-20 to +50°C

Table 3-11. Comparison Between FLIR GF320 and Opgal EyeCGas Specifications[33,73]

Specification	FLIR GF320	Opgal EyeCGas
Weight incl. lens and battery	2.48 kg (5.47 lbs)	2.68 kg (5.9 lbs)
Size incl. lens (LxWxH)	12.0 x 6.7 x 6.3 in.	9 x 5.1 x 4.3 in.
Accessory lenses (mid-wave band)	24°, f = 23 mm 14.5°, f = 38 mm 6°, f = 92 mm	18.2°, f = 30 mm 7.3°, f = 75mm

Table 3-12 presents the MDLRs claimed by the manufacturer for the FLIR GF320 as reported by Panek for the FLIR GF320 predecessor, the second generation FLIR GasFindIR.[75] There have not been any MDLR studies performed on the EyeCGas to date. Given the lack of studies involving the EyeCGas and, as a result, the lack of information available on its performance, it seems worthwhile to include the EyeCGas camera in future studies for model performance inter-comparisons, such as the laboratory studies described in Section IV of this document.

Table 3-12. Minimum Detected Leak Rates (MDLRs) for the FLIR GF320 per manufacturer[33]

Gas	MDLR (g/hr)	Gas	MDLR (g/hr)	Gas	MDLR (g/hr)
1-Pentene	5.6	Heptane	1.8	Octane	1.2
Benzene	3.5	Hexane	1.7	Pentane	3.0
Butane	0.4	Isoprene	8.1	Propane	0.4
Ethane	0.6	MEK	3.5	Propylene	2.9
Ethanol	0.7	Methane	0.8	Toluene	3.8
Ethylbenzene	1.5	Methanol	3.8	Xylene	1.9
Ethylene	4.4	MIBK	2.1		

* MDLR values for zero wind conditions from report by Panek, 2005.[75]

D. References and Reviewed Literature

1. American Petroleum Institute (API). 1997. Analysis of Refinery Screening Data. API Publication 310, Washington, DC.

2. American Petroleum Institute (API). 2004. Evaluation of Emissions Quantification Methods for Leak Detection and Repair (LDAR) Programs Using Optical Imaging Techniques. Discussion paper revised as of April 19, 2004.

3. American Petroleum Institute (API). 2004. Smart Leak Detection and Repair (LDAR) for Control of Fugitive Emissions. Washington, DC.

4. Bell, R.J. 1972. Introductory Fourier Transform Spectroscopy. Academic Press, New York, New York, USA.

5. Benson, R., R. Madding, R. Lucier, J. Lyons, and P. Czerepuszko. 2006. Standoff Passive Optical Leak Detection of Volatile Organic Compounds using a Cooled InSb Based Infrared Imager. AWMA 99th Annual Meeting, New Orleans, LA, (June).

6. Benson, R.G., and P.A. Czerepuszko. 2010. Infrared Camera Calibration Systems and Methods. US Patent # 7679046 B1, issued March 16, 2010.

7. Benson, R.G., J.A. Panek, and P. Drayton. 2008. Direct Measurements of Minimum Detectable Vapor Concentrations Using Passive Infrared Optical Imaging Systems. Proceedings of the 101st Annual Conference and Exposition (ACE) meeting of the AWMA, Paper 1025.

8. Benson, R.G., T.J. Scanlon, and P.A. Czerepuszko. 2008. Thermography Camera Configured for Leak Detection. US Patent # US2008/0231719 A1.

9. Bertin Technologies. 2012. Second Sight TC. Vendor data sheet available at www.secondsight-gasdetection.com.

10. Boczek, B., A. Dindal, and J. McKernan. 2010. FLIR Systems GasFindIR[TM] Midwave (MW) Camera. Environmental Technology Verification Report prepared by Battelle for the ETV Advanced Monitoring Systems Center.

11. Boczek, B., A. Dindal, and J. McKernan. 2010. Gas Imaging Technology, LLC Sherlock® VOC Camera. Environmental Technology Verification Report prepared by Battelle for the ETV Advanced Monitoring Systems Center.

12. Bruno, R.P. 1992. Tracking Gas Leaks With Active IR Scanning. Photonics Spectra, (February).

13. Bullock, Adam. 2009. TCEQ and Thermal Imaging Technology. Presented at FLIR Petrotherm 2009 Conference (February 24-25).

14. Bylin, C. 2008. Methane to Markets Overview – Oil & Gas Sector. Presented at the Methane to Markets and Natural Gas STAR Technology Transfer Workshop on Methane Emission in the Petroleum and Gas Sector, Buenos Aires, Argentina (November 5-6).

15. Carter, R.E, Jr., D.D. Lane, G.A. Marotz, M.J. Thomas, and J.L. Hudson. 1992. VOC Emission Rate Estimation from FTIR Measurements and Meteorological Data. Proceedings of the 1992 U.S. EPA/A&WMS International Symposium on the Measurement of Toxic and Related Air Pollutants (VIP-25), Air & Waste Management Association, Pittsburgh, PA, pp. 601 – 606.

16. Chakraborty, A.B. 2011. ONGC Experiences with Methane Leak Detection and Measurement Studies. Presented at the Global Methane Initiative Partnership-Wide Meeting, Krakow, Poland (October 12-14).

17. Clearstone Engineering, Ltd. 2002. Identification and Evaluation of Opportunities to Reduce Methane Losses at Four Gas Processing Plants. Technical report to the Gas Technology Institute and the U.S. EPA. June 20, 2002. Available from the U.S. EPA at http://www.epa.gov/gasstar/tools/related.html.

18. Clearstone Engineering, Ltd, Innovative Environmental Solutions, Inc., and National Gas Machinery Laboratory. 2006. Cost-Effective Directed Inspection and Maintenance Control Opportunities at Five Gas Processing Plants and Upstream Gathering Compressor Stations and Well Sites. Technical Report: EPA Phase II Aggregate Site Report. March 2006. Available from the U.S. EPA at http://www.epa.gov/gasstar/tools/related.html.

19. Coffey, Tom. 2009. Alternative Applications for GasFindIR. Presented at the 3rd Annual PetroTherm Conference in League City, Texas (February).

20. Colorado Department of Public Health and Environment. 2014. Control of Ozone via Ozone Precursors and Control of Hydrocarbons via Oil and Gas Emissions (Emissions of Volatile Organic Compounds and Nitrogen Oxides). State of Colorado Air Quality Control Commission (AQCC) Regulation 7, 5 CCR 1001-9. Available at https://www.colorado.gov/pacific/cdphe/aqcc-regs.

21. Colorado Oil and Gas Association (COGA). 2014. Air Quality Regulation Fast Facts. A Fact Sheet available at www.coga.org.

22. Drago, J. 2010. Enhanced Leak Detection and Repair Programs for the Chemical Processing Industries. ChemInnovations, Houston, TX. (October 19-21).

23. Emissions Inventory Improvement Program, Volume II: Chapter 16, Methods for Estimating Air Emissions from Chemical Manufacturing Facilities, August 2007, Final, http://www.epa.gov/ttnchie1/eiip/techreport/volume02/index.html.

24. Environ. 2004. Development of Emissions Factors and/or Correlation Equations for Gas Leak Detection, and the Development of an EPA Protocol for the Use of a Gas-imaging Device as an Alternative or Supplement to Current Leak Detection and Evaluation Methods. Final Report to the Texas Council on Environmental Technology and the Texas Commission on Environmental Quality.

25. Fernandez, R. 2013. EPA's Natural Gas STAR Program Overview. Presented at Natural Gas STAR Production Technology Transfer Workshop, Philadelphia, PA (September 24).

26. FLIR Systems, Inc. 2012. Technical Data: FLIR GF320 24°. Data sheet available at www.flir.com.

27. FLIR Systems. 2007. Data sheet: ThermaCam GasFindIR Infrared Camera for Leak Detection and Repair. Data sheet available at www.flir.com.

28. FLIR Systems. 2007. Data sheet: ThermaCam GasFindIR LW Infrared Camera for Leak Detection and Repair. Data sheet available at www.flir.com.

29. FLIR Systems. 2008. Data sheet: ThermaCam GasFindIR CO Infrared Camera for Leak Detection and Repair. Data sheet available at www.flir.com.

30. FLIR Systems. 2008. Data sheet: ThermaCam GasFindIR HSX Infrared Camera for Leak Detection and Repair. Data sheet available at www.flir.com.

31. FLIR Systems. 2009. Data sheet: ThermaCam GasFindIR GF300 Infrared Camera for Leak Detection and Repair. Data sheet available at www.flir.com.

32. FLIR Systems. 2009. Gas Detection: The Professional Guide. FLIR Systems AB.

33. FLIR Systems. 2013. FLIR GF300/320 Infrared Cameras. http://www.flir.com/thermography/americas/us/view/?id=55671. Accessed January 28, 2013.

34. FLIR Systems. 2013. Optical Gas Imaging. http://www.flir.com/thermography/americas/us/view/?id=49558. Accessed March 25, 2013.

35. Furry, D.W., G. Harris, D. Ranum, E.P. Anderson, V.M. Carlstrom, W.A. Sadik, C.M. Shockley, J.H. Siegell, and G.M. White. 2006. Development of Instrument Detection Limits for Smart LDAR Application: Chemical Plant Testing. Exxon Mobile Corporation.

36. Gagnon, J-P., Z. Habte, J. George, V. Farley, P. Tremblay, M. Chamberland, J. Romano, and D. Rosario. 2010. Hyper-Cam automated calibration method for continuous hyperspectral imaging measurements. Active and Passive Signatures, Proceedings of SPIE, 7687.

37. Goers, U-B., T.J. Kulp, P.E. Powers, and T.G. McRae. 1999. A PPLN-OPO-based Backscatter Absorption Gas Imaging (BAGI) System and its Application to the Visualization of Fugitive Gas Emissions. Proceedings of SPIE, 3758, Application of Tunable Diode and Other Infrared Sources for Atmospheric Studies and Industrial Processing Monitoring II, Denver, CO, 172 – 179.

38. Heath, M.W. 2006. Leak Detection and Measurement of Fugitive Methane Emissions: An EPA Best Management Practice for DI&M Programs. Presented at the Natural Gas STAR Producers Technology Transfer Workshop, Midland, TX (June 8).

39. Heath, M.W. III. 2011. Heath Consultants' Overview of Infrared Optical and Laser Leak Detection Technologies in the Natural Gas Industry. Presented at the Global Methane Initiative Partnership-Wide Meeting, Krakow, Poland (October 12-14).

40. Hinnrichs, M. 1999. Imaging Spectrometer for Fugitive Gas Leak Detection. Proceedings of SPIE 3853, Environmental Monitoring and Remediation Technologies II, Boston, MA, (September) 152 – 161.

41. Hinnrichs, M. Email communication between M. Hinnichs and Tracey Footer, Eastern Research Group. Dated April 2, 2013.

42. Hinnrichs, M., and B. Piatek. 2003. Hand Held Hyperspectral Imager for Chemical/Biological and Environmental Applications. SPIE Photonics East (October).

43. Hinnrichs, M., and G.M. Morris. 1995. Image Multispectral Sensing. US Patent # 5479258.

44. Hinnrichs, M., and N. Gupta. 2007. Miniature Optical Imaging Sensor for Smart LDAR Detection and Quantification Using Diffractive Optical Lenslet Arrays. 100th Annual Conference of the Air and Waste Management Association.

45. Hinnrichs, M., and N. Gupta. 2008. Comparison of QWIP to HgCdTe Detectors for Gas Imaging. Infrared Technology and Applications XXXIV, Proceedings of SPIE, 6940.

46. Hinnrichs, M., and R. Hinnrichs. 2004. Gas Leak Detector. US Patent # 6680778 B2.

47. Hinnrichs, M., R. Schmehl, L. McCrigler, P. Burke, and A. Engberg. 2006. Infrared Gas Imaging and Quantification Camera for LDAR Applications. AWMA 99th Annual Meeting, New Orleans, LA, June.

48. Howard, J. and A. Bouchard. 2011. LDAR and Flare Regulatory Update. EPA National Flares and LDAR Workshop, (June 15, 2011).

49. ICF International. 2014. Economic Analysis of Methane Emission Reduction Opportunities in the U.S. Onshore Oil and Natural Gas Industries. Report prepared for the Environmental Defense Fund (EDF), New York, NY and available at https://www.edf.org/sites/default/files/methane_cost_curve_report.pdf.

50. IEC Infrared Systems. Photovoltaic Infrared Cameras vs. Microbolometer Infrared Cameras. http://www.iecinfrared.com/photovoltaic-versus-microbolometer-cameras.html. Accessed December 21, 2012.

51. Intergovernmental Panel on Climate Change (IPCC). 2014. Climate Change 2014: Synthesis Report. Contribution of Working Groups I, II, and III to the 5th Assessment Report of the IPCC [Core Writing Team: R.K. Pachauri and L.A. Meyer (eds.)]. IPCC, Geneva, Switzerland, 151 pp.

52. Kastek, M., T. Piatkowski, and H. Polakowski. 2011. Infrared imaging Fourier-transform spectrometer used for standoff gas detection. Air Pollution XIX in WIT Transactions on Ecology and the Environment, 147: 161-172.

53. Kastek, M., T. Piatkowski, R. Dulski, M. Chamberland, P. Lagueux, and V. Farley. 2012. Method of Gas Detection Applied to an Infrared Hyperspectral Sensor. Photonics Letters of Poland 01/2012.

54. Kastek, M., T. Piatkowski, R. Dulski, M. Chamberland, P. Lagueux, and V. Farley. Hyperspectral imaging infrared sensor used for chemical agent detection and identification. Poster presentation at the Symposium on Photonics and Optoelectronics (SOPO), Shanghai, China, 21-23 May 2012.

55. Koren, N. 2012. Introduction to Resolution and MTF Curves. Retrieved December 26, 2012 from http://www.normankoren.com/Tutorials/MTF.html.

56. Kroll, A., W. Baetz, and D. Peretzki. 2009. On Autonomous Detection of Pressured Air and Gas Leaks Using Passive-IR Thermography for Mobile Robot Application. IEEE International Conference on Robotics and Automation, Kobe, Japan, 921 – 926.

57. Kulp, T.J., P.E. Powers, and R. Kennedy. The Development of a Laser-Illuminated Infrared Imager for Natural Gas Leak Detection. Proceedings of the U.S. DOE Natural Gas Conference, Houston, TX, (March 24-27), paper 2.7.

58. Lagueux, P., M. Chamberland, F. Marcotte, A. Villemaire, M. Duval, J. Genest, and A. Carter. 2008. Performance of a Cryogenic Michelson Interferometer. Advanced Optical and Mechanical Technologies in Telescopes and Instrumentation, Proceedings of SPIE, 7018.

59. Lev-On, M., D. Epperson, J. Siegell, K. Ritter. 2007. Derivation of New Emission Factors for Quantification of Mass Emissions When Using Optical Gas Imaging for Detecting Leaks. Journal of the Air & Waste Management Association, 57(**9**): 1061-1070.

60. Lev-On, M., H. Taback, D. Epperson, J. Siegell, L. Gilmer, and K. Ritter. 2006. Methods for Quantification of mass Emissions from Leaking Process Equipment When Using Optical Imaging for Leak Detection. Environmental Progress, 25(**1**): 49 – 55.

61. Lewis, A.W., S.T.S. Yuen, and A.J.R. Smith. 2003. Detection of Gas Leakage from Landfills using Infrared Thermography – Applicability and Limitations. Waste Management & Research, 21: 436 – 447.

62. Loukeris, K. 2011. Air Toxic Enhanced Leak Detection and Repair Program. EPA National Flares and LDAR Workshop, (June).

63. Maillart, J.L., O. Soupault, P. Bernascolle, E. Soulie, P. Adam, and M.F. Benassy. 2007. Second Sight: Stand-Off Equipment for Chemical Gas Detection. Presented at the 9th CBW Protection Symposium, Gothenburg, Sweden, (May 22-25).

64. Mammen, C.H., and R.G. Benson. 2010. Thermography Camera Configured for Gas Leak Detection. US Patent # 7649174.

65. Marotz, G.A., D.D. Lane, R.E. Carter, Jr., M.J. Thomas, and J.L. Hudson. 1992. A Comparison of VOC Concentrations Assessed by Open-path FTIR and Canisters. Proceedings of the 1992 U.S. EPA/A&WMS International Symposium on the Measurement of Toxic and Related Air Pollutants (VIP-25), Air & Waste Management Association, Pittsburgh, PA, pp. 607 – 614.

66. McRae, T.G. 1999. GasVue VOC and SF_6 Leak Location Field Test Results. Proceedings of SPIE, 3853, Environmental Monitoring and Remediation Technologies II, Boston, MA, 196 – 212.

67. McRae, T.G., and L.L. Altpeter. 1995. Natural Gas Leak Dispersion Studies Using an Infrared Gas Imaging System. Proceedings of SPIE, 2366, Optical Instrumentation for Gas Emissions Monitoring and Atmospheric Measurements, 124 – 134.

68. Meister, M. 2009. Smart LDAR—More Cost-Effective? A white paper prepared for Trinity Consultants. http://www.trinityconsultants.com/Templates/TrinityConsultants/News/Print.aspx?id=1293. Accessed September 28, 2012.

69. Meyer, L. 2009. Alternative Technologies for Leak Detection, Enhancement of Pipeline Integrity. Presented at the Gas STAR 16th Annual Implementation Workshop, San Antonio, TX, (October 19-21).

70. Miseo, E. V. and N. A. Wright. 2003. Developing a Chemical-Imaging Camera. The Industrial Physicist. 29-32.

71. Moeller, T., and T. Trefiak. 2009. Leak Detection and Measurement in the Transmission and Distribution Sectors. Presented at the Gas STAR 16th Annual Implementation Workshop, San Antonio, TX (October 19-21).

72. Moore, E.A., K.C. Gross, S.J. Bowen, G.P. Perram, M. Chamberland, V. Farley, J-P. Gagnon, P. Lagueux, and A. Villemaire. 2009. Characterizing and overcoming spectral artifacts in imaging Fourier-transform spectroscopy of turbulent exhaust plumes. Chemical, Biological, Radiological, Nuclear, and Explosives (CBRNE) Sensing X, Proceedings of SPIE, 7304.

73. Opgal. 2012. Benchmark Comparison Spec Sheet. Provided by Guardian Compliance.

74. Panek, J., P. Drayton, K. Ritter, and D. Fashimpaur. 2006. Controlled Laboratory Sensitivity Performance Evaluation of Optical Leak Imaging Infrared Cameras for Identifying Alkane, Alkene, and Aromatic Compounds. AWMA 99th Annual Meeting, New Orleans, LA (June).

75. Panek, J.A. 2005. Controlled Laboratory Testing to Determine the Sensitivity of FLIR GasFindIR Infrared Camera for Imaging Organic Compounds. Prepared by Innovative Environmental Solutions, Inc. for FLIR Systems.

76. Picard, D. 2008a. Reducing Methane Emissions through Directed Inspection and Maintenance (DI&M). Presented at the Methane to Markets and Natural Gas STAR Technology Transfer Workshop on Methane Emission in the Petroleum and Gas Sector, Buenos Aires, Argentina (November 5-6).

77. Picard, D. 2008b. Methane Emission Measurement Techniques. Presented at the Methane to Markets and Natural Gas STAR Technology Transfer Workshop on Methane Emission in the Petroleum and Gas Sector, Buenos Aires, Argentina (November 5-6).

78. Picard, D., J. Panek, D. Fashimpaur. 2006. Directed Inspection and Maintenance Leak Survey at a Gas Fractionation Plant Using Traditional Methods and Optical Gas Imaging. AWMA 99th Annual Conference, 06-A-119-AWMA.

79. Puckrin, E., C.S. Turcotte, P. Lahaie, D. Dubé, V. Farley, P. Lagueux, F. Marcotte, and M. Chamberland. 2009. Airborne measurements in the infrared using FTIR-based imaging hyperspectral sensors. Proceedings of SPIE, 7342-46, Orlando, FL (April 13-17).

80. Reese, D., C. Melvin, and W. Sadik. 2007. Smart LDAR: Pipe Dream or Potential Reality? Exxon Mobile Corporation.

81. Rice, J. 2008. Directed Inspection and Maintenance and Infrared Leak Detection. Lessons Learned from Natural Gas STAR. Presented at the Natural Gas STAR Producers Technology Transfer Workshop, Denver, CO. April 29, 2008.

82. Richards, L. 2009. Directed Inspection and Maintenance and Infrared Leak Detection. Lessons Learned from the Natural Gas STAR Program. Presented at the Natural Gas STAR Producers and Processors Technology Transfer Workshops, Billings, MT (August 31).

83. Robinson, D.R. 2003. Emerging Technology: Optical Imaging Leak Detection. Gas STAR 10th Annual Implementation Workshop, Houston, TX, (October 27-29).

84. Robinson, D.R., and R.E. Luke-Boone. 2003. Identifying Fugitive Emissions with Optical Imaging. Proceedings of the 10th Annual International Petroleum Environmental Conference (IPEC), Houston, TX. November 11-14, 2003.

85. Robinson, D.R., R Luke-Boone, V. Aggarwal, B. Harris, E. Anderson, D. Ranum, T.J. Kulp, K. Armstrong, R. Sommers, T.G. McRae, K. Ritter, J.H. Siegell, D. Van Pelt, and M. Smylie. 2007. Refinery Evaluation of Optical Imaging to Locate Fugitive Emissions. Journal of the Air & Waste Management Association, 57(**7**): 803-810.

86. Russwurm, G.M. 1992. Operational Considerations for the Use of FTIR Open Path Techniques under Field Conditions. Proceedings of the 1992 U.S. EPA/A&WMS International Symposium on the Measurement of Toxic and Related Air Pollutants (VIP-25), Air & Waste Management Association, Pittsburgh, PA, pp. 579 – 581.

87. Safitri, A. 2011. Infrared Optical Imaging Techniques for Gas Visualization and Measurement. Thesis dissertation for Doctor of Philosophy in Chemical Engineering from Texas A&M University.

88. Sandsten, J., U. Wållgren, M. Barenthin Syberg, and H. Hagman. 2015. Optical Gas Imaging Standard for Sensitivity and Detection of Gases. AWMA 108th Annual Meeting, Raleigh, NC (June).

89. Scherello, A. 2011. State-of-the-Art Methane Leak Detection CHARM® and GasCam®. Presented at the Global Methane Initiative Partnership-Wide Meeting, Krakow, Poland (October 12-14).

90. Secrest, C. 2011. Photo-Ionization Detectors for CAA Inspections. EPA National Flares and LDAR Workshop (June).

91. Siegell, J.H., K. Ritter, H. Taback, and M. Lev-On. 2006. Cheaper, Faster and Smarter: Next-Generation LDAR Programs. EM Magazine, April, 46-49.

92. Skoog, D.A., F.J. Holler, and S.R. Crouch (Eds). 2007. Principles of Instrumental Analysis, 6th Edition. Australia: Brooks/Cole: Thomson Learning.

93. Spectral Remote Sensing & Detection. 2009. Sensitivity Reliability of Gas Imaging Leak Detection of SF_6. Presented to the 2009 Workshop on SF_6 Emission Reduction Strategies (February).

94. TCEQ. 2012. Texas Commission on Environmental Quality Comments on National Uniform Emission Standards for Storage Vessels and Transfer Operations; Proposed Rule. Federal Docket ID: EPA-HQ-OAR-2010-0871-0048. Available at http://www.regulations.gov.

95. Tegstam, J. 2011. Optical Gas Imaging: Gas Leak Detection Using Infrared Cameras. Presented at the Global Methane Initiative Partnership-Wide Meeting, Krakow, Poland (October 12-14).

96. Thoma, E.D., R.C. Shores, E.L. Thompson, D.B. Harris, S.A. Thorneloe, R.M. Varma, R.A. Hashmonay, M.T. Modrak, D.F. Natschke, and H.A. Gamble. 2005. Open-Path Tunable Diode Laser Absorption Spectroscopy for Acquisition of Fugitive Emission Flux Data; Journal of Air and Waste Management Association. 55(5): 658-668.

97. Throwe, S., and M. Mia. 2011. EPA Air Enforcement Initiatives. EPA National Flares and LDAR Workshop (June).

98. Trefiak, T. 2006. Pilot Study: Optical Leak Detection and Measurement. Report to ConocoPhillips (October 16).

99. Tremblay, P. L. Belhumeur, M. Chamberland, A. Villemaire, P. Dubois, F. Marcotte, C. Belzile, V. Farley, and P. Lagueux. 2010. Pixel-wise real-time advanced calibration method for thermal infrared cameras. Infrared Imaging Systems: Design, Analysis, Modeling, and Testing XXI, Proceedings of SPIE, 7662.

100. Tremblay, P. S. Savary, M. Rolland, A. Villemaire, M. Chamberland, V. Farley, L. Brault, J. Giroux, J-L. Allard, E. Dupuis, and T. Padia. 2010. Standoff gas identification and quantification from turbulent stack plumes with an imaging Fourier-transform spectrometer. Advanced Environmental, Chemical, and Biological Sensing Technologies VII, Proceedings of SPIE, 7673.

101. Tupper, P., and J. Wilwerding. 2009. Comparison of Leak Detection and Measurement Methodologies. Presented at the Gas STAR 16th Annual Implementation Workshop, San Antonio, TX (October 19-21).

102. U.S. EPA. 1985. EPA Announces National Strategy for Toxic Air Pollutants. EPA press release published June 4, 1985.

103. U.S. EPA. 1990. EPA: A Retrospective. EPA press release published November 29, 1990.

104. U.S. EPA. 1990. Standards of Performance for Equipment Leaks of VOC in Petroleum Refineries. New Source Performance Standard (NSPS), Code of Federal Regulations (CFR), 40 CFR part 60, subpart GGG.

105. U.S. EPA. 1995. Protocol for Equipment Leak Emission Estimates, EPA-453/R-95-017, EPA-453/R-95-017. November 1995. http://www.epa.gov/ttnchie1/efdocs/equiplks.pdf.

106. U.S. EPA. 1995. Protocol for Equipment Leak Emission Estimates. U.S. Environmental Protection Agency (EPA), Office of Air Quality Planning and Standards, Report EPA 435-R-95-017, November 1995.

107. U.S. EPA. 1996. Methane Emissions from the Natural Gas Industry Volume 8: Equipment Leaks. Office of Research and Development, June 1996. EPA-600/R-96-080h. Available at http://www.epa.gov/gasstar/tools/related.html.

108. U.S. EPA. 1999. FT-IR Open-path Monitoring Guidance Document, Third Ed. Prepared by ManTech Environmental Technology, Inc., Research Triangle Park, NC. EPA/600/R-96-040.

109. U.S. EPA. 1999. Monte Carlo Simulation Approach for Evaluating Alternative Work Practices for Equipment Leaks, Final Report. Research Triangle Park, NC: Office of Air and Radiation, Office of Air Quality Planning and Standards.

110. U.S. EPA. 1999. Proper Monitoring Essential to Reducing 'Fugitive Emissions' Under Leak Detection and Repair Programs. EPA Enforcement Alert, 2(9); October 1999, EPA 300-N-99-014.

111. U.S. EPA. 2003. Directed Inspection and Maintenance at Compressor Stations. Lessons Learned from Natural Gas STAR Partners. Office of Air and Radiation. October 2003. EPA 430-B-03-008.

112. U.S. EPA. 2003. Directed Inspection and Maintenance at Gas Processing Plants and Booster Stations. Lessons Learned from Natural Gas STAR Partners. Office of Air and Radiation. October 2003. EPA 430-B-03-018.

113. U.S. EPA. 2003. Directed Inspection and Maintenance at Gate Stations and Surface Facilities. Lessons Learned from Natural Gas STAR Partners. Office of Air and Radiation. October 2003. EPA 430-B-03-007.

114. U.S. EPA. 2005. Natural Gas STAR Partner Update. Fall.

115. U.S. EPA. 2006. A New EPA Method: Leak Detection Beyond LDAR. Presented by R. Segall at AWMA 99th Annual Meeting, New Orleans, LA, June.

116. U.S. EPA. 2006. Alternative Work Practice to Detect Leaks from Equipment. Proposed rule amendment in the Federal Registrar, 71(66):17401-17409.

117. U.S. EPA. 2006. Directed Inspection and Maintenance and IR Leak Detection. Lessons Learned from Natural Gas STAR. Presented at the Natural Gas STAR Producers and Processors Technology Transfer Workshops, Gillette and Rock Springs, WY (May 9 & 11).

118. U.S. EPA. 2007. Final Amendments to Equipment Leak Regulations and New Standards for Synthetic Organic Chemicals Manufacturing Industry and Petroleum Refineries. Fact sheet prepared by the U.S. EPA Office of Air Quality Planning and Standards.

119. U.S. EPA. 2007. Leak Detection and Repair: A Best Practices Guide. Office of Enforcement and Compliance Assurance. October 2007. EPA-305-D-07-001. Available at http://www2.epa.gov/compliance/leak-detection-and-repair-best-practices-guide.

120. U.S. EPA. 2008. Alternative Work Practice to Detect Leaks from Equipment. 40 CFR Parts 60, 63, and 65. Revised as of December 19, 2008.

121. U.S. EPA. 2008. Alternative Work Practice to Detect Leaks from Equipment. Federal Register Volume 73, No. 246 (73 FR 78199 78199–78219; December 22, 2008.)

122. U.S. EPA. 2009. Investigation of Fugitive Emissions from Petrochemical Transport Barges Using Optical Remote Sensing. Final Report to the EPA National Risk Management Research Laboratory, Office of Research and Development, EPA/600/R-09/136.

123. U.S. EPA. 2011. Conduct DI&M at Remote Sites. Partner Reported Opportunities (PRO) for Reducing Methane Emissions, PRO Fact Sheet No. 901. Office of Air and Radiation.

124. U.S. EPA. 2011. EPA Handbook: Optical Remote Sensing for Measurement and Monitoring of Emissions Flux. U.S. Environmental Protection Agency, Office of Air Quality Planning and Standards, Air Quality Analysis Division, Measurement Technology Group, Research Triangle, NC, Guideline Document GD-52. http://www.epa.gov/ttn/emc/guidlnd.html.

125. U.S. EPA. 2012. Justification for Other than Full and Open Competition.

126. U.S. EPA. 2012. Oil and Natural Gas Sector: Standards of Performance for Crude Oil and Natural Gas Production, Transmission, and Distribution. Background Supplemental Technical Support Document for the Final New Source Performance Standards. U.S. EPA Office of Air and Radiation, Office of Air Quality Planning and Standards, Technical Support Document. Available at http://www.epa.gov/airquality/oilandgas/pdfs/20120418tsd.pdf. April 18, 2012.

127. U.S. EPA. 2012. Proposed National Uniform Emission Standards for Storage Vessels and Transfer Operation, Equipment Leaks, and Closed Vent Systems and Control Devices; and Revisions to the National Uniform Emission Standards General Provisions. Fact Sheet prepared by U.S. EPA Office of Air Quality Planning and Standards.

128. U.S. EPA. 2014. Report for Oil and Natural Gas Sector Leaks. White paper prepared by the U.S. EPA Office of Air Quality Planning and Standards (OAQPS). Available at http://www.epa.gov/airquality/oilandgas/methane.html.

129. U.S. EPA. 2015. Inventory of U.S. Greenhouse Gas Emissions and Sinks: 1990 – 2013. U.S. Environmental Protection Agency (EPA) report EPA 430-R-15-004. Published online at http://www.epa.gov/climatechange/ghgemissions/usinventoryreport.html on April 15, 2015.

130. Wilwerding, J. 2011. Fugitive emissions from valves: Update. Valves 2011: A Special Supplement to Hydrocarbon Processing, V-81 to V-83. June 2011.

131. Zeng, Y. 2012. White Paper on A Calibration/Verification Device for Gas Imaging Infrared Cameras. Providence, June 25, 2012.

132. Zeng, Y., and J. Morris. 2012. A New Technology for Measurement of Flare Combustion Efficiency in Real-Time. American Fuel & Petrochemical Manufacturers Environmental Conference, Denver, CO. ENV-12-14.

IV. ERG LABORATORY EVALUATIONS

This section summarizes the experimental laboratory studies conducted by ERG under EPA contracts EP-D-11-006 and EP-W-09-033 to evaluate the performance and application of OGI technology for leak detection. OGI has the potential to accurately identify leaking equipment and streamline the surveying process for LDAR programs. However, in order to fully understand the capabilities of OGI so that it can be implemented as a standalone monitoring technique, substantial technology performance testing needs to be conducted to better quantify and qualify the applicability, issues, and operation of OGI cameras for LDAR activities. In the work conducted for the EPA to date, ERG evaluated the following parameters (with more studies currently ongoing):

- Technology Feasibility Study – Initial demonstration of laboratory equipment and procedure used to determine the detection capabilities of an OGI camera at different gas concentrations and flow rates under controlled settings.

- Spectral Limitation Study – Documented the spectral operating window for multiple OGI cameras to define a predictable window-of-operation with known variability between same and different OGI camera makes and models.

- Gas Sensitivity Threshold Study – Evaluated the response of multiple OGI cameras to various test gases at different concentrations to develop a response curve with gas threshold detection levels. To be used for calculating OGI camera response factors relative to propane.

- Repeat Feasibility Study – Observed side-by-side comparisons of OGI camera operation and leak display with cameras from two different manufacturers.

- Horizontal Wind Shear Study – Observed the impact of various wind speeds perpendicular to the leak axis on OGI leak detection when all other parameters are controlled.

- Reynolds Number Study – Observed the impact of leak source exit face velocity (or gas leak exit pressure) by changing the size of the exit leak orifice and varying the mass emission rate.

- Temperature Differential Study – Investigated the impact of various temperature differentials (ΔTs) between the gas plume and the background scenery on OGI camera leak detection when the background is warmer and colder than the gas.

- Sky Background Data Collection – Observed the impact of different sky background conditions on OGI gas leak detection.

NOTE: All concentrations seen throughout this section represent the actual concentration of the gas before it is released as a simulated leak. Unless otherwise noted, the gas used for this study is nominally a 50/50 blend of propane and butane. The concentration of the gas should not be directly related to a Method 21 response without consideration of method specific

conditions (e.g., calibration gas, response factors, analyzer precision, environmental factors, leak geometry).

Similar to how regular cameras produce images using the visible light region (about 0.40 to 0.75 µm) of the electromagnetic spectrum, OGI cameras produce thermal images (called thermograms) from the infrared (IR) region (about 1.0 to 14.0 µm) of the electromagnetic spectrum. OGI cameras are a type of thermographic imager where a special optical component—called a band-pass filter—filters the incoming radiation to a very specific region. In the case of OGI cameras that target hydrocarbons (HCs), the region that is allowed to pass through to the camera's detector to make the image is from about 3.2 to 3.4 µm, which corresponds to the bandwidth of the energy absorbed by many compounds containing carbon-hydrogen (C-H) bonds. Therefore, the OGI camera produces a thermogram of the heat distribution in the field-of-view (FOV) where the presence of a plume of HC gas is represented by a change in heat. Like the way a shadow blocks incident light in the visible range, a plume of HC gas "blocks" the heat signature from the background thermal profile from being imaged in the IR, whether that background is hotter or colder than the gas plume. When the apparent background is hotter than the gas plume, the C-H bonds will absorb the heat signature and block the background thermal profile with a "cold" shadow. When the apparent background is colder, the C-H bonds will emit a hotter heat signature and block the background thermal profile with a "hot" shadow. Because OGI camera technology is based on thermal properties, some OGI cameras are developed with the ability to measure the apparent temperature of objects in the FOV; this capability is referred to as "thermometric" in this document.

The Stephan-Boltzmann Law explains the relationship where a change in the temperature of an object is proportional to the radiation output of that object; for example, an increase in the object's temperature results in an increase in the amount of IR radiation being emitted by that object. The total amount of radiation detected by the camera from an object is equal to the sum total of the amount of radiation emitted by the object, the amount of radiation transmitted by the object (unless the object is opaque) and the amount of radiation reflected by the object. Some OGI camera developers have created temperature calibration curves in the camera's firmware where, if the user inputs an accurate emissivity value (or ratio that describes the object's ability to emit radiation relative to a perfect blackbody emitter) and is able to view the object without transmissive or reflective interference, the intensity of the radiation received by the camera's detector is an accurate measure of the object's "apparent temperature." In the presence of an HC gas plume, an object's perceived radiation intensity will be partially occluded by HC gas absorption and the resulting apparent temperature of the object as measured by an OGI camera will change proportionally with the amount of gas between the object and the camera. Therefore, many of the studies presented in this section utilize measurements of apparent temperatures from FLIR GF320 cameras to objectively evaluate camera performance.

A. Feasibility and Detection Limit Study

ERG designed a custom controlled leak generation system (CLGS) to allow the observation of OGI technology leak detection performance under carefully controlled laboratory settings. The objective for the CLGS was to allow precise blending of pollutant gas with diluent gas so that a leak of known concentration, flow rate, and mass emission rate is released out a 2" opening in front of a background with a known temperature that is stable, controllable, and different from

the gas temperature. The blending system design is illustrated as a schematic in Figure 4-1 and the whole CLGS system is shown in Figure 4-2. Figure 4-2 also shows the equipment used to monitor the temperature of the gas, the temperature of the background plate, the temperature of the hood space, the relative humidity of the hood space, and the wind speed generated from the hood system ventilation (the last 3 conditions monitored by the "Met Sensors" labeled in Figure 4-2). The experimental gas plume is delivered from a 2" PVC pipe in front of a temperature controlled custom-built cold plate painted with Krylon #51602 Ultra Flat Black spray paint to reduce thermal reflection. See Appendix C.1 of this document for more detail on the CLGS design.
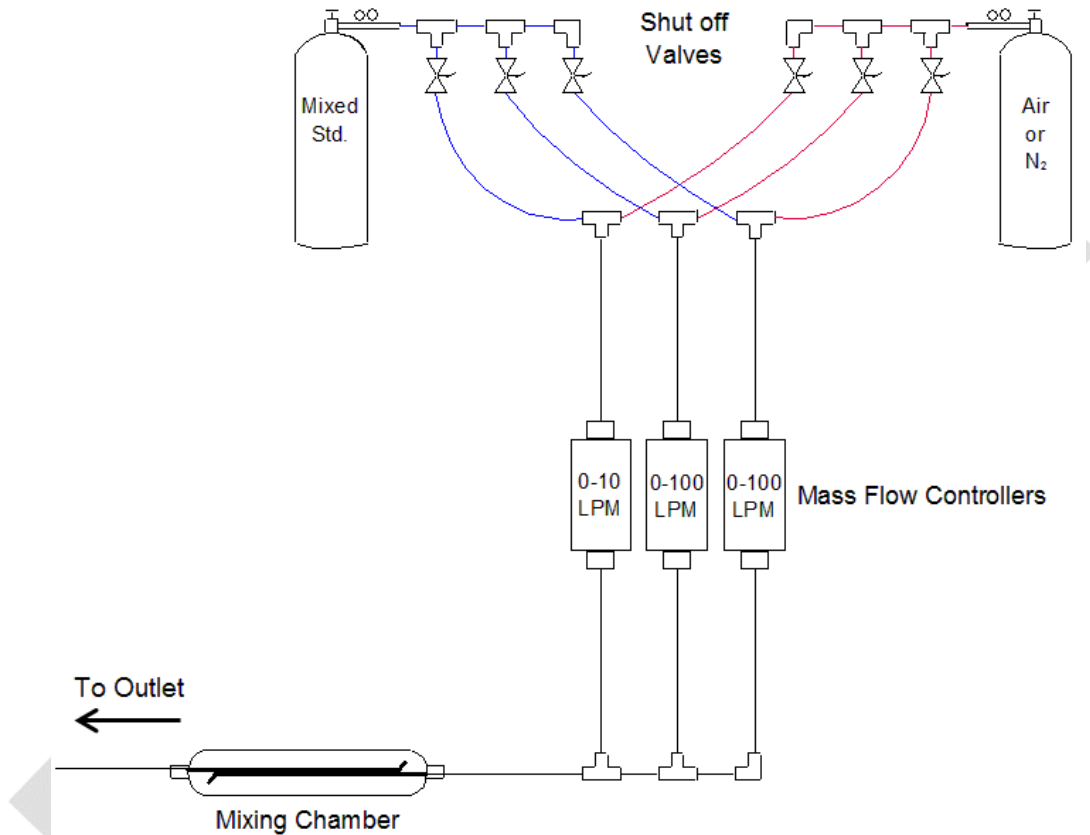
Figure 4-1. CLGS Gas Blending Component Developed by ERG for Preliminary Performance Tests
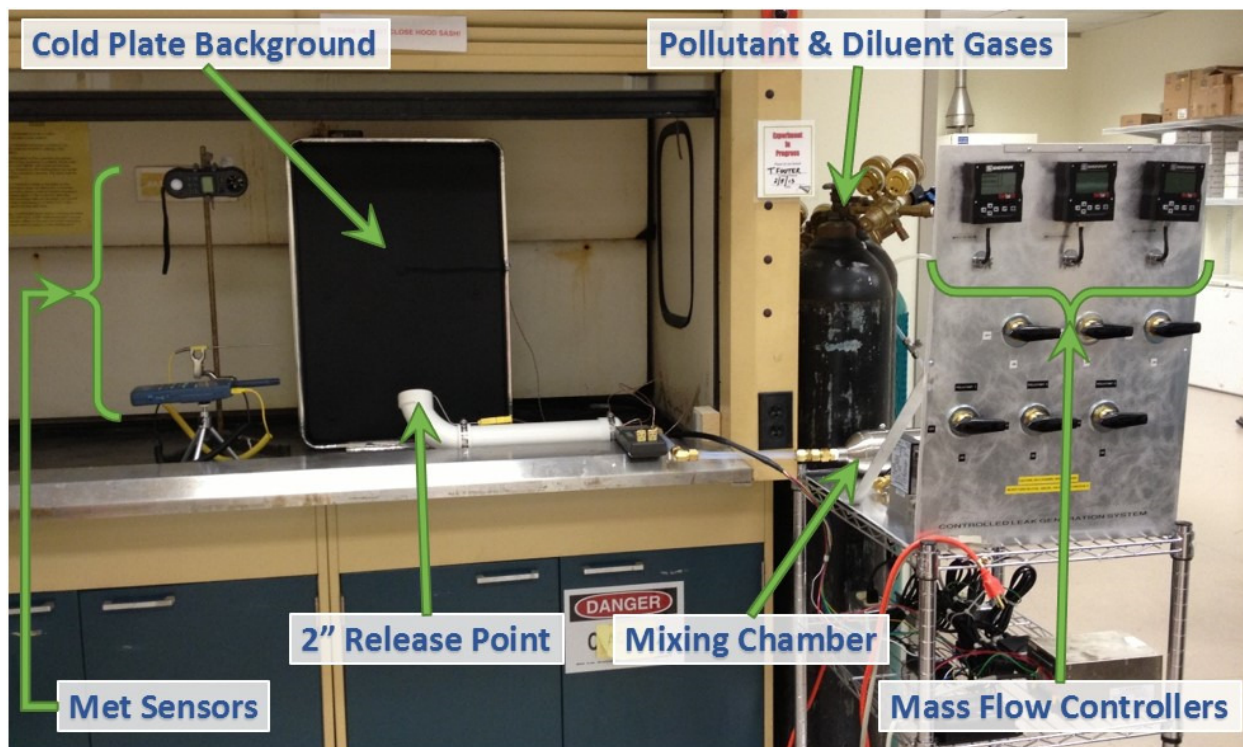
Figure 4-2. Overview of CLGS in Place at ERG's Laboratory

The first task conducted was a feasibility study using the CLGS, a 2% total hydrocarbon test gas blend of propane and butane, and a tripod mounted FLIR GF320 OGI camera. This initial study had two objectives: (1) to see if the CLGS design worked and was appropriate for FLIR GF320 camera performance testing; and (2) to determine at what concentration level and mass emission rate the FLIR GF320 camera lost detection when imaging leaks of various concentrations and mass rates. The settings on the OGI camera were held constant throughout the testing unless otherwise noted. More detail on the experimental design can be found in Appendix A.1: Test Plan.

For the purposes of this feasibility study, the leak had to be easily noticeable within 5 seconds of viewing the FLIR GF320 camera output displayed on a 40" flat screen TV (to assist with the execution of the tests by one analyst and verified by observing the FLIR GF320 camera LCD screen when leak detection was marginal). Lacking prior experience with the magnitude of the impact ΔT has on leak detection, the first attempt to execute this study did not find much success determining limits of detection at a $\Delta T = 15$ to $16°$ C, as all concentrations and mass rates were detected. The results shown in Tables 4-1 through 4-5 were collected later, with the effective ΔT lowered to 2 to 3°C. Using manual thermal tuning, the level and span of these tests at the lower ΔT where held equal to those of the higher ΔT tests for comparison and to challenge the observer.

NOTE: OGI camera software typically contains an automated display algorithm that defines the thermal tuning (grayscale profile) of an image based on establishing the range of temperatures in the FOV ("span") and calculating the midpoint of the span ("level"). Both the GF320 and Opgal have a setting ("auto mode") that allows the cameras to automatically

adjust the "span" and "level" so that all objects in the FOV are viewable. Additionally, the FLIR GF320 camera allows manual tuning, a process where the user can manually adjust the display thermal tuning (the "span" and "level"), thereby enabling us to perform a comparison between images produced by the two different ΔT conditions of our feasibility study while keeping all other conditions the same. The manual thermal tuning settings are not important when imaging in high sensitivity or enhanced modes due to the self-subtracting nature of the display algorithm. In other words, to increase OGI camera display sensitivity to a gas plume, camera developers designed an algorithm that subtracts the elements of the current frame from those of the previous frame (or average of a predetermined number of frames) to isolate (and, therefore, amplify) the difference between the frames due to the movement of the gas plume. In this way, the thermal tuning becomes less important, as the image is being constructed from differences in raw pixel intensity information from the detector.

A look into the increase in detection capabilities through the use of high sensitivity or enhanced modes was performed at the lowest concentration level (500 ppmv), and the results are shown in Tables 4-6 and 4-7. This test was repeated (Table 4-7 displays the results of the second run) to validate the results due to the challenging nature of trying to image a leak at a low concentration. Table 4-8 shows an overview of the total results, including the earlier test runs with ΔT ≈ 15°C. The green shading in the following tables indicates conditions where easy/definitive detection was lost.

Table 4-1. Results from Feasibility Study at About 20,000 ppmV (2%) Total Hydrocarbons (50/50 Propane-Butane Mix)

Run ID	Test Date	Total HC Conc. (ppmV)	Total Flow Rate (L/min)	Mass Release Rate (g/hr)	ΔT (°C)	Detected?
1A	2/7/2013	20220	100	255	2.4	Y
1B	2/7/2013	20220	90	229	2.6	Y
1C	2/7/2013	20220	80	204	2.8	Y
1D	2/7/2013	20220	70	178	2.7	Y
1E	2/7/2013	20220	60	153	2.6	Y
1F	2/7/2013	20220	50	128	2.7	Y
1G	2/7/2013	20220	40	102	2.9	Y
1H	2/7/2013	20220	30	77	2.7	Y
1I	2/7/2013	20220	20	51	2.8	Y
1J	2/7/2013	20220	10	26	2.8	Y
1K	2/7/2013	20220	5	13	2.7	N
1L	2/7/2013	20220	10	26	2.7	Y
1K	2/7/2013	20220	5	13	3.0	N

* Reversing the camera's polarity and adjusting the thermal tuning allowed the 13 g/hr leak (1K) to be detected after this test run.

Table 4-2. Results from Feasibility Study at About 10,000 ppmV (1%) Total Hydrocarbons (50/50 Propane-Butane Mix)

Run ID	Test Date	Total HC Conc. (ppmV)	Total Flow Rate (L/min)	Mass Release Rate (g/hr)	ΔT (°C)	Detected?
2A	2/7/2013	10110	100	128	3.1	Y
2B	2/7/2013	10110	90	115	3.1	Y
2C	2/7/2013	10110	80	102	3.1	Y
2D	2/7/2013	10110	70	89	3.2	Y
2E	2/7/2013	10110	60	77	3.0	Y
2F	2/7/2013	10110	50	64	3.1	Y
2G	2/7/2013	10110	40	51	3.1	Y
2H	2/7/2013	10110	30	38	3.0	Y
2I	2/7/2013	10110	20	26	2.9	Y
2J	2/7/2013	10110	10	13	3.2	Y
2K	2/7/2013	10110	5	6	2.8	N
2L	2/7/2013	10110	10	13	2.9	Y

Table 4-3. Results from Feasibility Study at About 5,000 ppmV (0.5%) Total Hydrocarbons (50/50 Propane-Butane Mix)

Run ID	Test Date	Total HC Conc. (ppmV)	Total Flow Rate (L/min)	Mass Release Rate (g/hr)	ΔT (°C)	Detected?
3A	2/8/2013	5055	100	64	2.6	Y
3B	2/8/2013	5055	90	57	2.7	Y
3C	2/8/2013	5055	80	51	2.6	Y
3D	2/8/2013	5055	70	45	2.7	Y
3E	2/8/2013	5055	60	38	2.6	Y
3F	2/8/2013	5055	50	32	2.5	Y
3G	2/8/2013	5055	40	26	2.7	Y
3H	2/8/2013	5055	30	19	2.5	Y
3I	2/8/2013	5055	20	13	2.3	N
3O	2/8/2013	5055	25	16	2.6	Y
3P	2/8/2013	5055	30	19	2.5	Y

Table 4-4. Results from Feasibility Study at About 500 ppmV Total Hydrocarbons

Run ID	Test Date	Total HC Conc. (ppmV)	Total Flow Rate (L/min)	Mass Release Rate (g/hr)	ΔT (°C)	Detected?
4A	2/8/2013	506	100	6	2.9	N

* Detection at this concentration level and flow rate was not achieved; therefore, further tests were not attempted according to original work plan.

Table 4-5. Results from Feasibility Study Holding Mass Emission Rate Equal to 10 g/hr with OGI Camera Thermal Tuning on Auto (50/50 Propane-Butane Mix)

Run ID	Test Date	Total HC Conc. (ppmV)	Total Flow Rate (L/min)	Mass Release Rate (g/hr)	ΔT (°C)	Detected?
5A	2/21/2013	809	100	10	2.0	N
5B	2/21/2013	1011	80	10	2.1	Y
5C	2/21/2013	1348	60	10	2.2	Y
5D	2/21/2013	2022	40	10	2.3	Y
5E	2/21/2013	2696	30	10	2.3	Y
5F	2/21/2013	4044	20	10	2.0	Y

Table 4-6. Results from Feasibility Study at About 500 ppmV Total Hydrocarbons on High Sensitivity Mode (50/50 Propane-Butane Mix)

Run ID	Test Date	Total HC Conc. (ppmV)	Total Flow Rate (L/min)	Mass Release Rate (g/hr)	ΔT (°C)	Detected?
10A	2/21/2013	506	100	6.4	2.4	Y
10B	2/21/2013	494	90	5.6	2.5	Y
10C	2/21/2013	506	80	5.1	2.5	Y
10D	2/21/2013	491	70	4.3	2.4	Y
10E	2/21/2013	506	60	3.8	2.4	Y
10F	2/21/2013	485	50	3.1	2.7	N
10G	2/21/2013	506	40	2.6	2.4	N
10H	2/21/2013	539	30	2.0	2.3	N
10I	2/21/2013	506	20	1.3	2.6	N
10T	2/21/2013	485	50	3.1	2.2	N
10U	2/21/2013	478	55	3.3	2.4	N
10V	2/21/2013	515	55	3.6	2.5	Y

* Video files were not recovered from this test run. Test run was repeated due to video recording error. Results for rerun are shown in Table 4-7.

Table 4-7. Results from Feasibility Study at About 500 ppmV Total Hydrocarbons on High Sensitivity Mode, Rerun (50/50 Propane-Butane Mix)

Run ID	Test Date	Total HC Conc. (ppmV)	Total Flow Rate (L/min)	Mass Release Rate (g/hr)	ΔT (°C)	Detected?
10A	3/12/2013	506	100	6.4	1.9	Y
10B	3/12/2013	494	90	5.6	2.1	Y
10C	3/12/2013	506	80	5.1	2.2	Y
10D	3/12/2013	491	70	4.3	2.1	Y
10E	3/12/2013	506	60	3.8	2.1	Y
10F	3/12/2013	485	50	3.1	2.1	Y
10G	3/12/2013	506	40	2.6	2.0	N
10H	3/12/2013	539	30	2.0	1.9	N
10I	3/12/2013	506	20	1.3	2.0	N
10T	3/12/2013	485	50	3.1	2.1	Y
10U	3/12/2013	478	55	3.3	2.0	Y
10V	3/12/2013	515	55	3.6	2.1	Y

Table 4-8. Overall Results from the Feasibility Study Showing Both ΔT Conditions

Test Conditions		Detection Limit	Mass Emission (g/hr)	Concentration (ppmV)	Total Flow Rate (L/min)
ΔT ≈ 15°C Manual Mode	Run 1	None reached	-	-	-
	Run 2	None reached	-	-	-
	Run 3	None reached	-	-	-
	Run 4	4O	1.5	485	25
High Sensitivity Mode	Run 10	None reached	-	-	-
ΔT ≈ 2 – 3°C Manual Mode	Run 1	1K	12.8	20220	5
	Run 2	2K	6.4	10110	5
	Run 3	3I	12.8	5055	20
	Run 4	4A	6.4	506	100
Auto Mode	Run 5*	5B	10.2	1011	80
High Sensitivity Mode	Run 10	10G	2.6	506	40

* Due to the nature of this test run, this is the maximum total flow rate for detection at the 10.2 g/hr rate of emission.

The results shown in Table 4-8 indicate that the FLIR GF320 camera should be able to detect a propane/butane gas mixture mass emission rate of 10.7 g/hr (average of runs 1 through 3) or greater under controlled laboratory conditions, with less-than-optimal manual thermal tuning, and with a ΔT ≈ 2°C. Using the FLIR GF320 camera's High Sensitivity Mode, the camera could potentially achieve a limit of detection down to 2.6 g/hr under controlled laboratory conditions. The controlled laboratory conditions that were present during this study but that would generally not be found in the field were:

- Tripod-mounted camera

- Consistently low and calm winds produced by the hood face velocity

- Homogenous and non-reflective thermal background

- Knowledge of the leak source

- No thermal interference from the surrounding infrastructure.

Other parameters contribute to a leak being detected by an OGI camera beside just mass emission rate, such as the speed at which the gas is exiting. A leak with a high flow rate will be harder to detect due to the more diffuse nature of the turbulent plume, and, conversely, a very slow leak will be harder to detect because it will appear smaller in volume, will be found closer to the leaking equipment, and will sometimes be intermittent depending on the wind conditions. By plotting the flow rate data from the feasibility study by the mass emission rate and highlighting the limits of detection (Figure 4-3), it is obvious that leak detection at the extremes of gas flow rate will be more challenging in addition to leaks with low mass emission rates.
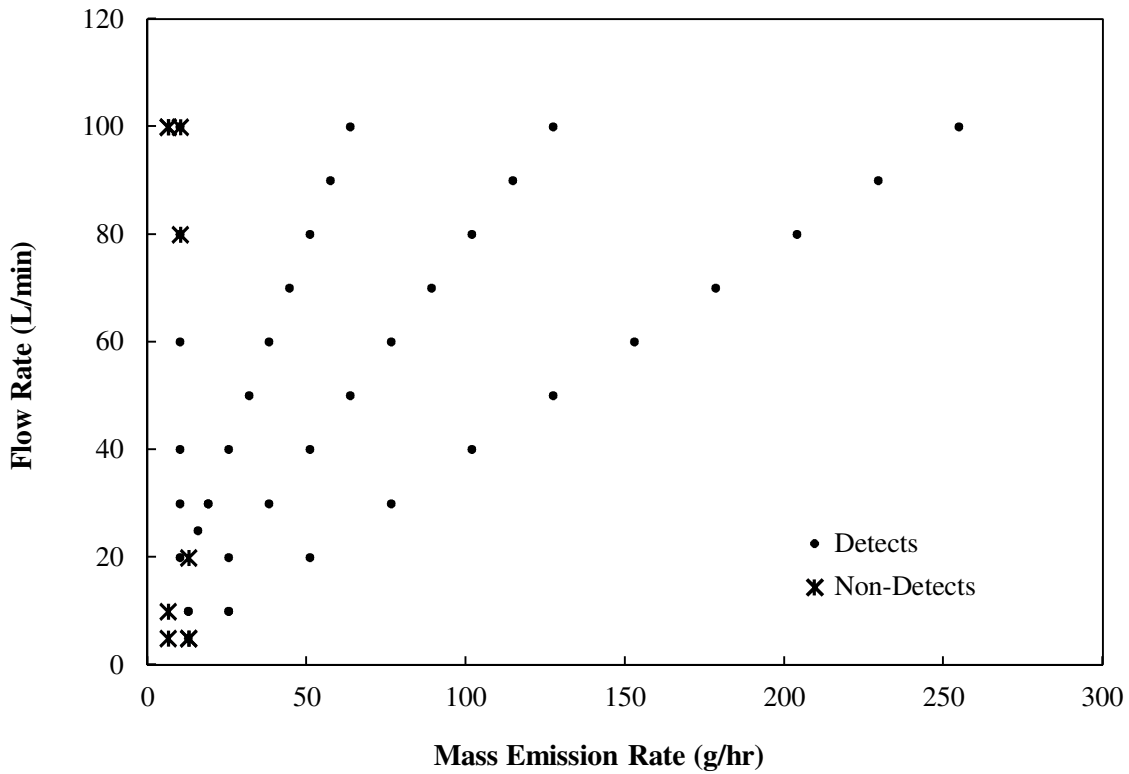
Figure 4-3. Feasibility Study Results by Flow Rate and Mass Emission Rate for Measurements in Manual and Auto Modes

B. Spectral Limitations and Gas Sensitivity Studies

The performance capabilities of an OGI camera are a direct result of the spectral properties of the IR optics used to construct the camera. The Office of Research and Development (ORD) of the EPA designed the custom-built spectral test platform shown in Figure 4-4 to specifically evaluate the spectral limitations of OGI cameras. One side of the spectral test platform (the left side in Figure 4-4) had a monochromator capable of emitting an IR source from 0.105 to 4.00 µm at a resolution of 1 Å (or 0.0001 µm), which was used to measure the spectral intensity curve of nine OGI cameras. The other side of the spectral test platform (the right side in Figure 4-4) had optical test cells with internal temperature and pressure sensors placed in front of a temperature controlled hot plate background. ERG integrated the precise gas dilution system from the CLGS described in Section IV-A of this document to deliver test gas to the cells on the spectral test platform at known concentrations. This was designed such that the spectral sensitivity of OGI cameras to different test gases at various concentrations could be evaluated.
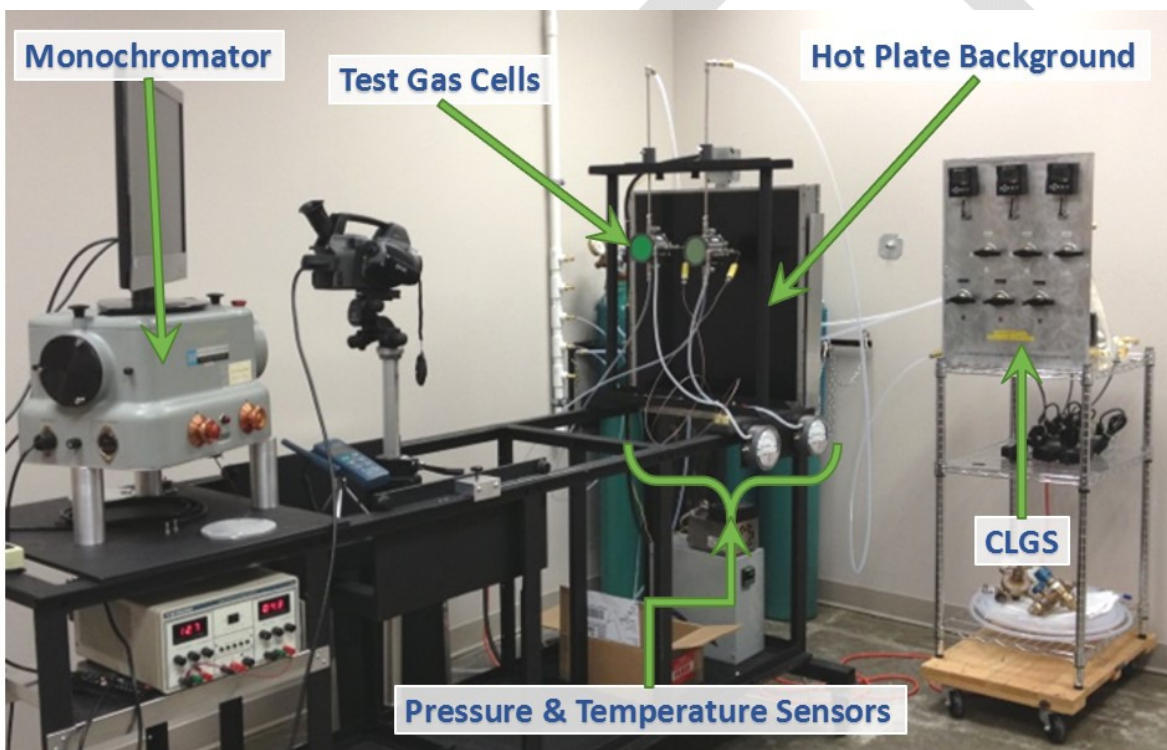
Figure 4-4. EPA ORD Custom-built Spectral Test Platform

ERG conducted spectral evaluations on seven FLIR GF320 cameras, one Opgal EyeCGas camera, and one older model FLIR GasFindIR camera (predecessor to the FLIR GF320 camera). The details for the OGI IR cameras used for these evaluations are presented in Table 4-9. The experimental design for these evaluations was initially based on the thermometric function (or ability to provide measurements of apparent temperature) available with the FLIR GF320 camera model. The addition of non-thermometric cameras (Opgal EyeCGas and FLIR GasFindIR) into the study required an augmentation to the study design for these cameras. Grayscale intensity from IR images recorded by these OGI cameras is used as a proxy for optical intensity. By adding neutral density filters of known optical densities into the field of view during the gas cell

tests, a grayscale calibration curve can be developed and used to evaluate the grayscale values measured from the optical test cells at different concentrations. A curve of the normalized grayscale intensity from the monochromator exit image is currently in process for both non-thermometric OGI cameras. An example of this technique[g] is provided in Figure 4-5 in the visible and the IR. As the preparation of the data collected from non-thermometric cameras is ongoing, the results presented at this time are from only the FLIR GF320 cameras evaluated.

Table 4-9. OGI Cameras Evaluated for Spectral Limitations and Gas Sensitivity

Make	Model	Serial Number	Owner/Location
FLIR	GF320	44401313	ERG
FLIR	GF320	44400966	EPA OECA
FLIR	GF320	44400816	EPA R8
FLIR	GF320	44401085	EPA OECA
FLIR	GF320	44401204	Southern Ute
FLIR	GF320	44401135	EPA R3
Opgal	EyeCGas*	TCG1005011*	Guardian Compliance
FLIR	GF320	44400819	EPA NEIC
FLIR	GasFindIR*	BH0115*	EPA R6

* These OGI camera models do not have thermometric capabilities. Therefore, the data collected from these cameras are still being processed.
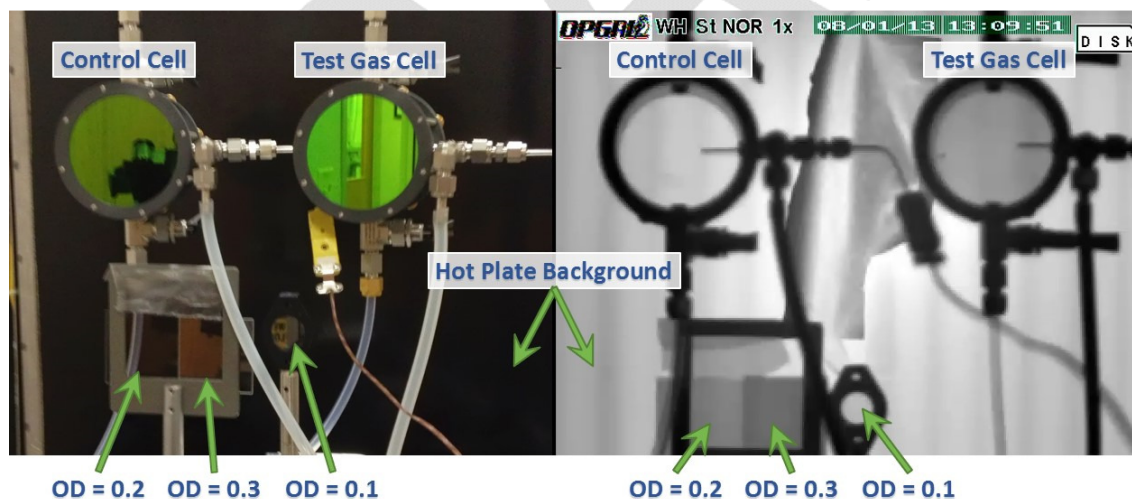
Figure 4-5. Example Placement of Neutral Density Filters for Non-Thermometric IR Spectral Tests in the Visible (Left) and IR (Right)

Each FLIR GF320 camera was mounted onto the spectral testing platform facing the monochromator and optimized such that the camera's cooled internal components contributed

---

[g] The data from the two non-thermometric OGI cameras using this technique are currently being processed under EPA Contract No. EP-D-11-006 Work Assignment 5-09.

minimal thermal interference (examples shown in Figures 4-6 and 4-7). After allowing the monochromator to thermally equilibrate, the optical intensity (as apparent temperature in °C) for each FLIR GF320 camera was measured from 3.00 to 3.65 µm in increments of 0.01 µm twice; once ascending from 3.00 to 3.65 µm, and then repeated descending from 3.65 to 3.00 µm for verification purposes. Each spectral curve was normalized to the maximum apparent temperature measured for that curve before being averaged over the entire collection of spectral curves for all FLIR GF320 cameras tested and plotted with 1σ standard deviation error bars by wavelength (in µm) in Figure 4-8. The error bars in Figure 4-8 highlight how the FLIR GF320 cameras all respond nearly identically, demonstrating the consistency of performance for the same make and model camera (the FLIR GF320), regardless of the original date of manufacture.
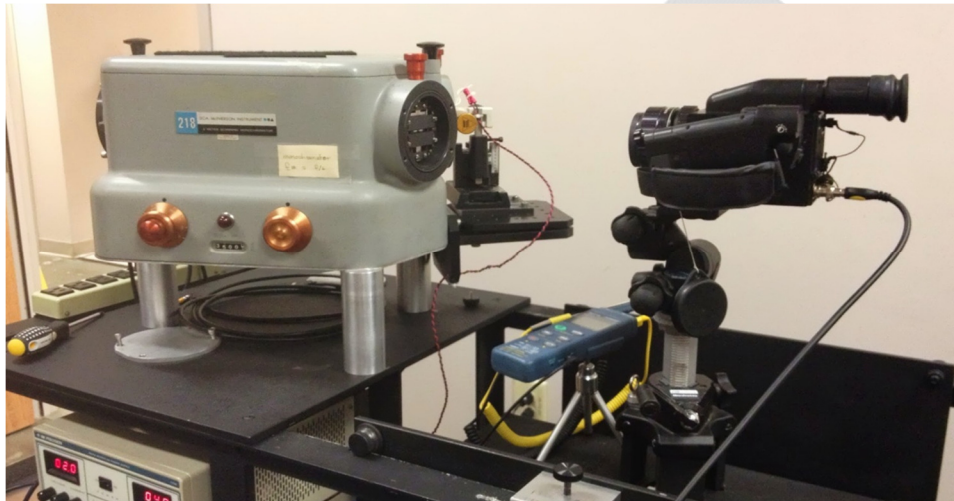
Figure 4-6. A FLIR GasFindIR Mounted and Aligned to the Monochromator Exit Slit

Figure 4-7. The Exit Slit of the Monochromator as Imaged by the FLIR GF320
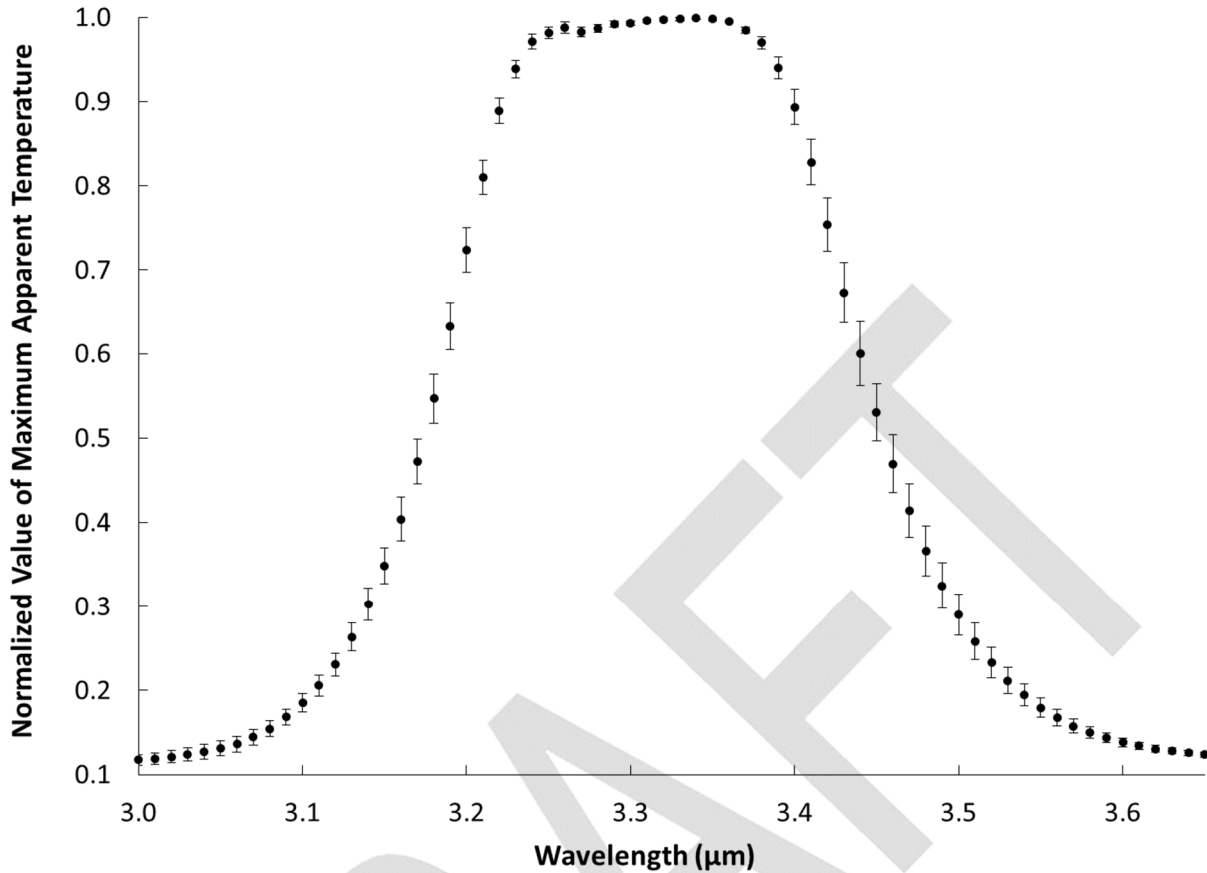
Figure 4-8. Average Spectral Window Curve for FLIR GF320 Cameras

In order to clearly define the spectral limitations of the OGI camera's optical system (called the "spectral window"), a feature of the spectral curve, termed the "point of limitation" (or POL) was defined as an increase in the optical intensity greater than 30% of the baseline value (evaluated beyond the fringe of the spectral window). The two locations on the spectral curve where this occurs are called the POL1-low and POL1-high. A case can be made that only the peak area of optical transmission (the plateau at the top of the spectral curve in Figure 4-8) should be considered as the camera's spectral window. Therefore, Category 2 POLs were calculated to be the region within which the optical intensity measurements stay within 5% of the maximum apparent temperature. Table 4-10 lists the results for all FLIR GF320 cameras tested and shows that POLs for Category 1 range from about 3.1 to 3.6 um and the POLs of Category 2 range from about 3.2 to 3.4 μm. Figure 4-9 shows a graphical representation of the spectral window POL locations for the FLIR GF320 cameras. The Category 2 POLs seem to correspond to the operating range of 3.2 to 3.4 um advertised by the camera manufacturer.

Table 4-10. FLIR GF320 Spectral Window Results

Camera ID	Camera Make and Model	Camera Owner	T_{max} (°C)	POL 1 (Å)		POL 2 (Å)	
				Low	High	Low	High
44401313	FLIR GF320	ERG	229	30900	35800	32400	33900
44400816	FLIR GF320	EPA OECA	231	30900	35700	32300	33800
44400966	FLIR GF320	EPA Region 8	236	30800	35600	32400	33900
44401085	FLIR GF320	EPA OECA	232	30900	35700	32400	33800
44401204	FLIR GF320	Southern Ute	228	31000	35700	32400	33800
44401135	FLIR GF320	EPA Region 3	228	30800	35500	32400	33800
44400819	FLIR GF320	EPA NEIC	236	30800	35700	32400	33800
Average				**30900**	**35700**	**32400**	**33800**
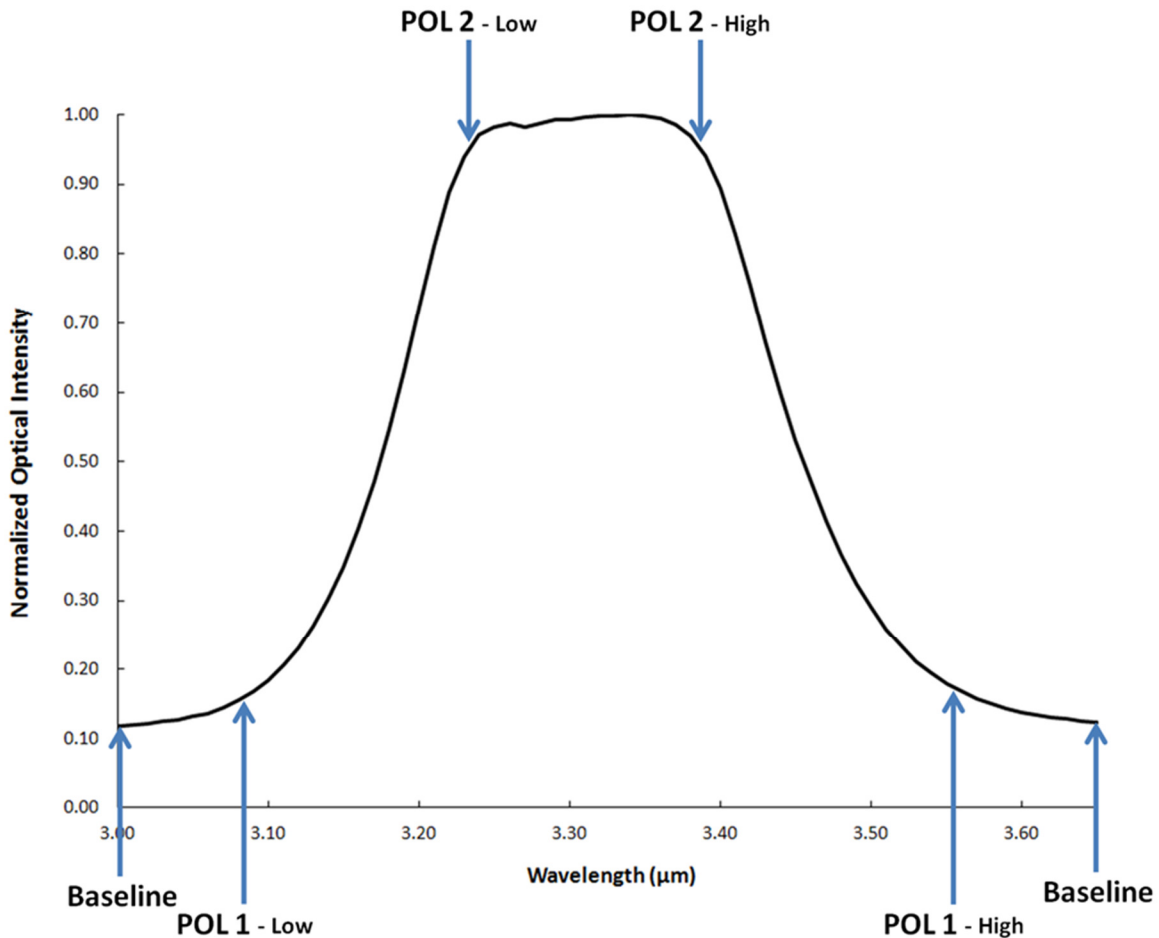
Figure 4-9. Average FLIR GF320 Spectral Window Curve Illustrating POL Locations

By developing an average OGI camera spectral performance curve, ERG was able to calculate response factors for various gases relative to propane (propane relative response factors). Spectral data from the Pacific Northwest National Laboratory (PNNL) were obtained and analyzed for each of the compounds listed in Table 4-11. The absorbance spectrum for each compound in the range of 3.00 to 3.70 µm was individually scaled by the average OGI camera spectral performance curve and then integrated to calculate the total integrated absorbance value presented in Table 4-11. These values were then divided by the total absorbance integrated value for propane in order to determine theoretical response factors relative to propane (propane relative response factors or propane RRFs).

Table 4-11. Integrated Spectral Absorbance and Propane Relative Response Factors

Compound	Total Integrated Absorbance	Propane Relative Response Factors
1,3-butadiene	0.009	**0.26**
1,3,5-trimethylbenzene	0.034	**0.95**
Acetic Acid	0.003	**0.08**
Acetaldehyde	0.004	**0.12**
Acetone	0.007	**0.21**
Acetylene	0.000	**0.01**
Acrylic Acid*	0.002	**0.05**
Benzene	0.013	**0.36**
Butane	0.043	**1.21**
Butene	0.025	**0.70**
Carbon tetrachloride	0.000	**0.00**
Dimethylformamide	0.019	**0.53**
ETBE	0.048	**1.35**
Ethylbenzene	0.030	**0.84**
Ethylene	0.006	**0.17**
Formaldehyde	0.007	**0.18**
Heptane	0.064	**1.80**
Hexane	0.057	**1.61**
Isoprene	0.016	**0.45**
MEK	0.017	**0.47**
Methane	0.011	**0.30**
Methanol	0.016	**0.44**
Methyl chloride	0.006	**0.15**
Methylene chloride	0.001	**0.03**
MTBE	0.045	**1.25**
m-Xylene	0.027	**0.76**
Octane	0.051	**2.00**
o-Xylene	0.024	**0.76**
Pentane	0.051	**1.43**

Table 4-11. Integrated Spectral Absorbance and Propane Relative Response Factors

Compound	Total Integrated Absorbance	Propane Relative Response Factors
Pentene	0.024	**0.68**
Propane	0.036	**1.00**
Propene	0.015	**0.42**
p-Xylene	0.029	**0.80**
Styrene	0.015	**0.42**
Toluene	0.020	**0.56**
Vinyl chloride	0.001	**0.03**
Water	0.000	**0.00**
Propane+Butane	0.039	**1.10**

* The spectra for Acrylic Acid was available from PNNL at only 50°C, versus 25°C as with all other gas spectra listed here.

Changes in the method for calculating the propane RRFs (such as range of integration and saturation as a function of optical depth) will alter the resulting propane RRF values. Therefore, to determine the most accurate method of integration, the theoretical propane RRF values in Table 4-11 need to be empirically validated. ERG is currently evaluating gas sensitivity assessments as a way to empirically validate the theoretical propane RRFs that we calculated.

The spectral testing platform shown in Figure 4-4 has two optically transmissive, air-tight, gas cells in front of a temperature controlled hot plate. By integrating the CLGS gas delivery component to the test cells of the spectral testing platform, we are able to carefully control the concentration of test gas delivered to the test cells. As discussed earlier in this section, the apparent temperature as measured by the FLIR GF320 camera provides a proxy for optical intensity received by the camera when the background apparent temperature is held constant. An example gas sensitivity curve is provided in Figure 4-10, where each blue asterisk represents the individual measurement for each of the seven FLIR GF320 tested at various concentration levels and the red circle is the average of all camera responses with black error bars representing 1σ standard deviation. The dashed line indicates a polynomial Classical Least Squares line of best fit through the averaged data. By extrapolating the equation for this line of best fit, we can calculate the temperature differential of the OGI camera response at a pre-determined concentration level for all test gases and develop a ratio of temperature differential responses for each gas to propane and compare this ratio to our theoretical propane RRFs. This work is currently ongoing.
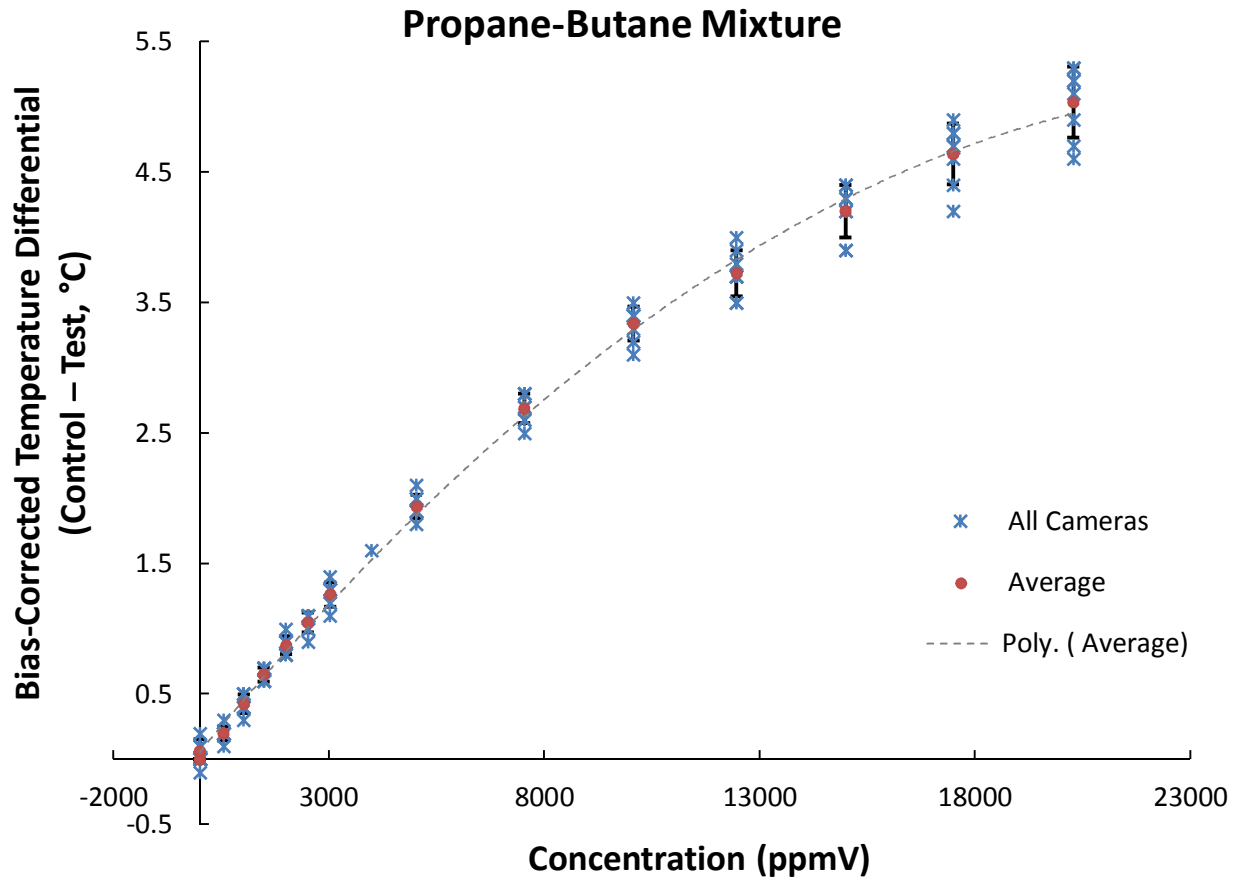
Figure 4-10. Example Gas Sensitivity Curve for 50/50 Propane-Butane Mixture

According to the Beer-Lambert law, which describes the relationship between the intensity of light signal as it passes through a media and the properties of that media, the IR signal detected by an OGI camera will be attenuated exponentially with increasing concentration. It is hypothesized that the curve at the top end of the line of best fit in Figure 4-10 indicates the beginning of that exponential attenuation towards optical saturation. This will be investigated further and any influence this may have on the calculated propane RRFs will be evaluated.

C. Assessment of Parameters that Influence Plume Characteristics/Detection

It is common knowledge that parameters beyond the camera's technical design will influence leak detection success. When attempting to characterize the performance and application of a technology (especially if used for method development purposes), the proper identification and quantification of the impact that various parameters will have on data quality is paramount. As directed by the EPA, ERG evaluated the influence from parameters that potentially impact OGI camera leak detection capability by isolating these parameters in carefully designed laboratory experiments. Some of the parameters tested to date are:

- Different manufacturers – a visual comparison

- Horizontal wind shear

- Reynolds number or leak face velocity

- Hot vs. cold ΔT.

The side-by-side visual comparison, horizontal wind shear, and Reynolds number parameters were investigated as part of Work Assignment 3-08 on EPA contract # EP-D-11-006.

The results from these studies are presented in Tables 4-12 through 4-26. For images results from both OGI cameras, see Appendix C.2 of this document. Each OGI camera was set to Auto mode unless otherwise specified. The green shading in the following tables indicates conditions where easy/definitive detection was lost, and the orange shading indicates a discrepancy in results between the two cameras. Due to camera design and equipment restraints during these tests, it is reasonable to expect a difference of results between the two cameras when investigating the limits of detection.

Table 4-12. Repeat Feasibility Study Run 1 (2% concentration) with FLIR and Opgal OGI Cameras

Run ID	Conc. (ppmV)	Total Flow Rate (L/min)	Mass Release Rate (g/hr)	ΔT (°C)	Detected by FLIR?	Detected by Opgal?
1A	20297	100	255	1.3	Y	Y
1B	20297	90	229	1.4	Y	Y
1C	20297	80	204	1.8	Y	Y
1D	20297	70	178	1.8	Y	Y
1E	20297	60	153	1.7	Y	Y
1F	20297	50	127	1.9	Y	Y
1G	20297	40	102	2.0	Y	Y
1H	20297	30	76	1.6	Y	Y
1I	20297	20	51	1.8	Y	Y
1J	20297	10	26	1.7	Y	Y
1K	20297	5	13	1.6	Y	Y

Table 4-13. Repeat Feasibility Study Run 3 (5000 ppmV) with FLIR and Opgal OGI Cameras

Run ID	Conc. (ppmV)	Total Flow Rate (L/min)	Mass Release Rate (g/hr)	ΔT (°C)	Detected by FLIR?	Detected by Opgal?
2A	5074	100	64	1.6	Y	Y
2B	5074	90	57	1.7	Y	Y
2C	5074	80	51	1.8	Y	Y
2D	5074	70	45	1.5	Y	Y
2E	5074	60	38	1.9	Y	Y
2F	5074	50	32	1.9	Y	Y
2G	5074	40	26	1.7	Y	Y
2H	5074	30	19	1.7	Y	Y
2I	5074	20	13	1.7	Y	Y
2J	5074	10	6.4	1.7	Y	Y
2K	5074	5	3.2	1.6	N	N
2L	5074	10	6.4	1.4	Y	Y

Table 4-14. Repeat Feasibility Study Run 4 (500 ppmV) with FLIR and Opgal OGI Cameras

Run ID	Conc. (ppmV)	Total Flow Rate (L/min)	Mass Release Rate (g/hr)	ΔT (°C)	Detected by FLIR?	Detected by Opgal?
3A	507	100	6.4	2.1	N	N
3B	507	90	5.7	1.8	N	N
3C	507	80	5.1	1.6	N	N
3D	507	70	4.5	2.0	N	N
3E	507	60	3.8	2.1	N	N
3F	507	50	3.2	1.8	N	N
3G	507	40	2.5	2.1	N	N
3H	507	30	1.9	2.0	N	N
3I	507	20	1.3	1.8	N	N
3J	507	10	0.64	2.0	N	N
3K	507	5	0.32	2.0	N	N

Table 4-15. Repeat Feasibility Study Run 5 (10.2 g/hr held constant) with FLIR and Opgal OGI Cameras

Run ID	Conc. (ppmV)	Total Flow Rate (L/min)	Mass Release Rate (g/hr)	ΔT (°C)	Detected by FLIR?	Detected by Opgal?
4A	812	100	10.2	2.3	N	N
4B	1015	80	10.2	2.2	N	N
4C	1353	60	10.2	2.0	Y	N*
4D	2030	40	10.2	1.8	Y	Y
4E	2706	30	10.2	1.6	Y	Y
4F	4059	20	10.2	2.2	Y	Y
4G	8119	10	10.2	1.9	Y	Y

* The viewing set up during these tests for the Opgal was not identical to that for the FLIR. The display TV was smaller and the video output had to be converted from analog to digital before being displayed. These discrepancies at the margins of detection are not anticipated to be representative of actual in-field performance.

Table 4-16. Rerun of Repeat Feasibility Study Run 5

Run ID	Conc. (ppmV)	Total Flow Rate (L/min)	Mass Release Rate (g/hr)	ΔT (°C)	Detected by FLIR?	Detected by Opgal?
4A	812	100	10.2	1.5	N	N
4B	1015	80	10.2	1.5	N	N
4C	1353	60	10.2	1.5	N	N
4D	2030	40	10.2	1.6	N	N
4E	2706	30	10.2	1.5	N	N
4F	4059	20	10.2	1.4	Y	Y
4G	8119	10	10.2	1.3	Y	Y

Table 4-17. Repeat Feasibility Study Run 10 (500 ppmV on High Sensitivity/Enhanced Modes) with FLIR and Opgal OGI Cameras

Run ID	Conc. (ppmV)	Total Flow Rate (L/min)	Mass Release Rate (g/hr)	ΔT (°C)	Detected by FLIR?	Detected by Opgal?
5A	507	100	6.4	1.5	N	N
5B	507	90	5.7	1.7	N	N
5C	507	80	5.1	1.5	N	N
5D	507	70	4.5	1.5	N	N
5E	507	60	3.8	1.8	N	N
5F	507	50	3.2	1.8	N	N
5G	507	40	2.5	1.6	N	N
5H	507	30	1.9	1.9	N	N

Table 4-18. Repeat of Feasibility Study Run 5 with FLIR and Opgal on High Sensitivity/Enhanced Mode

Run ID	Conc. (ppmV)	Total Flow Rate (L/min)	Mass Release Rate (g/hr)	ΔT (°C)	Detected by FLIR?	Detected by Opgal?
6A	812	100	10.2	1.6	Y	N*
6B	1015	80	10.2	2.1	Y	Y
6C	1353	60	10.2	1.5	Y	Y
6D	2030	40	10.2	1.9	Y	Y
6E	2706	30	10.2	1.7	Y	Y
6F	4059	20	10.2	1.9	Y	Y
6G	8119	10	10.2	1.8	Y	Y

* The viewing set up during these tests for the Opgal was not identical to that for the FLIR. The display TV was smaller and the video output had to be converted from analog to digital before being displayed. These discrepancies at the margins of detection are not anticipated to be representative of actual in-field performance.

Table 4-19. Horizontal Wind Shear, Normal/Auto Mode

Run ID	Conc. (ppmV) Total Flow Rate (L/min) Mass Release Rate (g/hr)	Horizontal Wind Velocity (m/s)	ΔT (°C)	Detected by FLIR?	Detected by Opgal?
2-1	20297, 50, 127	1.0	1.8	Y	Y
2-2	20297, 50, 127	2.0	1.9	Y	Y
2-3	20297, 50, 127	5.0	2.1	N	N
2-4	20297, 50, 127	9.0	2.1	N	N
2-5	20297, 50, 127	12	2.0	N	N

Table 4-20. Horizontal Wind Shear, High Sensitivity/Enhanced Mode

Run ID	Conc. (ppmV) Total Flow Rate (L/min) Mass Release Rate (g/hr)	Horizontal Wind Velocity (m/s)	ΔT (°C)	Detected by FLIR?	Detected by Opgal?
2-3	20297, 50, 127	5.0	2.0	Y	Y
2-4	20297, 50, 127	9.0	2.1	N	N
2-5	20297, 50, 127	12.0	2.1	N	N

Table 4-21. Reynolds Number Study Results with 2" Orifice

Run ID	Conc. (ppmV)	Total Flow Rate (L/min)	Mass Release Rate (g/hr)	Reynolds Number	ΔT (°C)	Detected by FLIR?	Detected by Opgal?
3-1A	20297	10	26	244	1.8	Y	Y
3-1B	20297	20	51	488	1.8	Y	Y
3-1C	20297	30	76	732	1.8	Y	Y
3-1D	20297	40	102	977	1.6	Y	Y
3-1E	20297	50	127	1221	1.9	Y	Y
3-1F	20297	60	153	1465	1.8	Y	Y
3-1G	20297	70	178	1709	1.8	Y	Y
3-1H	20297	80	204	1953	2.1	Y	Y

Table 4-22. Reynolds Number Study Results with 1" Orifice

Run ID	Conc. (ppmV)	Total Flow Rate (L/min)	Mass Release Rate (g/hr)	Reynolds Number	ΔT (°C)	Detected by FLIR?	Detected by Opgal?
3-2A	20297	10	26	475	1.7	Y	Y
3-2B	20297	20	51	950	1.9	Y	Y
3-2C	20297	30	76	1425	2.0	Y	Y
3-2D	20297	40	102	1900	1.8	Y	Y
3-2E	20297	50	127	2375	2.0	Y	Y
3-2F	20297	60	153	2850	1.8	Y	Y
3-2G	20297	70	178	3325	1.8	Y	Y
3-2H	20297	80	204	3800	1.9	Y	Y

Table 4-23. Reynolds Number Study Results with 1/2" Orifice

Run ID	Conc. (ppmV)	Total Flow Rate (L/min)	Mass Release Rate (g/hr)	Reynolds Number	ΔT (°C)	Detected by FLIR?	Detected by Opgal?
3-3A	20297	10	26	1009	1.9	Y	Y
3-3B	20297	20	51	2018	2.2	Y	Y
3-3C	20297	30	76	3027	2.1	Y	Y
3-3D	20297	40	102	4035	2.1	Y	Y
3-3E	20297	50	127	5044	2.1	Y	Y
3-3F	20297	60	153	6053	2.2	Y	Y
3-3G	20297	70	178	7062	2.0	Y	Y
3-3H	20297	80	204	8071	2.3	Y	Y

Table 4-24. Reynolds Number Study Results with 1/4" Orifice

Run ID	Conc. (ppmV)	Total Flow Rate (L/min)	Mass Release Rate (g/hr)	Reynolds Number	ΔT (°C)	Detected by FLIR?	Detected by Opgal?
3-4A	20297	10	26	1992	1.9	N	N
3-4B	20297	20	51	3984	1.9	Y	Y
3-4C	20297	30	76	5976	2.1	Y	Y
3-4D	20297	40	102	7968	1.8	Y	Y
3-4E	20297	50	127	9960	2.0	N	N
3-4F	20297	60	153	11952	1.9	N	N
3-4G	20297	70	178	13944	1.9	N	N
3-4H	20297	80	204	15937	2.0	N	N

Table 4-25. Reynolds Number Study Results with 1/8" Orifice

Run ID	Conc. (ppmV)	Total Flow Rate (L/min)	Mass Release Rate (g/hr)	Reynolds Number	ΔT (°C)	Detected by FLIR?	Detected by Opgal?
3-5A	20297	10	26	3979	2.0	N	N
3-5B	20297	20	51	7958	2.0	N	N
3-5C	20297	30	76	11936	1.8	N	N
3-5D	20297	40	102	15915	1.8	N	N
3-5E	20297	50	127	19894	1.7	N	N
3-5F	20297	60	153	23873	1.9	N	N
3-5G	20297	70	178	27852	1.6	N	N
3-5H	20297	80	204	31830	1.6	N	N

**Table 4-26. Reynolds Number Study Results with 1/8" Orifice and High/Enhanced Sensitivity Modes**

Run ID	Conc. (ppmV)	Total Flow Rate (L/min)	Mass Release Rate (g/hr)	Reynolds Number	ΔT (°C)	Detected by FLIR?	Detected by Opgal?
3-5A	20297	10	26	3979	1.2	Y	Y
3-5B	20297	20	51	7958	1.1	Y	Y
3-5C	20297	30	76	11936	1.4	Y	N*
3-5D	20297	40	102	15915	1.1	N	N
3-5E	20297	50	127	19894	1.3	N	N
3-5F	20297	60	153	23873	1.0	N	N
3-5G	20297	70	178	27852	0.9	N	N
3-5H	20297	80	204	31830	0.7	N	N

* The viewing set up during these tests for the Opgal was not identical to that for the FLIR. The TV display was smaller and the video output had to be converted from analog to digital before being displayed. These discrepancies at the margins of detection are not anticipated to be representative of actual in-field performance.

Two observations were made after plotting the Reynolds number data in a scatter plot (as shown in Figure 4-11). First, it appears detection becomes more challenging around a Reynolds number of 8000. Also, the lower mass emission rate values appear to be more difficult to visualize. However, due to the limited dimensions of this chart, it is not readily apparent that the mass emission rates from this test also correspond to flow rates. And, as observed with the initial

feasibility study data, the leaks that are being emitted at the lower flow rates (and, therefore, mass rates) will be harder to detect.
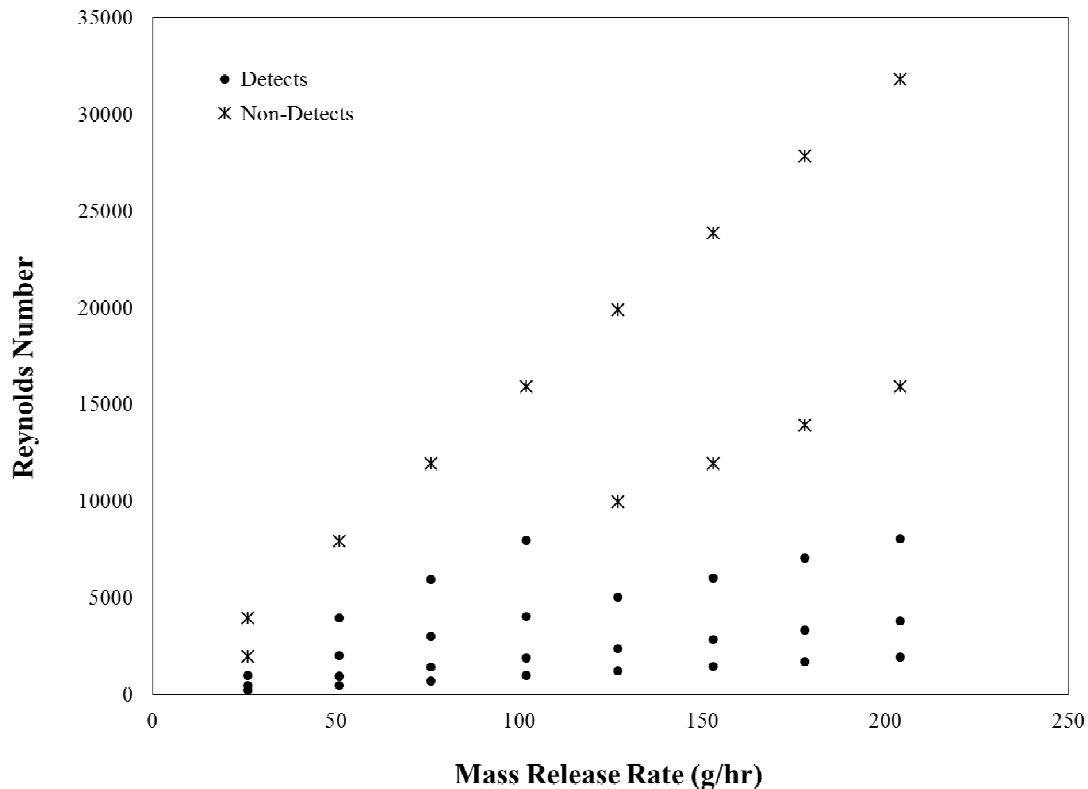
Figure 4-11. Overview of Reynolds Number Data

D. Camera Field Operation

Laboratory studies are good for isolating specific parameters and making observations under carefully controlled conditions. However, the types of conditions experienced in the laboratory are rarely ever encountered in the field. ERG designed and constructed the leak simulation platform (LSP, shown in Figure 4-12) to evaluate the operation of OGI cameras for leak detection in the field. Three flow meters allow for up to three leak simulations to be flowing at one time. This allows the evaluation of detecting multiple leaks in close proximity.

Volunteers of all experience levels ranging from never having used an OGI camera before to hundreds of hours of OGI camera use in the field and representing the EPA, industrial contractors, and camera vendors participated in a blind leak survey study using the LSP. Table 4-27 lists all possible leak simulations with the LSP, and Table 4-28 shows the experimental matrix that was adopted partway through the testing (changes were made due to time and resource constraints). Table 4-29 lists each test participant and their experience level prior to running the blind test, and Table 4-30 represents an overview of the results.
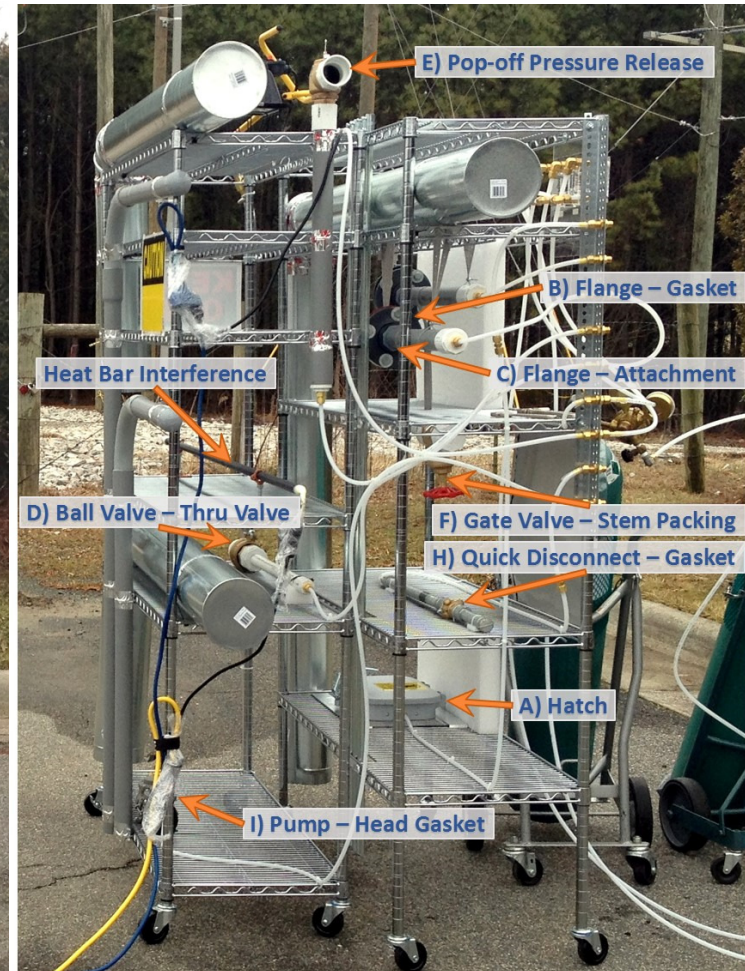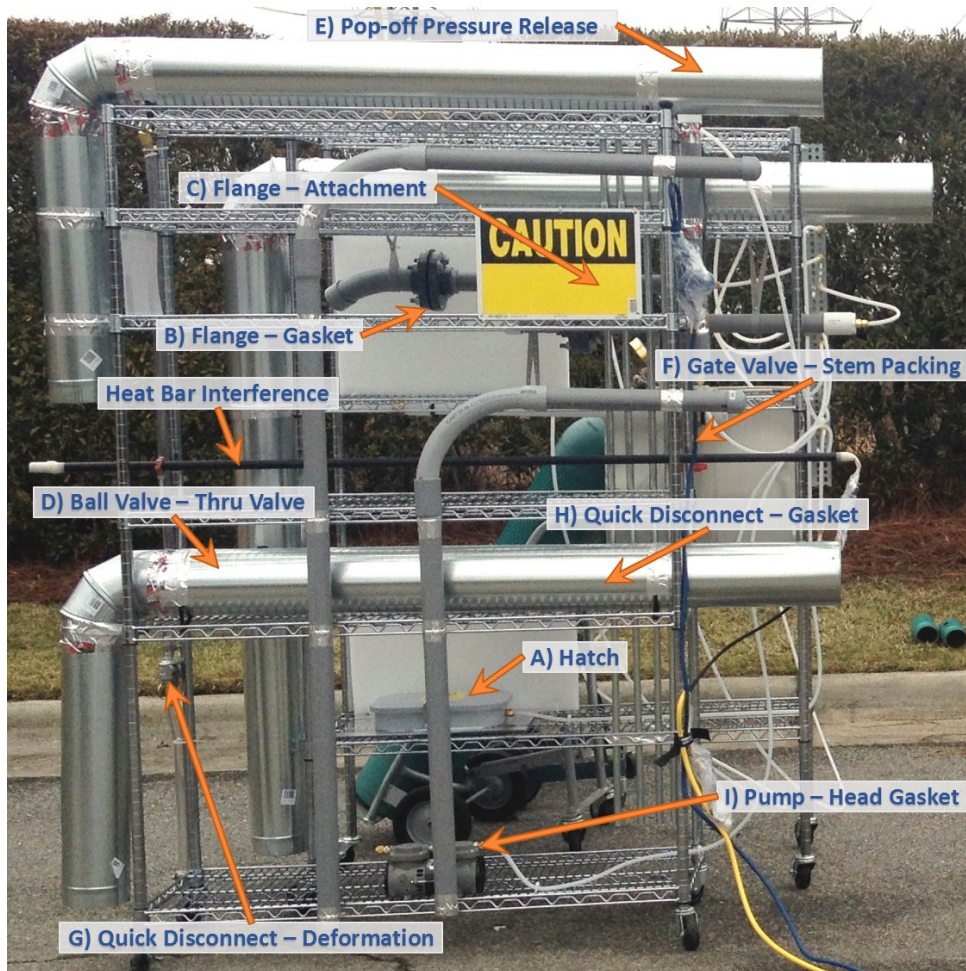
Figure 4-12. Custom-built LSP by ERG from the Front (left) and Side (right) Showing Leak Locations

Table 4-27. List of LSP Leaking Elements

Leak Identifier	Leak Description
A1	Hatch – Gasket
A2	Hatch – Closure
B	Flange – Gasket
C	Flange – Attachment
D	Ball Valve – Thru-valve leak
E	Pop-off pressure release valve
F	Gate Valve – Thru-stem leak
G	Quick Disconnect – Leak from deformation
H	Quick Disconnect – Gasket leak
I	Pump – Head gasket

Table 4-28. Initial Experimental Matrix for Blind Surveys

Run ID	Leak 1			Leak 2			Survey Duration (seconds)	Survey Zone
	Leak ID	Conc.	Flow Rate (L/min)	Leak ID	Conc.	Flow Rate (L/min)		
1	E	2%	40	D	0.2%*	60	15	Point
2	B	2%	60	G	0.2%*	60	15	Point
3	C	2%	20	F	2%	60	300	Free
4	I	2%	60	B	2%	40	300	Free
5	I	2%	60	A1	2%	60	300	Free
6	C	2%	40	--	--	--	300	Free
7	H	2%	20	F	2%	20	300	Free
8	E	2%	60	D	0.2%*	60	15	Point
9	A2	0.2%*	60	--	--	--	15	Point
10	G	2%	60	D	0.2%*	60	300	Free
11	E	2%	60	D	0.2%*	60	300	Free

* It was later determined that the 0.2 % (2000 ppmv) concentration level was not detectable due to the conditions encountered during testing.

Table 4-29. List of OGI Camera Operators and Experience Level

Operator	Experience Level	Description
A	3. Advanced	*Laboratory Scientist – Designed Study* * Operator had > 100 hours of camera operation experience in the past year. None of which was in a field setting.
B	1. Novice	*Environmental Engineer* Operator had < 10 hours of camera operation experience. None of which was in a field setting.
C	4. Expert	*LDAR Survey and Training Director* Operator had > 300 hours of camera operation experience in the past 2 years. Almost all of which was in a field setting.
D	3. Advanced	*LDAR Survey Technician* Operator had ~ 40 hours of camera experience in 2013, with a total of about 150 camera hours over entire career. Almost all of which was in a field setting.
E	3. Advanced	*EPA Compliance Engineer* Operator had 90 hours of camera operational experience in 3 years. Hours were a mix of laboratory and field settings.
F	3. Advanced	*Camera Vendor Technical Design Engineer/Scientist* Operator had > 400 hours of camera operation experience strictly in controlled/laboratory conditions.
G	2. Intermediate	*Camera Vendor Salesman* Operator had ~ 40 hours of camera operation experience in 2013, typically in an office or laboratory setting.
H	1. Novice	*EPA Policy Scientist* † Operator had < 10 hours of camera operation experience. None of which was in a field setting.

* This participant was the designer of the study and was therefore biased.

† This participant was a part of the EPA review team and therefore saw example footage of the leaking equipment prior to the test day.

Table 4-30. Overall Blind Survey Results for Leaks Released at 2% Concentration

Leak ID/Type	Operator/Camera										
	A/1	B/1	C/1	C/2	D/1	D/2	E/1	E/2	F/2	G/2	H/1
A1 Hatch - Gasket	Y	N	N	-	Y	-	Y	-	-	-	-
B Flange - Gasket	Y	N	N	-	Y	Y	N	Y	Y	Y	N
C Flange - Attachment	N	Y	N	N	Y	-	Y	-	-	-	-
E Pop-off	Y	Y	N	Y	Y	Y	Y	Y	Y	N	Y
F Stem Valve	Y	Y	N	Y	Y	Y	Y	Y	Y	Y	N
G QD - Deform	Y	Y	-	Y	Y	Y	Y	Y	Y	Y	Y
H QD - Gasket	Y	N	-	Y	N	N	N	N	Y	N	N
I Pump	Y	Y	Y	-	N	Y	Y	N	Y	Y	N

1 = FLIR GF320, 2 = Opgal EyeCGas
Green = Leak was detected at least 1 time, Red = Leak was not detected, Gray = Not tested due to time and resource constraints. See Appendix C.3 for more information.

The efforts from this study resulted in the following observations:

- Some leaks were harder to visualize than others.

- Although level of experience generally predicted operator performance, it was not the rule in all cases.

- There was no real discernible difference between the two camera types, although % detected by camera type (see Appendix C.3 of this document) indicates that the Opgal camera or users of the Opgal camera may have been more successful at identifying leaks.

- The 2,000 ppmv (0.2%) test gas was not detectable under non-ideal conditions.

- Capturing video footage is imperative for reviewing and qualifying leak detection.

- The presence of a heat/steam source during the cold, rainy conditions resulted in interference in leak identification.

V. SUMMARY

Through our evaluations and literature research, we identified a number of parameters that impact the detection capability of the OGI cameras. The parameters that have been evaluated by ERG and have an impact on the detection capability are:

- ΔT – The temperature differential between the gas plume and the apparent background
- Gas matrix of the plume or leak (speciation and concentration)
- Mass rate of the leak
- Camera configuration (both equipment and software parameters)
- Operator ability
- Wind speed
- Reynolds number of the leak.

Other parameters that were evaluated but are not deemed to substantially impact the detection capability are intra-model variability and performance degradation over lifespan of camera.

Other potential parameters that have been identified in the literature research as potentially impacting the detection capabilities of the OGI cameras but that have not been evaluated by ERG to date are the line of sight, ratio of FOV to the plume size and the standoff distance, and thermal interferences (e.g., steam, glint).

Despite the numerous parameters that may affect the detection capabilities of the OGI camera, the empirical testing in the lab and under proper field conditions with the LSP showed the ability of the FLIR GF320 and Opgal EyeCGas to detect leaks of 60 g/hr propane at a level of 10,000 ppmv with a knowledgeable camera operator.

While our testing focused on each parameter in isolation, it is important to remember that all these parameters can work in concert to affect the detection capability of the OGI camera. Figure 5-1 shows an example concept of an OGI performance envelope for a camera operating during normal conditions. Once developed, all the points within the highlighted pentagon would define the conditions necessary for valid operation of the OGI camera in order to detect any fugitive emissions that are present. As the point of operation gets closer to the middle of the envelope, the conditions for use of the camera become more optimal, allowing for easier detection of fugitive emissions using the OGI camera. As the point of operation moves toward the outer boundaries of the highlighted pentagon, the conditions for use of the camera become less optimal, presenting more challenges to detection of fugitive emissions using the OGI camera.
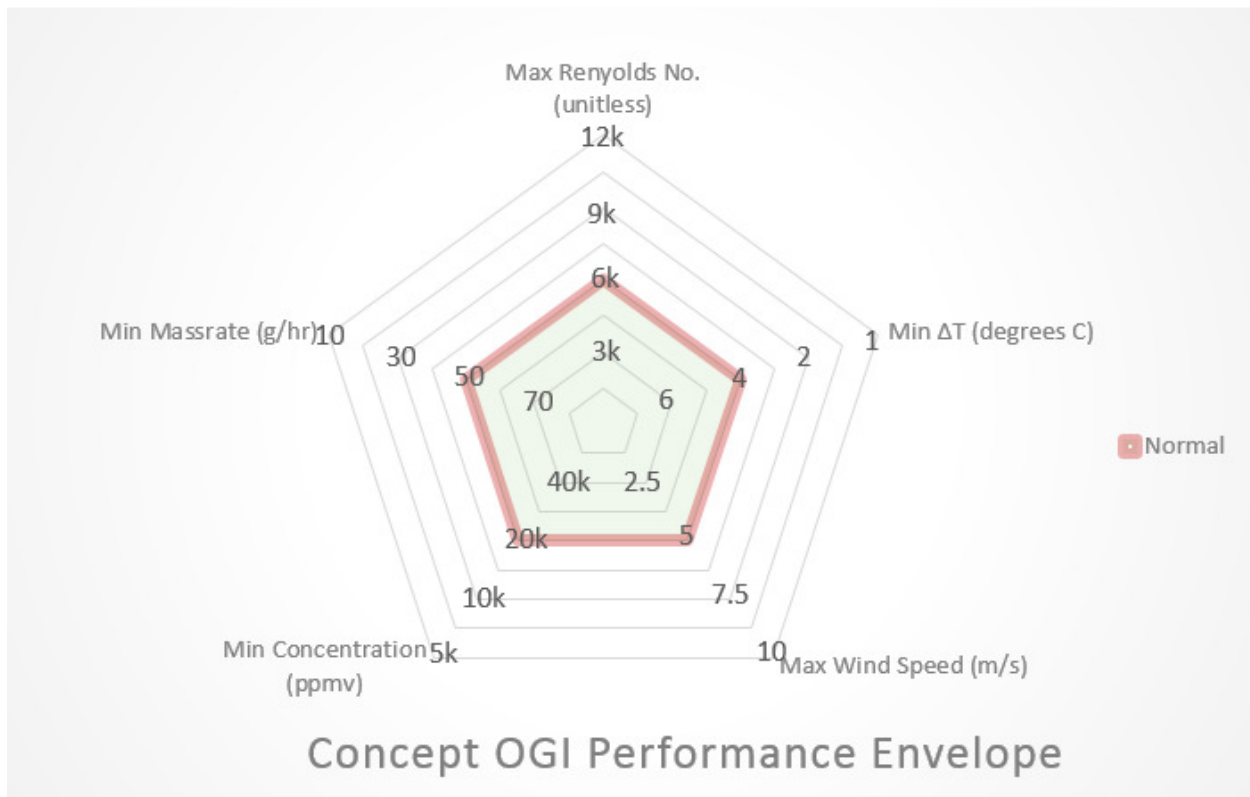
Figure 5-1. Concept Diagram of OGI Camera Performance Envelope

If there are parameters beyond the operator's control (e.g., wind speed) that cause the point of operation to be outside of the normal performance envelope, there may be a need to develop alternative envelopes to deal with these parameters. For example, requiring a higher ΔT or higher concentration can compensate for higher wind speeds to allow for a similar mass rate detection. Examples of these adjusted performance envelopes for higher wind speed and higher ΔT and for higher wind speed and higher concentration as compared to the normal performance envelope are shown in Figure 5-2. This concept of maintaining the performance capabilities of the camera by requiring one parameter to move inward in order to compensate for another parameter that falls outside the performance envelope would be applicable to any of the parameter that define the performance envelope.
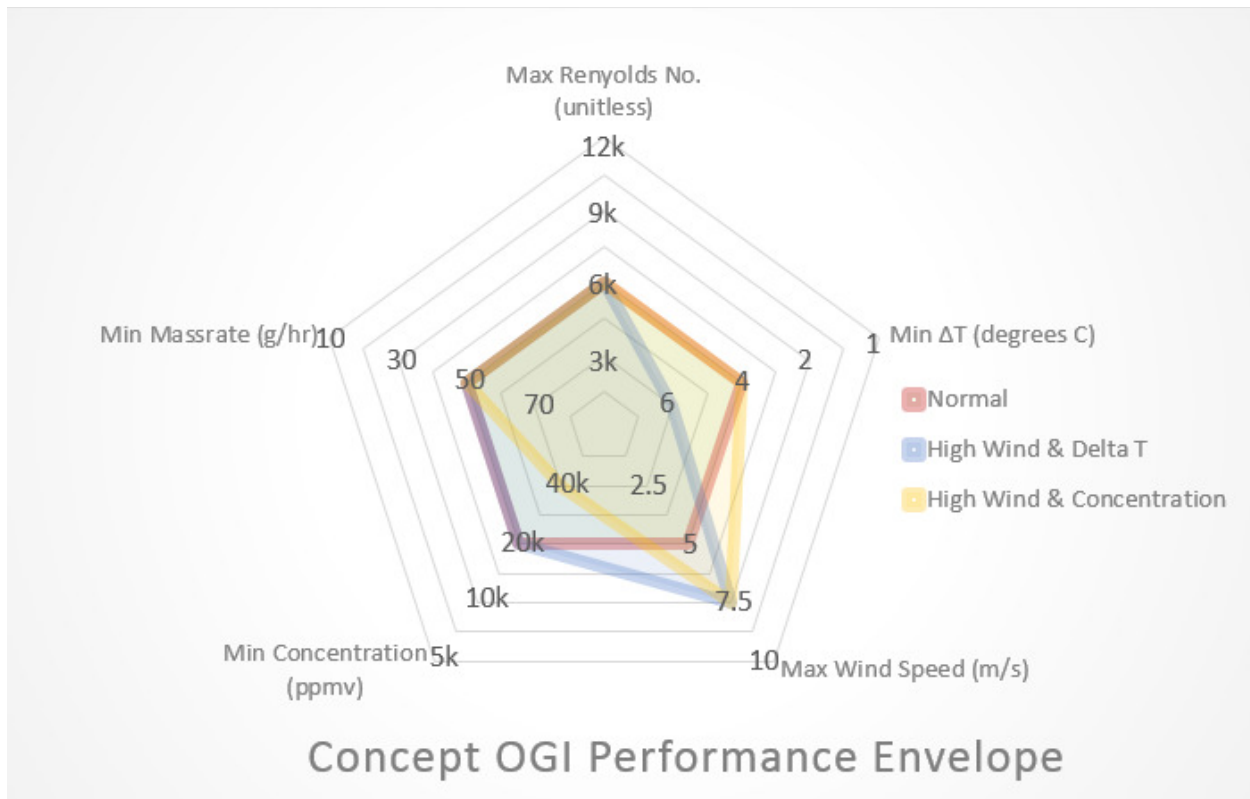
Figure 5-2. Concept Diagram of the OGI Camera Performance Envelope in the Presence of Non-Ideal Conditions

NOTE: The performance envelopes presented in Figures 5-1 and 5-2 represent only a draft concept OGI performance envelope for a FLIR GF320 or Opgal EyeCGas. Only after further empirical tests of the parameters have been completed and robust empirical correlations have been derived can a final envelope be determined. Also, these draft concept performance envelopes may not represent all potential parameters that will impact the detection capability.

With the possibility for a variety of technological advances of OGI cameras in the future, the development of these performance envelopes may be specific to camera models, camera modes, certain standards, and specific leak profiles such that parameters like the gas composition of the leak and the overall concentration of the leak affect the performance envelope while certain parameters such as wind have a consistent impact across all types of cameras.

VI.   LIST OF APPENDICES AND SUPPLEMENTAL DOCUMENTS

Appendix A: Feasibility Study (WA 2-09)

1. Test Plan

2. Final Report

Appendix B: Spectral Testing (TD-19)

1. Spectral Testing QAPP

2. Final Report

Appendix C: Parameters that Influence Detection (WA 3-08)

1. Parameter Testing QAPP

2. Final Report

3. Blind Study Report

Appendix D: BIC® Lighter Study Report

Appendix E: SOP for FLIR Temperature Calibration Verification